Behaviour of Shear-Critical Reinforced Concrete Beams Strengthened with Fiber Reinforced Cementitious Mortar

by

Rizwan Azam

A thesis

presented to the University of Waterloo

in fulfillment of the

thesis requirement for the degree of

Doctor of Philosophy

in

Civil Engineering

Waterloo, Ontario, Canada, 2016

AUTHOR'S DECLARATION

I hereby declare that I am the sole author of this thesis. This is a true copy of the thesis, including any required final revisions, as accepted by my examiners.

I understand that my thesis may be made electronically available to the public.

Abstract

Extensive research has been conducted on strengthening of shear-critical reinforced concrete (RC) beams, particularly using fiber reinforced polymer (FRP) strengthening systems. This previous research has helped to better understand the behaviour of shear strengthening systems and has improved the performance of existing shear strengthening systems. However, there is still a potential to further improve upon the performance of existing shear strengthening systems. A cement-based composite system is an innovative strengthening system that has similar benefits (such as light weight, ease of installation and non-corroding) to FRP systems, but overcomes some of the draw backs (such as poor compatibility with concrete substrate, lack of vapour permeability and fire resistance) of using epoxy as bonding agent in FRP systems. A cement-based composite replaces the epoxy with cementitious mortar and the fiber sheets with fabric or grids.

The current study presents the results of an experimental study conducted to investigate the effectiveness of cement-based composite systems in comparison to an existing epoxy-based system (carbon fiber reinforced polymer, CFRP) to strengthen shear-critical RC beams. Two types of cement-based systems were investigated in this

study: carbon fiber reinforced polymer (CFRP) grid embedded in mortar (CGM) and carbon fabric reinforced cementitious mortar (CFRCM).

The experimental study consisted of two phases. Phase I focused on flexural testing of seven medium-scale shear-critical reinforced concrete (RC) beams. The objective of this phase was to evaluate the potential of FRCM shear strengthening. The test variables included the type of FRCM (carbon FRCM or CFRCM and glass FRCM or GFRCM) and the strengthening scheme (side bonded vs. U-wrapped). Phase II was designed based on results of Phase I study, and it consisted of flexural testing of twenty (20) large-scale shear-critical RC beams strengthened with cement-based systems. The objective of this phase was to evaluate the effectiveness of the two types of cement-based strengthening systems in comparison to the existing epoxy-based FRP system. The test variables included: the shear span to depth ratio (slender and deep beams), amount of internal transverse steel reinforcement and type of strengthening system (CFRCM, CGM and CFRP).

The results showed that the cement-based systems (CFRP grid in mortar and CFRCM) performed better compared to the epoxy-based system (CFRP sheet) in terms of the increase in shear capacity relative to the ultimate strength of the strengthening systems. The results also showed that the bond of cement–based system with the concrete substrate was sufficient that u-wrapping may not be required; the studied side-bonded

systems did not exhibit signs of premature debonding. This is in contrast to most FRP fabric strengthening systems were u-wrapping is required for adequate bond. In addition, cement-based systems exhibited a better ability to control diagonal (shear) crack widths compared to the epoxy-based system tested, providing a greater reduction in diagonal crack width despite the relative lower ultimate strength and stiffness of the cement-based systems. Shear strengthening resulted in reduced shear strength contribution from stirrups. The strengthened beams with stirrups exhibited steeper shear cracks compared to control unstrengthened beams with stirrups. Similarly, the presence of stirrups reduces the shear strength contribution from strengthening. Again, the addition of stirrups results in steeper shear cracks which intersect fewer fibers tows in the strengthening system which results in a reduced shear strength contribution from strengthening layer. Lastly, the existing models to predict the ultimate load of strengthened shear-critical RC beams were evaluated and modifications to these methods were proposed.

Acknowledgements

I am grateful to have had the opportunity of working with my late supervisor, Professor Khaled Soudki, whose support, encouragement and dedication has been exceptional throughout my PhD tenure under his supervision. I am also very thankful to Professor Jeffrey S. West to take over the responsibility after passing away of Professor Khaled Soudki and for his guidance and valuable advice at later stages of my PhD which greatly helped me finish my PhD.

Thanks to my committee members, Professors Tim Topper, Steve Lambert and Rania Al-Hammoud for reviewing my thesis.

I would like to thank Civil Engineering Laboratory technicians Richard Morrison, Doug Hirst, Robert Sluban and Terry Ridgeway for their help in my experimental work.

I would like to thank my colleagues, office mates and friends: Mohamed Zawam, Olivier Daigle, Rayed Alyousef, Hesham Elhuni, Martin Noel, Adham El Menoufy, Liam butler, Mohamed Yakhlaf, Abdulaziz Alaskar, Hisham Alabduljabbar A. Shihata and S. Krem for their support in laboratory work and discussions.

I would also like to express my gratitude to Sika Canada for material donation and to the Natural Science and Engineering Research Council of Canada (NSERC) for their financial support.

Dedication

To My Late Supervisor Khaled A. Soudki

Table of Contents

List of Figures

List of Tables

Chapter 1: Introduction

1.1 General

1.1.1 State of Infrastructure

Infrastructure all over the world is aging and deteriorating. At the same time, traffic loads are increasing day by day. As a result, there are large numbers of deficient structures in the infrastructure; e.g.: there are more than 200,000 deficient bridges in United States and approximately 30,000 deficient bridges in Canada. Approximately over 150 spans collapse each year in North America. Canada's deteriorating infrastructure needs $49 billion for rehabilitation (Mufti 2003).

1.1.2 Shear-Critical Reinforced Concrete Members

Different design standards are used to design reinforced concrete (RC) structures in different parts of the world. All design standards agree on one basic design principle that RC members should be proportioned in such a way that they are governed by a ductile flexure failure mode and that brittle shear failure is avoided. Flexural failure of RC members is easily predictable as flexural design of RC members is based on Bernoulli's hypothesis (Bernoulli's beam theory) which state that plane section remains plane after bending. The ultimate flexural capacity of RC members can be determined by using a linear strain distribution for all stages of loading as per Bernoulli's hypothesis along with material (concrete, steel, FRP, etc.) appropriate stress-strain relationships and ensuring that equilibrium is satisfied. In contrast, shear failures of RC

members are more difficult to predict as most shear design provisions are not directly based on rational theory and rely upon empirical equations. The majority of tests used to calibrate code empirical equations are based on small scale shear-critical RC beams. Recent studies on the size effect on shear strength of concrete members found that the shear strength of the some members designed in 20th century was overestimated (Sneed et al., 2008, Sherwood et al., 2006). For example, there are structures in service without stirrups or with minimum stirrups that have a low margin of safety with higher probability of experiencing a shear failure (Collins et al., 2009). The partial collapse of Viaduc de la Concorde overpass in Laval, Quebec in 2006 highlighted this problem. The collapsed portion of the overpass was a thick cantilever slab which was constructed without stirrups. Investigation of the failure indicated that the slab experienced shear failure (Johnson et al., 2007). Therefore, there is a need for innovative methods to strengthen shear-critical RC member in-service.

1.1.3 Fiber Reinforced Cementitious Mortar (FRCM) Strengthening

Fiber reinforced polymers (FRPs) have been applied to strengthen/repair reinforced concrete (RC) members worldwide. A number of studies reported in the literature have demonstrated the effectiveness of FRPs to strengthen shear-critical RC members (Belarbi et al. 2011). However, the use of epoxy as a bonding agent in FRPs has some drawbacks that may limit the desirability of FRP systems for some strengthening applications. These drawbacks include poor compatibility with the concrete substrate,

lack of vapour permeability, hazardous working environment for workers, and most importantly, post-repair inspection and assessment of the structure are difficult .(De Caso et al., 2012; Ombres, 2011; Hashemi et al., 2011; Blanksvard et al., 2009; Tariantafillou et al., 2006).

Fiber reinforced cementitious mortar (FRCM) is a relatively new strengthening and rehabilitation system. It has all of the benefits of the fiber reinforced polymer (FRP) system but overcomes the draw backs of using epoxy as the bonding agent since FRCM replaces epoxy with cementitious mortar. The direct replacement of epoxy with cementitious mortar may result in poor bond if used with FRP sheets since the mortar does not penetrate through continuous or tightly woven fiber sheets. To avoid this problem, the continuous fiber sheets used in FRP systems are also replaced with fiber grids and oven-weave meshes in the FRCM system.

1.1.4 Current State-of-the-Art in FRCM Strengthening

A number of studies have been conducted to investigate the effectiveness of FRCM to strengthen reinforced concrete structures. These studies have mainly investigated the confinement of RC members with FRCM, bond behaviour of FRCM with concrete, flexural behaviour of FRCM strengthened RC members, and shear behaviour of FRCM strengthened RC members. Almost all of these studies were exploratory studies (a

review of the studies related to shear strengthening with FRCM is presented in Chapter 2).

Keeping in mind the current state of deteriorated North American Infrastructure, novel emerging technologies should be explored to rehabilitate deficient structures to increase their in-service life without compromising post-repair inspection. Therefore, there is need to conduct a comprehensive study to investigate the effectiveness of FRCM strengthening of RC members especially for shear-critical RC members and to develop design guidelines for FRCM shear strengthening.

1.2 Significance of FRCM Research

FRCM strengthening is an emerging strengthening system with great potential. However, the behaviour of shear-critical RC beams strengthened with FRCM has not been well studied. The research presented in this thesis provides data on the behaviour of shear-critical RC beams strengthened with FRCM compared to FRP. The research also evaluates the applicability of existing FRP shear strengthening code provisions and proposes modifications to existing design provisions for FRCM shear strengthening of RC beams.

1.3 Research Objectives

The main objective of the study was to examine the feasibility of FRCM strengthening for shear-critical RC deep and slender beams. The specific objectives were as follows:

- Investigate the effectiveness of FRCM strengthening for shear-critical RC beams.
- Compare the effectiveness of FRCM strengthening to that of FRP strengthening for shear-critical RC beams.
- Investigate the effect of internal transverse reinforcement on the effectiveness of FRCM strengthening systems applied to shear-critical RC beams.
- Evaluate the applicability of existing FRP shear strengthening code provisions for use with FRCM systems, and propose modifications to existing models as required.

1.4 Research Approach

To achieve the research objectives stated above, a comprehensive research program was designed. The research program consisted of an experimental and an analytical program.

The experimental program consisted of two phases, as shown in Figure 1.1. Phase I consisted of flexural testing of seven medium scale shear-critical reinforced concrete (RC) beams. The objective of this phase was to evaluate the potential of FRCM shear strengthening. The test variables included the type of FRCM (carbon FRCM, CFRCM and glass FRCM, GFRCM) and the strengthening scheme (side bonded vs. U-wrapped). One journal paper was published from this work and is presented in thesis as chapter 3. Based on results of Phase I, the Phase II experimental program was designed. Phase II consisted of flexural testing of twenty (20) large-scale shear-critical RC beams. The

objective of this phase was to evaluate the effectiveness of cement-based strengthening system in comparison to existing epoxy-based system. The test variables included: the shear span to depth ratio (slender and deep beams), transverse steel reinforcement and type of strengthening system (CFRCM, CGM and CFRP). Four journal papers were prepared based on the Phase II research and are presented in this thesis as chapter 4-7.

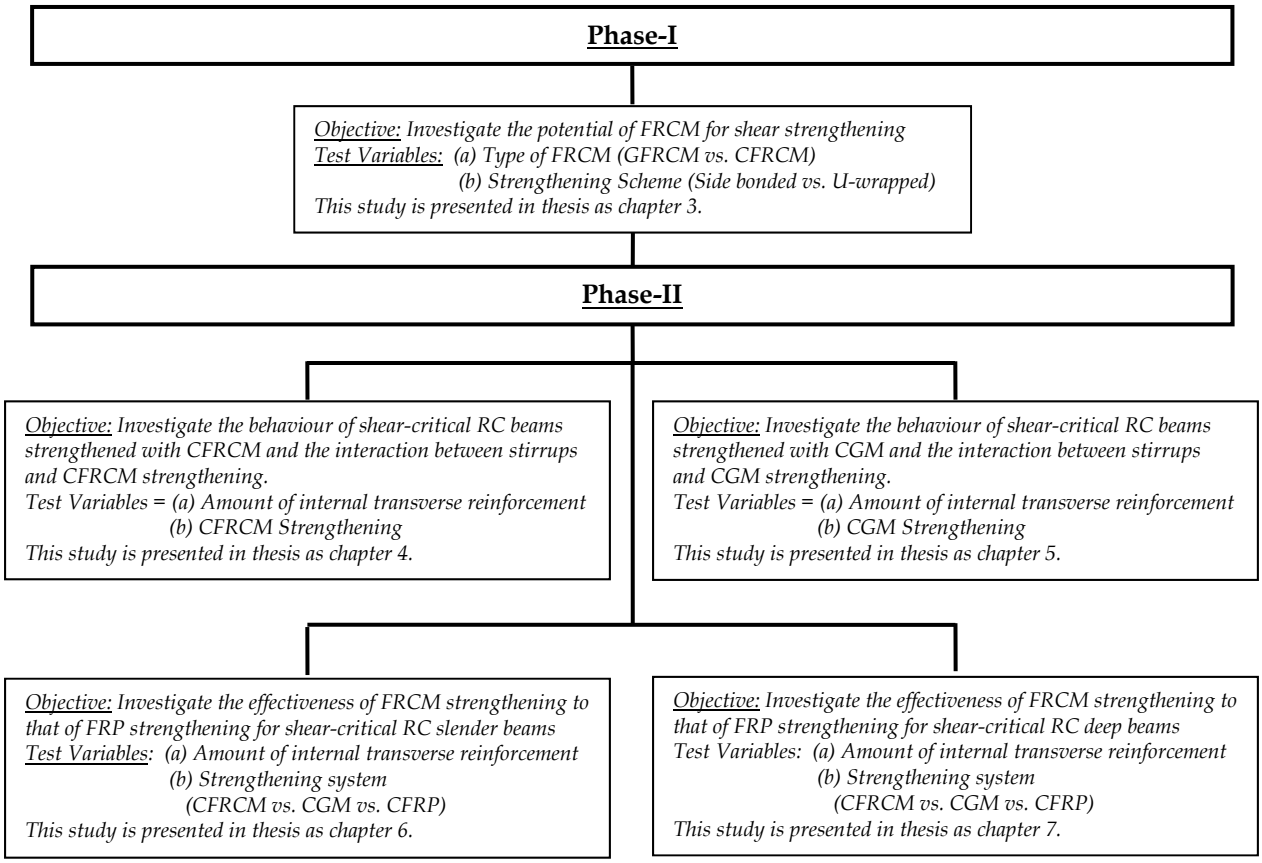

Figure 1.1 : Experimental program flow chart

The analytical portion of the research involved the evaluation of the existing models to predict the ultimate load of strengthened shear-critical RC beams and proposing

modifications to existing models to predict the ultimate load of FRCM strengthened shear-critical RC beams. Modified analytical models to predict the ultimate load of FRCM strengthened shear-critical RC deep and slender beams were validated against the Phase I and Phase II experimental results. The evaluation of the existing models and new modifications to existing models are presented along with the experimental results in chapters 3-7.

1.5 Organization of Thesis

The thesis is divided into eight chapters as follows:

Chapter-1: This chapter describes the problem statement, objectives of the research program, research approach and organization of the thesis.

Chapter-2: This chapter presents the background and literature review on strengthening of shear-critical RC beams with FRCM and FRP.

Chapter-3: This chapter presents the first published journal paper from this research. In this paper the effectiveness of different types of glass and carbon FRCMs (GFRCM, CFRCM1 and CFRCM2) to strengthen shear-critical RC was investigated.

Chapter-4: This chapter presents the second journal paper submitted from this research. This paper builds on paper 1. In this paper, the FRCM system that showed the best performance to strengthen shear-critical RC beams in paper 1 was investigated further.

In addition, the interaction between the internal transverse (shear) steel reinforcement and external strengthening was investigated.

Chapter-5: This chapter presents the third journal paper submitted from this research. This study builds on results of paper 1 and paper 2. In this paper, effectiveness of a new type of cement-based system (CFRP grid embedded in mortar (CGM)) to strengthen shear-critical RC beams was investigated.

Chapter-6: This chapter presents the fourth journal paper submitted from this research. In this paper, the effectiveness of cement-based strengthening systems (FRCM and CGM) was compared to that of the well-established FRP strengthening system for shear-critical RC beams.

Chapter-7: This chapter presents the fifth paper submitted from this research. In this paper, the effectiveness of both types of cement-based strengthening systems (FRCM and CGM) to strengthen RC deep beams was investigated in comparison to existing FRP system.

Chapter-8: This chapter presents the overall conclusions from this research, as well as recommendations for future studies.

Chapter 2: Background and Literature Review

2.1 Shear -Critical RC Beams

In general, RC beams fall into two categories: shear-critical RC beams and flexural critical RC beams. The flexural critical RC beams fail in a ductile manner compared to a sudden brittle failure in shear-critical RC beams. To avoid a sudden catastrophic shear failure and take advantage of the ductility possible in a flexural failure, RC beams are always designed as flexural-critical (Jumaat et al., 2011). However, certain situations could result in the occurrence of shear-critical RC beams such as: inaccuracy of the prevailing design standards, increase in applied loads, deterioration due to corrosion, and other conditions. Recent studies related to the size effect on RC beams indicated that during the late 20^{th} century major design standards overestimated the shear strength of RC beams and that beams considered to be flexural critical were actually shear-critical (Sneed et al., 2008, Sherwood et al., 2006). The studies on the effect of corrosion on RC beams have found that corrosion of transverse reinforcement results in significant reduction of the shear capacity in RC beams (Higgins et al., 2006 and Suffern et al., 2011). As a result, there is a need to find new methods to strengthen in-service shear-critical RC beams.

2.2 Mechanism of Shear Transfer

Shear in reinforced concrete beams is transferred by two load transfer mechanisms: beam action and arch action. The extent of the beam action and arch action depends on the shear span to depth ratio (a/d ratio). In general, beam action is the governing load transfer mechanism in slender beams (a/d ratio greater than 2.5) whereas arch action is the dominant load transfer mechanism in deep beams (a/d ratio less than 2.5). The two shear transfer mechanisms can be expressed mathematically as follows.

Consider a free body diagram of the portion of a reinforced concrete beam between two cracks as shown in Figure 2.1. The relationship between the shear force (V) and the tensile force in the bar (T) can be written as:

$$V = \frac{d}{dx}(TJd) \qquad \text{Equation 2.1}$$

$$\Rightarrow V = \frac{d(T)}{dx} + \frac{d(Jd)}{dx} \qquad \text{Equation 2.2}$$

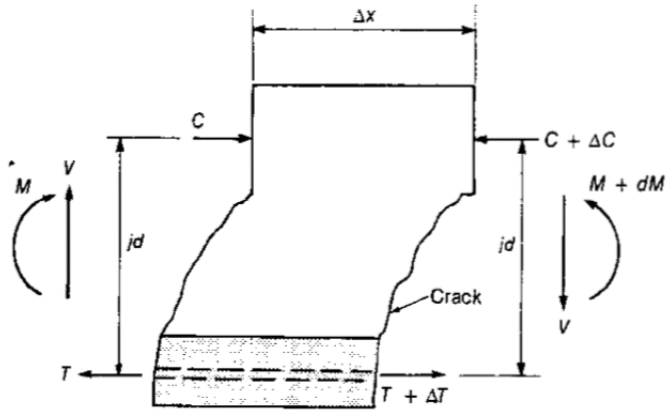

Figure 2.1 Free body diagram of beam between two cracks (MacGregor, 1997)

If the lever arm(Jd) remains constant as assumed in elastic beam theory, the shear force is transferred in beam action (V_b) as follows:

$$\frac{d(Jd)}{dx} = 0 \quad and \quad V = V_b = \frac{d(T)}{dx} \qquad \text{Equation 2.3}$$

Where $V = \frac{d(T)}{dx}$ is the shear flow across any horizontal plane between the reinforcement and the compression zone. For beam action to exist shear flow must be present.

On the other hand if the shear flow, $\frac{d(T)}{dx}$, equals zero, then the shear force is transferred to arch action(V_a) as follows:

$$V = V_a = \frac{d(Jd)}{dx} \qquad \text{Equation 2.4}$$

This happens when the reinforcing steel is unbonded and the shear flow cannot be transmitted, or when an inclined crack extend from the load point to the support

preventing the transfer of shear flow. In such cases, shear is transferred by arch action instead of beam action (MacGregor, 1997).

2.3 Strengthening of Shear-Critical RC Beams

2.3.1 Existing Techniques to Strength Shear-Critical RC Beams

Typical shear strengthening techniques include: section enlargement with additional transverse reinforcement, steel plate bonding and external post tensioning. These techniques have some draw backs such as time consuming, requirement of form work and labor intensive.

2.3.2 Strengthening of Shear-Critical RC Beams with FRP

In recent years, shear strengthening using advanced composite materials or fiber reinforced polymer (FRP) has gained popularity due to ease in installation and reduced construction time. FRP is a composite material that consists of fibers (carbon, glass, aramid or basalt) and a polymer matrix (epoxy or vinylester). FRP is manufactured in the form of bars, laminates and sheets. The laminates and bars are pre-cured, while the sheets are supplied dry and are impregnated with resin on site. To strengthened shear-critical RC beams, FRP sheets are used (Khalifa et al., 1998).

A large number of studies and field applications have been conducted to investigate the effectiveness of FRP sheets to strengthen shear-critical RC beams (Belarbi et al., 2011).

The effectiveness of FRPs to strengthen corroded shear-critical RC beams has also been highlighted in the literature (Azam and Soudki, 2012).

The factors that affect the FRP shear strengthening are presented in section 2.2.2.1. Existing models to predict FRP shear strength contribution are presented in section 2.2.2.2.

2.3.2.1 Factors Affecting Contribution from FRP Shear Strengthening

Bouselham and Chaallal (2004) reviewed an experimental database with over 100 tests on FRP shear strengthened RC beams and identified the following factors as the most important factors that affect the contribution from FRP shear strengthening: FRP material properties, internal transverse reinforcement, shear span to depth ratio, longitudinal reinforcement ratio and geometry of specimen. Recently, Belarbi et al. (2011) reviewed a large experimental database (over 500 tests) and identified some additional factors that influences the FRP shear strengthening contribution: concrete strength, fatigue loading, anchorage details, pre-cracking and pre-stressed concrete.

2.3.2.2 Models to Predict FRP Shear strength Contribution

A number of models have been reported in the literature to calculate the shear strength contribution from FRP strengthening. These models mainly use four conceptual approaches: the approach that use the experimentally determined limiting FRP stress/strain value (Al-Sulaimani et al., 1994 and Chajes et al., 1995), the effective strain

approach (Triantafillou, 1998; Khalifa et al., 1998; Khalifa and Nanni, 2000; Triantafillou and Antonopoulos, 2000), the approach that accounts for the non-linear strain in FRP over a shear crack (Chen and Teng, 2003a,b; Carolin and Taljten, 2005b) and a mechanics based approach (Monti and Loitta 2005).

Most FRP codes and design guidelines have adopted the model based on the effective strain approach. The effective FRP strain for fully wrapped beams is limited to 0.004 based on loss of aggregate interlock in concrete by ACI 440.2R 2008 and CAN/CSA-S6 2008. The model by Khalifa et al. (1998) is adopted for members failing by debonding of FRP sheet.

The ACI 440 procedure for calculating shear strength of FRP strengthened beams is presented in the following.

The shear strength contribution from FRP can be calculated using Equation 2.5 to Equation 2.7.

$$V_f = \frac{A_{fv} \cdot f_{fe}(sin\alpha + cos\alpha) d_{fv}}{S_f} \qquad \text{Equation 2.5}$$

$$A_{fv} = 2nt_f w_f \qquad \text{Equation 2.6}$$

$$f_{fe} = \varepsilon_{fe} E_f \qquad \text{Equation 2.7}$$

Where V_f is the shear strength contribution from FRP, A_{fv} is the area of FRP shear reinforcement with spacing S_f, f_{fe} is the effective stress in FRP (stress level attained at

section failure), α is the angle between FRP strip direction and longitudinal axis of member, d_{fv} is the effective depth of FRP shear reinforcement, S_f is the spacing of FRP shear reinforcement, n is the number of plies of FRP reinforcement, t_f is the nominal thickness of one ply of FRP reinforcement, w_f is the width of FRP reinforcing plies, ε_{fe} is the effective strain level in FRP reinforcement attained at failure and E_f is the tensile modulus of elasticity of FRP reinforcement.

The effective FRP strain for fully wrapped beams is limited to 0.004 based on loss of aggregate interlock in concrete by ACI 440.2R 2008. The effective FRP strain (ε_{fe}) for beams completely wrapped with FRP can be computed using Equation 2.8.

$$\varepsilon_{fe} = 0.004 \leq 0.75\varepsilon_{fu} \qquad \text{Equation 2.8}$$

For beams with side bonded or U-wrapped FRP, the effective FRP strain (ε_{fe}) can be computed using Equation 2.9 to Equation 2.13.

$$\varepsilon_{fe} = k_v\varepsilon_{fu} \leq 0.004 \qquad \text{Equation 2.9}$$

Where k_v is the bond reduction coefficient and ε_{fu} is the FRP rupture strain. The bond reduction coefficient (k_v) can be computed using Equation 2.10 to Equation 2.13 (Khalifa et al. 1998).

$$k_v = \frac{k_1 k_1 L_e}{11{,}900\varepsilon_{fu}} \leq 0.75 \ (in\ SI\ Units) \qquad \text{Equation 2.10}$$

$$L_e = \frac{23{,}300}{(n_f t_f E_f)^{0.58}} \leq 0.75\ (in\ SI\ units) \qquad \text{Equation 2.11}$$

$$k_1 = \left(\frac{f_c'}{27}\right)^{2/3} \quad (in\ SI\ Units) \qquad \text{Equation 2.12}$$

$$k_2 = \begin{cases} \dfrac{d_{fv} - L_e}{d_{fv}} & for\ U - wraps \\ \dfrac{d_{fv} - 2L_e}{d_{fv}} & for\ side\ bonded \end{cases} \qquad \text{Equation 2.13}$$

Where k_1 and k_1 are modification factors for the bond- reduction coefficient (k_v), L_e is the active bond length over which majority of bond stress is maintained, n_f is the modular ratio of elasticity between FRP and concrete (E_f/E_c), t_f is the nominal thickness of one ply of FRP reinforcement, E_f is the tensile modulus of elasticity of FRP reinforcement and f_c' is the specified compressive strength of concrete.

2.3.3 Strength Prediction for Strengthened Beams

In general, the additive approach is used to calculate the ultimate strength of strengthened shear critical RC beams. The total shear strength of RC beams is the sum of the shear strength contribution from concrete, the shear strength contribution from steel stirrups and the shear strength contrition from strengthening system. The shear strength contributions from the concrete and steel stirrups (strength of control unstrengthen beams) are calculated using the concrete design code approaches,

whereas the shear strength contribution from the strengthening system is determined using the truss analogy approach.

The truss analogy states that beams reinforced with stirrups can be analyzed as a truss. The tensile reinforcement in reinforced concrete beams is assumed as the tension chord and the compression zone (or compression reinforcement) is assumed as the top (compression) chord of the truss. Stirrups are assumed to be the vertical tension ties and the diagonal compressive stresses in the concrete are assumed to be the compression struts (Ritter, 1899). Morsch (1908 and 1922). The truss analogy is further simplified by assuming the angle between compression strut and the tension chord is 45˚. In the 45˚ truss model, the compression struts are assumed be a continuous field of diagonal compression instead of a discrete compression strut that starts from top of a stirrup and ends at the bottom of the next stirrups. The 45˚ truss model, along with forces and stresses are shown in Figure 2.2. The shear stresses are assumed to be uniformly distributed over an effective shear area of width, b_w, and effective depth, z (internal lever arm), of the cross section as shown in Figure 2.2 a.

The principal diagonal compressive stress (f_2) can be determined using equilibrium of forces as shown in Figure 2.2b. Since the total diagonal compressive force is $f_2.\left(b_w.\frac{z}{\sqrt{2}}\right)$ and the diagonal component of the shear force is $\sqrt{2}V$, the diagonal compressive stress (f_2) can be expressed as:

$$f_2 = \frac{2V}{b_w.z}$$ Equation 2.14

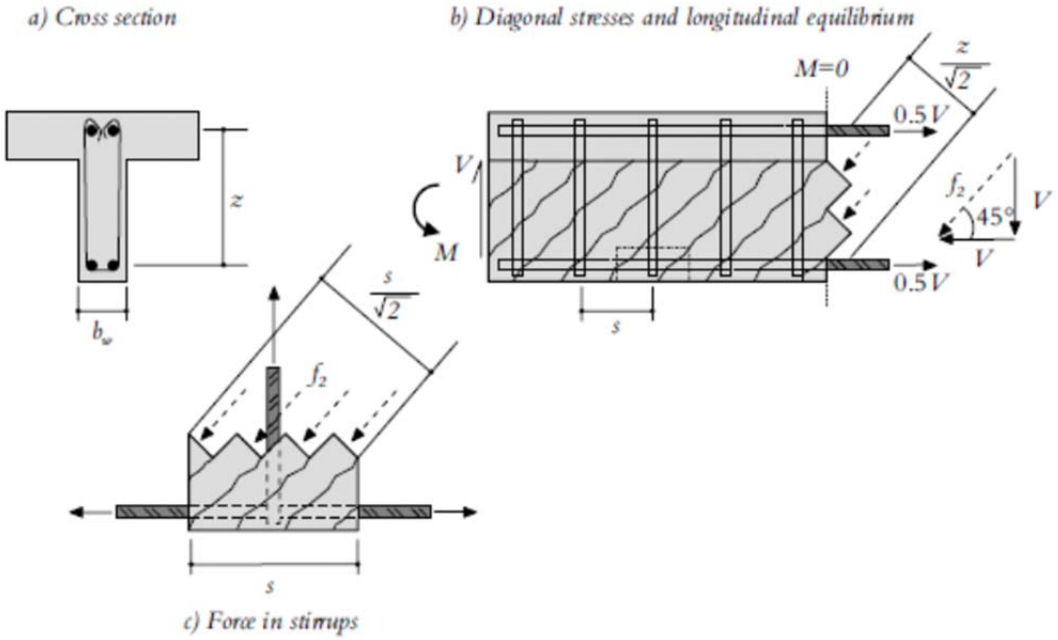

Figure 2.2 :45˚ Truss model (adopted from Blanksvard 2007)

To satisfy the equilibrium, the horizontal component of the compressive force (horizontal shear force) will be resisted by the longitudinal reinforcement as shown in Figure 2.2b. The vertical component of the compressive force will be resisted by the stirrups, $A_s f_y$. Taking the vertical component of the diagonal compressive force from Figure 2.2c, the tensile force in stirrups (Vs) will be:

$$V_s = \frac{A_s f_y . z}{s}$$ Equation 2.15

Equation 2.15 based on a 45˚ truss analogy is used in the current ACI Building Code for Structural Concrete (ACI 318-14) to determine the shear strength contribution from stirrups. Whereas the Canadian design code approach (CSA A23.3-04), also uses the truss analogy but the angle of compressive strut with tension chord is not taken as 45˚ and instead is treated as a variable to be determined using modified compression field theory. If the angle θ is considered as a variable in the truss model, the Equation 2.15 will take the form as:

$$V_s = \frac{A_s f_y . z \cot \theta}{s}$$ Equation 2.16

For the case of FRP strengthening, the ultimate condition is FRP sheet rupture or debonding rather than yielding of the steel stirrups. Triantafillou (1998) noted that FRP sheet used for FRP strengthening typically ruptures at a stress well below its ultimate strength due to stress concentration, and the corresponding strain at rupture should be considered as the effective strain for prediction and design purposes. This approach is used to determine FRP shear contribution in ACI 440 (2008) and ISIS Canada (2008). Considering a similar effective strain approach for FRCM, the shear strength contribution from FRCM (V_{FRCM}) strengthening can be computed.

2.4 Fiber Reinforced Cementitious Mortar (FRCM)

Fiber Reinforced Cementitious Mortar (FRCM) is a cement-based composite strengthening system that consists of fiber textile/grid/mesh and mortar. FRCM is an alternative strengthening/rehabilitation system to epoxy-based composite strengthening system (FRPs).

A number of cement-based composite strengthening systems has been developed; Textile Reinforced Concrete (TRC), Textile Reinforced Mortar (TRM), Fiber Reinforced Concrete (FRC), Mineral Based Composites (MBC) and Fiber Reinforced Cementitious Mortar (FRCM). All of these systems are conceptually similar with mortar used as the bonding agent. However, different fiber orientations are used in these cement-based strengthening systems; in TRC the fibers are placed in multi-directions, in FRC unidirectional continuous fiber sheet is used, and in the other cement-based systems (TRM, MBC and FRCM) fibers are placed in two orthogonal directions. In addition, the fibers used in the cement-based strengthening systems are either dry (TRC, TRM and FRC), or coated (FRCM) or impregnated with epoxy (MBC). The fibers are coated to improve their bond characteristics with the mortar. The epoxy impregnated fibers are stiffer than coated fibers and can only be placed on plane surfaces, whereas coated fiber grids are flexible and can be wrapped around corners. Thus, the systems with coated fibers may have a practical advantage over those with epoxy impregnated fibers for some applications.

Two types of mortars are commonly used in FRCM as a bonding agent: ordinary cement mortar and polymer modified mortar. Al-Salloum et al. (2012) compared the performance of polymer-modified mortar to that of cementitious mortar and concluded that polymer-modified mortar performs better in terms of enhancing the shear capacity of RC members.

The stress-strain behaviour of the FRCM system is essential to evaluate their performance for shear strengthening. For shear strengthening applications, not only the ultimate load of the FRCM matters but also the strain at ultimate load is important. Research conducted on the tensile behaviour of FRCM has revealed that they exhibit a non-linear stress strain behaviour which may be approximated as a tri-linear curve (Hegger et al., 2004). Figure 2.3 shows the typical stress strain curve of FRCM. In addition, due to cracking in the mortar of the FRCM, the ultimate strength is attained at a higher strain compared to FRP system (Hegger et al., 2004 and Hegger et al., 2006). Due to the non-linearity in their stress strain behaviour, FRCM are more comparable to shotcrete and ferrocement rather than FRP products (Ortlepp et al., 2006)

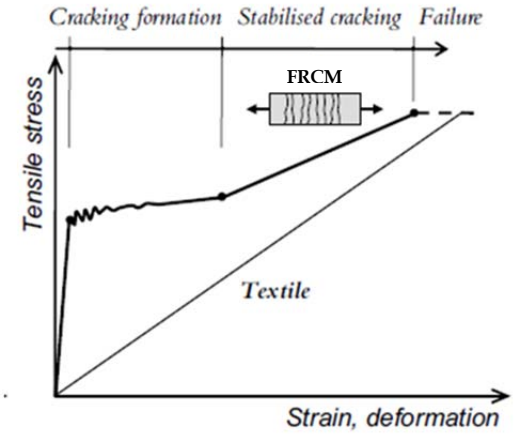

Figure 2.3: Typical stress strain behaviour of FRCM (adopted from Hegger et al., 2004)

2.5 Shear Strengthening of RC Elements with FRCM

2.5.1 Experimental Studies on Shear Strengthening of RC Elements with FRCM

A number of experimental studies have been reported in the literature to investigate the behaviour of RC beams strengthened in shear with FRCM. Table 2.1 presents a summary of available experimental studies. A review of these studies is presented in the following with a critical discussion and the gaps in the state-of-knowledge are highlighted.

Table 2.1: Summary of experimental studies

Author	Year	No. of tests	Geometry (T-shape or Rectangular)	Type of beams (slender or deep)	Strengthening scheme	Type of cement based system	Comments
Triantafillou et al.	2006	6	Rectangular	Slender	Fully wrapped	Carbon fiber textile with mortar	45% less effective than epoxy-based systems
Bruckner et al.	2006 & 2008	12	T-shape	Deep	U-wrapped (UW)	Glass fiber textile with mortar	A promising strengthening system
Blanksvard et al.	2009	23	Rectangular	Slender	Side bonded (SB)	CFRP grid with mortar	**Better than epoxy-based systems**
Al- Salloum et al.	2012	10	Rectangular	Deep	Side bonded	Carbon fiber textile with mortar	-
Tzoura E. et al.	2014	13	T-shape	Slender	U-wrapped (UW)	Carbon fiber textile with mortar	If system used with anchors, than marginally inferior to epoxy-vs. based systems
Escrig C. et al.	2015	9	Rectangular	Slender	Side bonded (SB)/U-warped (UW) or fully wrapped	Glass, basalt, carbon and PBO fibers in mortar	Further research needed to better understand strengthening response

Triantofillou et al. (2006) conducted an exploratory study to investigate the effectiveness of FRCM shear strengthening for RC members. The FRCM used in this study was denoted as textile reinforced mortar (TRM) that consisted of carbon fiber textile and polymer modified cementitious mortar. In addition, carbon fiber textile with epoxy, denoted as FRP, was tested for comparison purposes. The carbon fiber textile had a guaranteed tensile strength of 3350 MPa and elastic modulus of 225 GPa. The weight of the carbon textile was 168 g/m^2. The clear spacing between the rovings of the textile was 6 mm in both directions. A commercially available polymer modified mortar with cement to polymer ratio of 10:1 and binder to water ratio of 3:1 was used.

The variables examined in the study were: the type of bonding agent (epoxy vs. mortar), number of TRM/FRP strengthening layers (one or two), method of wrapping (conventional vs. spiral) and type of loading (static and cyclic).A total of six beams were tested: one control unstrengthened beam, two beams strengthened with one composite layer (TRM or FRP), two beams strengthened with two composite layers (TRM or FRP) and one beam strengthened with two spirally wrapped TRM layers. Two beams strengthened with one strengthening layer (FRP/TRM) were tested under cyclic loading, whereas the remaining four beams were tested monotonically. All beam specimens were 300 mm deep, 150 mm wide, and 2600 mm in length and were simply supported over a clear span of 2200 mm. The shear span to depth ratio for all beams was 2.8. Both the tension and compression reinforcement consisted of 3-16 mm bars.

The internal shear reinforcement consisted of 5.6 mm diameter stirrups at 230 mm c/c. The shear spans of five beams were completely wrapped with TRM/FRP.

The three beams strengthened with two composite layers (TRM or FRP) failed by flexure. The two beams strengthened with one composite layer (TRM or FRP) failed by either flexure (FRP) or shear (TRM). The TRM strengthening was 45% less effective compared to FRP. The strengthening effect increased with an increase in the number of composite layers. The authors concluded that TRM system is promising for shear strengthening of RC members; however more studies are required to optimize the mortar used in the TRM and to better understand the mechanics of this strengthening system. It is important to note that the findings in this study were based on beams that were tested under cyclic loading and the observed difference in the effects of strengthening could be related to the type of loading.

Bruckner et al. (2006 & 2008) investigated the performance of FRCM for shear strengthening of RC beams. The FRCM used consisted of alkali-resistant glass fiber textile with cementitious bonding agent and was denoted as textile reinforced concrete (TRC). The glass fiber textile had fibers in multi directions and a tensile strength of 560 MPa. The weight of the glass textile was 470 g/m^2. Fine grained concrete with a compressive strength of around 80 MPa was used as bonding agent. A total of twelve T-shaped beams were tested: three identical control beams, three beams strengthened with TRC without mechanical anchorage with different number of TRC layers (2, 4 and

6), three beams strengthened with TRC with mechanical anchorage type-1 with different number of TRC layers (2, 4 and 6) and three beams strengthened with TRC with mechanical anchorage type-2 with different number of TRC layers (3, 3 and 4). The beams were 550 mm deep with a flange width of 480 mm, a web width of 120 mm and a flange depth of 120 mm. The tensile reinforcement consisted of 6-20 mm bars and the compression reinforcement consisted of 8-12 mm bars. The internal shear reinforcement consisted of 8 mm diameter stirrups spaced at 100 mm or 200 mm c/c. The beams were 2400 mm long and simply supported over a clear span of 2000 mm. The entire span of beam was strengthened with U-wrapped TRC. The specimens were tested in three-point bending with a shear span to depth ratio of about 2.1. The test variables included the number of textile layers (2, 3, 4, and 6), presence of mechanical anchorage (without anchorage and with anchorage) and different anchorage methods.

The results showed that the load carrying capacity of the beams was increased by TRC strengthening; however, in order to fully utilize the TRC strengthening, mechanical anchorage is needed. The load carrying capacity of the strengthened beams was increased by 17% with the application of two or four TRC layers without mechanical anchorage, whereas the increase in strength was 33 % with the application of four TRC layers with mechanical anchorage.

It should be noted that the three control beams failed at different loads (476 kN, 590 kN and 577 kN). The authors used the control beam with lowest failure load in the

comparison with the strengthened beams. If the strengthened beams were compared with the average failure load of the control beams, then the strengthening results are not promising.

Blanksvard et al. (2009) investigated the behaviour of shear-critical RC beams strengthened with FRCM. The FRCM used consisted of carbon fiber grids with cementitious bonding agent and was denoted as Mineral Based Composite (MBC). The carbon fiber grids had a tensile strength of 3800 MPa and elastic modulus of 253 GPa. The weight of the carbon grids ranged between 66 to 159 g/m^2. Three types of mortars were used as bonding agent: one cementitious mortar with compressive strength of 22 MPa and two polymer based mortars with compressive strengths of 45 and 77 MPa. A total of twenty three beams were tested. All beam specimens were 500 mm deep, 180 mm wide, and 4500 mm in length and were simply supported over a clear span of 4000 mm. The tension and compression reinforcement consisted of 12-16 mm bars and 2-16 mm bars, respectively. In order to force the failure in one shear span, the beams were heavily reinforced with stirrups in one shear span compared to the other span. 12 mm diameter stirrups spaced at 100 mm c/c were used in the heavily reinforced shear span compared to either no stirrups or 10 mm diameter stirrups at 250 mm and 350 mm c/c in the test shear span. Only the test span was strengthened with side bonded MBC layer. The test variables included the concrete strength (49 MPa, 56 MPa and 74 MPa), amount of stirrups (no stirrups, 10 mm diameter stirrups @250 mm and 10 mm

diameter stirrups @350 mm), type of mortar (three different mortars with different amount of polymer and fibers), and the type of CFRP grid (three types of grids with different spacing and carbon amount (66g/cm^2, 98g/cm^2, and 159 g/cm^2). Two beams were also strengthened with an FRP system to compare them with the performance of MBC system. The beams were tested in four-point bending with a shear span to depth ratio of 3.0.

The results demonstrated that the MBC strengthening system was better compared to FRP system. The authors concluded that using mortar with a high modulus of elasticity performs better compared to a mortar with a low modulus of elasticity as a bonding agent. The CFRP grids with higher fiber content had higher failure loads. CFRP grids with small grid spacing performed better compared to those with large grid spacing. The authors were unable to conclude the effect of amount of stirrups on the effectiveness of MBC strengthening since almost all of the MBC strengthened beams containing stirrups failed by flexure. No conclusion was made on the effect of concrete strength on the effectiveness of MBC strengthening since all MBC strengthened beams cast with 76 MPa concrete failed by flexure. The remaining beams had almost the same concrete strength 49 and 56 MPa as opposed to the intended concrete strength of 35 MPa and 50MPa. The MBC strengthened beams that failed in shear exhibited rupture of the carbon fibers because the concrete strengths were high and the fiber content of the CFRP grids was too low to cause peeling failure.

This study revealed that FRCM shear strengthening exhibited favorable response compared to FRP strengthening. The study had a large number of full-scale specimens; however it was not well designed. Half of the specimens (beams containing stirrups) failed by flexure and thus their results were not conclusive. The concrete strengths of the beams were high (50 MPa or higher), and as such no peeling failures were obtained. If lower concrete strength (25MPa - 30MPa) was used peeling failure (bond failure) may have occurred which might have helped understand the effect of concrete strength on the effectiveness of FRCM. This study was a good exploratory study that highlighted the potential of FRCM shear strengthening but nevertheless, more research is needed.

Al-Salloum et al. (2012) investigated the effectiveness of FRCM strengthening to increase the shear resistance of RC beams. The FRCM used in this study consisted of basalt textile with cementitious bonding agent and was denoted as textile reinforced mortar (TRM). The basalt fiber textile had a tensile strength of 623 MPa and elastic modulus of 31.9 GPa. The weight of the textile was not reported by the authors. Two types of mortars were used as bonding agent: cementitious mortar with compressive strength of 24 MPa and polymer modified mortar with compressive strength of 56 MPa. A total 10 small scale RC beams were tested. The beams were 200 mm deep, 150 mm wide and 1500 mm in length. The test variables included: the type of mortar (cementitious vs. polymer modified cementitious), the number of TRM layers (2 or 4) and the textile/grid orientation in the shear spans (0˚/90˚ or 45˚/-45˚). The beams were

tested in four-point bending with shear span to depth ratio of 2.5. The test results indicated that the shear strength of RC beams increased when strengthened with basalt-based TRM; the increase in strength ranged between 36-86% for 2-4 TRM layers. It was also observed that a polymer modified cementitious mortar performed slightly better than cementitious mortar and that the 45˚/-45˚ orientation of textile showed better shear resistance than 0˚/90˚ orientation when four TRM layers were applied. The shortcoming of the above study is that it was performed on very small scale specimens.

Tzoura et al. (2016) investigated the effectiveness of U-shaped FRCM for shear strengthening of RC T beams. The FRCM used in this study was denoted as textile reinforced mortar (TRM) that consisted of carbon fiber textile and polymer modified cementitious mortar. In addition, carbon fiber textile with epoxy was denoted as FRP. The carbon fiber textile had a guaranteed tensile strength of 3375 MPa and elastic modulus of 225 GPa. The weight of light and heavy carbon textile was 174 g/m^2 and 348 g/m^2, respectively. The clear spacing between the rovings of the textile was 3 mm in one direction and 10 mm in other direction. A commercially available polymer modified mortar with binder to water ratio of 5:1 was used.

A total of thirteen beams were tested. The test variables included the cyclic loading, fixed support conditions, types of textiles, the number of TRM layers (1 or 2), use of anchors and TRM vs. FRP. To simulate the fixed boundary condition of a beam near a column support, a beam column connection was tested. The test results indicated that

the increase in ultimate load of TRM strengthened beam without anchors was not proportional. TRM strengthened beams without anchors were 50% as effective as FRP strengthened beams without anchors. However, TRM strengthened beams with anchors were marginally less effective compared to FRP strengthened beams with anchors.

Escrig et al. (2015) investigated the effectiveness different types of FRCM for shear strengthening of RC beams. The FRCM used in this study was denoted as textile reinforced mortar (TRM) that consisted of different types of fiber textile and cementitious mortars.

A total of nine beams were tested. The beams were 300 mm deep, 300 mm wide and 1700 mm in length. The test variables included: types of fiber textiles (glass, basalt, carbon and PBO), strengthening scheme (side bonded, u wrapped or fully wrapped). The beams were tested in three-point bending with shear span to depth ratio of 2.5 - 2.8. The test results indicated that the shear strength of RC beams increased on average 36 % when strengthened with TRM.

It should be noted that, in this study, TRM strengthening layer was applied over partial shear span (450 mm) close to the support compared as opposed to the more common application to the full shear span (800 mm). Most of the beams experienced a major shear crack close to mid span where there was no strengthening layer. As a result, contribution of TRM strengthening to load carrying capacity is less than expected.

All of the studies on cement-based strengthening systems found in the literature were exploratory studies. Most of the previous work was conducted on small-scale specimens. It is well known that the shear behaviour of RC beams is significantly affected by size of the specimens. The reported results are contradictory: some studies concluded that FRCM shear strengthening is better that FRP while others concluded that FRCM shear strengthening was significantly less effective compared to FRP strengthening. Also, in two studies a number of strengthened beams failed by flexure as opposed to expected shear failure. Therefore, there is need for a detailed study on shear strengthening of large-scale RC beams strengthened with FRCM.

2.5.2 Analytical Studies on Shear Strengthening of RC Elements with FRCM

A limited number of analytical models have been reported in the literature to predict the ultimate strength of shear-critical RC beams strengthened with FRCM. A review of these models is presented in this section along with a critical evaluation of their applicability. The gaps in the state-of-knowledge on modeling the shear behaviour of RC beams strengthened with FRCM are also highlighted.

The existing models to calculate the ultimate strength of shear-critical RC beams strengthened with FRCM use the additive approach:

$$V_u = V_c + V_s + V_{FRCM} \qquad \text{Equation 2.17}$$

Where V_c is the concrete is shear contribution, V_s is the steel stirrup contribution and V_{FRCM} is the FRCM shear strength contribution.

In the models, V_c and V_s are calculated using the existing code provisions for RC beams, and different expressions are proposed for the shear contribution from FRCM. As is the case for FRP shear strengthening, the FRCM shear strength contribution is based on the well-known truss analogy.

Triantafillou and Papanicolaou (2006) proposed Equation 2.18 to calculate the shear strength contribution from FRCM. The equation considers that the textile (fiber grid) is mainly made of continuous fiber rovings in two orthogonal directions.

$$V_{FRCM} = \sum_{i=1}^{2} \frac{A_{ti}}{S_i} (\varepsilon_{te,i} E_{ib}) 0.9d(cot\theta + cot\beta_i) sin\beta_i \qquad \text{Equation 2.18}$$

Where $\varepsilon_{te,i}$ is the effective strain of FRCM in direction i; E_{ib} is the elastic modulus of fibers; d is the effective depth of section; A_{ti} is twice the cross sectional area of each roving in the direction i; S_i is the spacing of roving along member axis, θ is the angle between shear crack and member axis and β_i is the angle between continuous fiber roving and member axis.

The authors adopted the effective strain approach used for FRP systems by multiplying the effective strain of the FRP with an effectiveness coefficient to obtain the effective strain of FRCM ($\varepsilon_{te,i}$).

Blanksvard et al., 2009 proposed a simple approach to calculate the shear strength contribution from FRCM, presented in Equation 2.19 to Equation 2.22.

$$V_{FRCM} = V_{FRP} + V_{MBA} \qquad \text{Equation 2.19}$$

Where V_{FRCM} is the shear strength contribution for FRCM, V_{FRP} is the shear strength contribution from vertical tows of the fiber grid and V_{MBA} is the shear strength contribution from the mortar. The shear strength contribution from fiber grid is given in Equation 2.13-2.14.

$$V_{FRP} = \frac{2.\varepsilon_{ver,ef}.E_{ver}.A_{ver}.h_{ef}.cot\theta}{S_{ver}} \qquad \text{Equation 2.20}$$

$$\varepsilon_{ver,ef} = \frac{2}{3}.\boldsymbol{\varepsilon_{ver,ult}} \qquad \text{Equation 2.21}$$

Where $\varepsilon_{ver,ef}$ is the effective strain of the fiber grid tows in the vertical direction; E_{ver} is the elastic modulus of the vertical FRP grid tow; A_{ver} is the area of one fiber tow in the vertical direction; h_{ef} is the effective height of section; S_{ver} is the spacing of vertical FRP grid tows; θ is the angle between shear crack and member axis; $\varepsilon_{ver,ult}$ is the ultimate strain of the fiber grid tows in the vertical direction. The shear strength contribution from the mortar is given in Equation 2.15.

$$V_{MBA} = \frac{1}{3}t_{MBA,tot}.h_{ef}.f_{MBA,t} \qquad \text{Equation 2.22}$$

Where $t_{MBA,\,tot}$ is the total thickness of the mineral-based bonding agent (mortar); h_{ef} is the effective height of section and $f_{MBA,t}$ is the tensile strength of mineral-based bonding agent (mortar).

Both models presented above use the effective strain approach that is typically used for FRP systems. Triantafillou and Papanicolaou (2006) proposed an effectiveness coefficient to be multiplied with the effective FRP strain to obtain the effective strain of FRCM. The authors obtained the effectiveness coefficient based on the experimental results of two beams (one strengthened with FRP and the other strengthened with FRCM). Blanksvard (2009) multiplied the ultimate strain of the CFRP grid with a reduction factor to obtain the effective strain in the FRCM. The reduction factor was obtained as the ratio between the maximum shear stress to the average shear stress in a rectangular section. It is worth mentioning that the equations for the effective strain of FRP at failure were obtained based on regression analysis of a large data base. In case of FRCM, only very limited test data is available and so there is a need to expand the existing data or explore other mechanics-based design approaches.

2.6 Summary

The literature review has revealed that FRCM shear strengthening is a promising repair technique for RC members. However, very limited research has been conducted on this topic and almost all of the previous work is exploratory.

The existing studies have reported contradictory results: Triantifillou and Papanicolaou (2006) found that FRCM is 45% less effective compared to FRP while Blanksvard et al. (2009) found that FRCM is more effective than FRP. Triantifillou and Papanicolaou (2006) used dry carbon fiber textiles embedded in mortar whereas Blanksvard et al. (2009) used CFRP grid embedded in mortar. The different types of FRCM system could have been the cause of the contradictory results. It should be noted that the system used by Blanksvard et al. (2009) can only be applied on the sides of specimens while the system used by Triantifillou and Papanicolaou (2006) can be applied around the beam cross-section as U or full wraps. The results of these exploratory studies are used to calculate the effective strain used in analytical models.

There are gaps in the state–of-the-art understanding of the behaviour of shear-critical RC beams strengthened with FRCM. The behaviour of FRCM strengthened shear-critical RC with different span to depth ratios is not fully understood. Therefore, it can be concluded that before we can fully utilize FRCM in shear strengthening of RC beams, there is need to conduct a comprehensive study on understanding the mechanism of FRCM shear strengthening of large-scale RC beams. In particular, the effect of the effect of internal transverse reinforcement and the effect of shear span to depth ratios (slender vs. deep beams) on the behaviour of FRCM shear strengthening of RC beams should be examined.

Chapter 3: FRCM Strengthening of Shear-Critical RC Beams

This chapter has been published in the Journal of Composites for Construction, American Society of Civil Engineering (ASCE), Volume 18, No. 5, 2014.

The contributing authors are:

Azam, R. and Soudki, K.

Contributors to this chapter include: -

Rizwan Azam: Ph.D. candidate, who researched, analyzed, and wrote the paper.

Khaled Soudki: Supervisor to Rizwan Azam and assisted with research direction, editing, and general advice.

3.1 Introduction

In general, RC beams fall into two categories: shear-critical RC beams and flexural critical RC beams. The flexural critical RC beams fail in a ductile manner compared to the sudden brittle failure in shear-critical RC beams. To avoid sudden catastrophic shear failure, RC beams are always designed as flexural critical (Jumaat et al., 2011). However, certain situations could result in shear-critical RC beams such as: inaccuracy of the prevailing design standards, increases in design loading due to changed use, deterioration due to corrosion, and other conditions. Recent studies related to the size effect on RC beams indicated that during the late 20th century major design standards overestimated the shear strength of RC beams and that beams considered to be flexural critical were actually shear-critical (Sneed et al., 2008, Sherwood et al., 2006). A recent survey of the shear strength of RC members constructed without stirrups has indicated that there are structures in service with an increased probability of experiencing shear failure (Collins et al., 2008). The studies on the effect of corrosion on RC beams have found that corrosion of transverse reinforcement may result in a significant reduction of the shear capacity in RC beams (Higgins et al., 2006 and Suffern et al., 2011). As a result, there are a significant number of in-service shear-critical RC members that may require shear strengthening.

Fiber reinforced polymer (FRP) systems have been applied to strengthen and repair many reinforced concrete (RC) members worldwide. A number of studies reported in

the literature have demonstrated the effectiveness of FRPs to strengthen shear-critical RC members (ACI 440.2R 2008, Belarbi et al. 2011). However, the use of epoxy as a bonding agent in FRPs has some drawbacks: poor compatibility with concrete substrate, diffusion tightness, hazardous working environment for manual workers, and most importantly post-repair inspections and assessment of the structure become difficult since the FRP effectively hides the conditions underneath the repair system.

The fabric reinforced cementitious matrix (FRCM) composite system is a relatively new strengthening and rehabilitation system. FRCM has all the benefits (such as light weight, easy to install and non-corroding characteristics) of typical FRP systems, but overcomes some of the draw backs (such as poor compatibility with concrete substrate, diffusion tightness, non-applicability on wet surfaces and fire resistance) of using a epoxy as bonding agent in FRP system; FRCM replaces epoxy with cementitious mortar and fiber sheets with fabric/textiles. FRCM is also known as textile reinforced concrete (TRC) and textile reinforced mortar (TRM).

Few studies have been conducted to investigate the effectiveness of FRCM to strengthen shear-critical RC beams (Al-Salloum et al., 2012; Blanksvard et al., 2009; Bruckner et al., 2008; Bruckner et al., 2006; Triantafillou et al., 2006). Different type of FRCMs were used in these studies including: carbon fabric reinforced cementitious matrix, CFRCM (Triantafillou et al., 2006), glass fabric reinforced cementitious matrix, GFRCM

(Bruckner et al., 2008; Bruckner et al., 2006), and basalt fabric reinforced cementitious matrix, BFRCM (Al-Salloum et al., 2012).

Triantofillou et al. (2006) conducted an experimental study to investigate the effectiveness of CFRCM shear strengthening for RC beams. The CFRCM used in this study was denoted as textile reinforced mortar (TRM) that consisted of carbon fabric and polymer modified cementitious mortar. In addition, carbon fabric with epoxy was denoted as FRP. The variables examined in the study were: the type of bonding agent (epoxy vs. mortar), number of TRM/FRP strengthening layers (one or two), method of wrapping (conventional vs. spiral) and type of loading (static and cyclic). A total of six beams were tested: one control un-strengthened beam and five strengthened beams. Two beams were tested under cyclic loading, whereas the remaining four beams were tested monotonically. Test results revealed that the TRM strengthening was 45% less effective compared to the FRP system. The authors concluded that the TRM system is promising for shear strengthening of RC members, although they suggested that more studies are required to optimize the mortar used in the TRM and to better understand the mechanics of this strengthening system.

Bruckner et al. (2006 & 2008) investigated the performance of GFRCM for shear strengthening of RC beams. The GFRCM used consisted of alkali-resistant glass fabric with cementitious bonding agent and was denoted as textile reinforced concrete (TRC). A total of twelve T-shaped beams were tested: three identical control beams and nine

strengthened beams. The test variables included the number of fabric layers (2, 3, 4, and 6), presence of mechanical anchorage (without anchorage and with anchorage) and different anchorage methods. The results showed that the load carrying capacity of the beams was increased by TRC strengthening; however, in order to fully utilize the TRC strengthening, mechanical anchorage was needed. The load carrying capacity of the strengthened beams was increased by 17% with the application of two or four TRC layers without mechanical anchorage, whereas the increase in strength was 33 % with the application of four TRC layers with mechanical anchorage.

Al-Salloum et al. (2012) investigated the effectiveness of BFRCM strengthening to increase the shear resistance of RC beams. The FRCM used in this study consisted of basalt fabric with cementitious bonding agent and was denoted as textile reinforced mortar (TRM). A total of 10 RC beams were tested. The test variables included: the type of mortar (cementitious vs. polymer modified cementitious), the number of TRM layers (2 or 4) and the fabric orientation in the shear spans (0˚/90˚ or 45˚/-45˚). The test results indicated that the shear strength of RC beams increased when strengthened with basalt-based TRM; the increase in strength ranged between 36-86% for 2-4 TRM layers. It was also observed that a polymer modified cementitious mortar performed slightly better than cementitious mortar, and that the 45˚/-45˚ orientation of the textile showed better shear resistance than 0˚/90˚ orientation when four TRM layers were applied.

The literature review has revealed that FRCM shear strengthening is a promising repair technique for RC members. However, very limited research has been conducted on this topic. Therefore, there is a need for further investigation of the effectiveness of FRCM strengthening for shear-critical RC beams. There is also a need to evaluate the applicability of the existing FRP design guidelines for the shear strengthening of RC beams using FRCM systems.

3.2 Test Program

A total of seven reinforced concrete beams were tested: one control unstrengthened beam and six strengthened beams. The test variables included the strengthening material (glass FRCM (GFRCM), and carbon FRCM (CFRCM-1, CFRCM-2)) and the strengthening scheme (side bonded and u-wrapped). The test matrix is given in Table 3.1.

Table 3.1: Test matrix

Strengthening scheme	Strengthening material			
	None	GFRCM	CFRCM-1	CFRCM-2
Control (unstrengthened)	1	-	-	-
Side bonded	-	1	1	1
U-wrapped	-	1	1	1

3.2.1 Test Specimens

The details of the beam specimens are presented in Table 3.2 and Figure 3.1. All beams were 150 mm wide, 350 mm deep and 2400 mm long. The longitudinal tensile

reinforcement in all of the beams was 2-25M bottom bars. The side and vertical covers to the tension reinforcement were kept at 30 mm for all beams. The beams were not provided with shear reinforcement, although three stirrups were provided in the anchorage zone for the longitudinal reinforcement.

The beam designation used in this study is as follows: YY-ZZ with YY = strengthening scheme and ZZ= strengthening material. The strengthening scheme is specified as C (control), SB (side bonded) and UW (U-wrapped) and the strengthening material is specified as N (none), GT (glass fabric/textile), CT1 (carbon fabric/textile-1), and CT2 (carbon fabric/textile-2).

Table 3.2: Details of test specimens (pilot study)

Sr. No.	Beam Designation	Target f_c' (MPa)	Longitudinal Reinforcement			Shear Reinforcement		Comment
			Amount of Rebar	ρ (%)	ρ/ρ_b	Internal Steel	External FRCM/FRP	
1	C-N	35	2-25M	2.17	0.50	None	None	
2	UW-G	35	2-25M	2.17	0.50	None	GFRCM (U-Wrapped)	Glass grid
3	SB-G	35	2-25M	2.17	0.50	None	GFRCM (side bonded)	Glass grid
4	UW-C1	35	2-25M	2.17	0.50	None	CFRCM-1 (U-Wrapped)	Carbon grid-1
5	SB-C1	35	2-25M	2.17	0.50	None	CFRCM-1 (side bonded)	Carbon grid-1
6	UW-C2	35	2-25M	2.17	0.50	None	CFRCM-2 (U-Wrapped)	Carbon grid-2
7	SB-C2	35	2-25M	2.17	0.50	None	CFRCM-2 (side bonded)	Carbon grid-2
8	UW-CS	35	2-25M	2.17	0.50	None	CFRP (U-Wrapped)	Carbon sheet

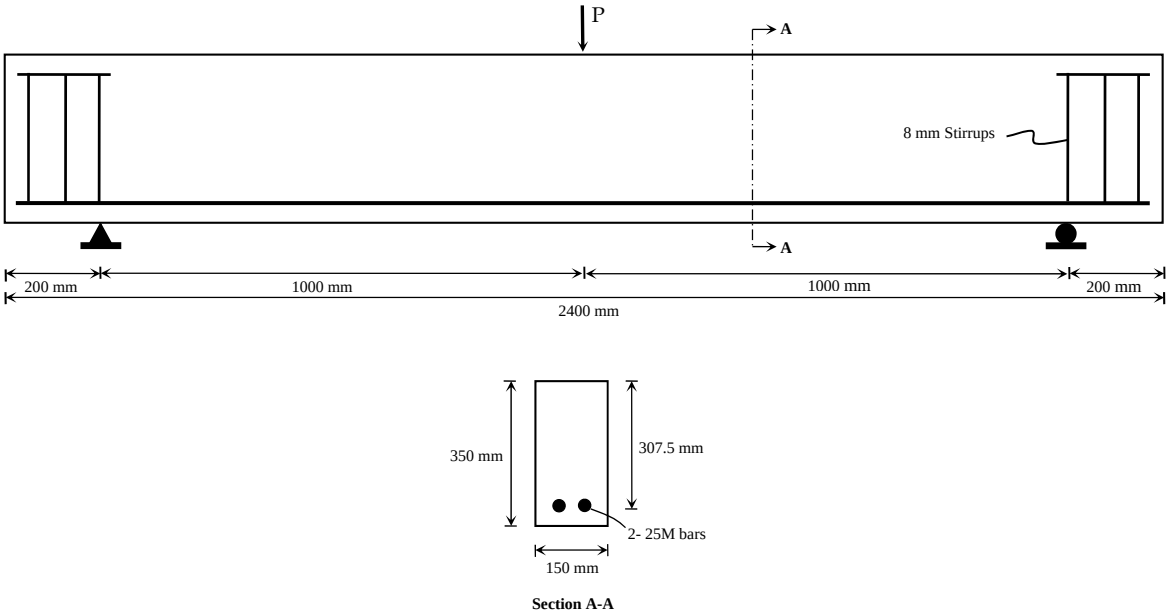

Figure 3.1: Beam specimen geometry and reinforcement details (pilot study)

3.2.2 Material Properties

The concrete used to fabricate the test beams was supplied by Hogg Ready-mix concrete. The concrete was batched with Type GU portland cement with a maximum coarse aggregate size of 19 mm and a water cementing material ratio of 0.45. Six concrete cylinders (100 mm x 200 mm) were also cast from the same concrete batch. The 28 day compressive strength of the concrete was 37.5 ± 2 MPa. Grade 400 reinforcing steel bars were used as longitudinal reinforcement: 25M bars as tensile reinforcement and 8 mm stirrups in the anchorage zone. The longitudinal steel had yield strength of 480 MPa as reported by the supplier.

Three different fabrics (textiles) were used in the FRCM strengthening layer: glass fabric/ textile (GT), carbon fabric/ textile-1 (CT1) and carbon fabric/textile-2 (CT2) (Figure 3.2). The glass fiber used to make the glass fabric/textile (GT) had a tensile strength of 2300 MPa (measured on roving), tensile modulus (nominal) of 75 GPa and an elongation at break of 2.8% (measured on roving). The carbon fibers used to make the carbon fabric/textile (CT1 and CT2) had a tensile strength of 3800 MPa, tensile modulus of 230 GPa and an elongation at break of 1.6%. The manufacturer provided geometrical and mechanical properties of the fabrics/ textiles as reported in Table 3.3. The glass fabric/ textile (GT) had an ultimate tensile strength of 100 kN/m in both directions. The weight of the GT was 350 g/m^2. The orthogonal spacing of the fiber tows in GT was 15.7 x 10.1 mm. The carbon fabric/textile-1 (CT1) had an ultimate strength of 135 kN/m and 105 kN/m in the longitudinal and transverse direction, respectively. The weight of CT1 was 270 g/m^2. The orthogonal spacing of the fiber tows in CT1 was 30 x 30 mm. The carbon fabric/textile-2 (CT2) had an ultimate strength of 325 kN/m and 250 kN/m in longitudinal and transverse direction, respectively. The weight of CT2 was 609 g/m^2. The orthogonal spacing of the fiber tows in CT2 was 10 x 18 mm. It is important to note that fabrics/ textiles used in this study were Styrene-butadiene rubber (SBR) coated. The weight of coating ranged between 15-20% of total weight of the fiber textiles.

Table 3.3 : Geometric and mechanical properties of fiber textiles used in FRCM systems

Fiber Textile	Weight* (g/m^2)	Spacing of fiber tows (mm)	Tensile Strength (kN/m)		Tensile** Modulus (GPa)	Ultimate** elongation (%)
			Longitudinal	Transverse		
Glass fabric/textile (GT)	350	15.7 x 10.1	100	100	75	2.8
Carbon fabric/textile -1 (CT1)	270	30 x 30	135	105	230	1.6
Carbon fabric/textile -2 (CT2)	609	10 x 18	325	250	230	1.6

* Weight of textiles includes 15-20 weight of coating.

**Tensile modulus and ultimate elongations are measured on rovings.

Sika Monotop 623, polymer modified, one component, and early strength-gaining cementitious mortar was used as the bonding agent in the FRCM composite layer. The compressive strength of the mortar was measured using 50 mm cubes. The compressive strengths of the mortar at 3, 7 and 28 days were 41±3.3, 45±2.4 and 58±2.8 MPa, respectively.

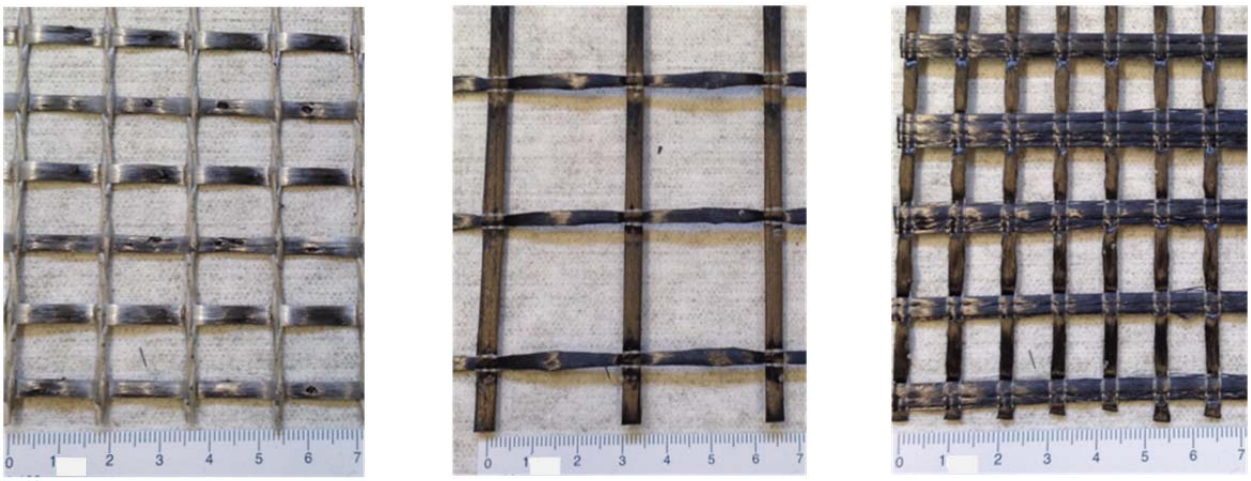

(a) (b) (c)

Figure 3.2 : Types of fiber textiles (a) glass fiber textile (b) carbon fiber textile-1 (c) carbon fiber textile-2

3.2.3 FRCM Strengthening

Six beams were strengthened with three types of FRCM; two beams were strengthened with each type of textile, one side bonded and one u-wrapped. The entire span length of the beam was strengthened with FRCM. The FRCM strengthening procedure followed the manufacturer's specifications and is shown in Figure 3.3.

The concrete surfaces were sand-blasted to expose the aggregates. The edges of the beam cross section were rounded to a radius of 12 mm. Water was sprayed on the dry concrete surfaces of the beams until saturated surface dry (SSD) condition was achieved. Once the SSD condition was achieved, the first layer of mortar was applied. After the application of the first layer of mortar, the fabric was pressed into the mortar. The fabrics were applied in such a way that the direction of stronger fabric tows is

perpendicular to the longitudinal axis of the beam. Then a final layer of mortar was applied to completely cover the fiber textile. Finally, the beam surface was finished with a trowel. Total thickness of the strengthening system was about 6-8 mm.

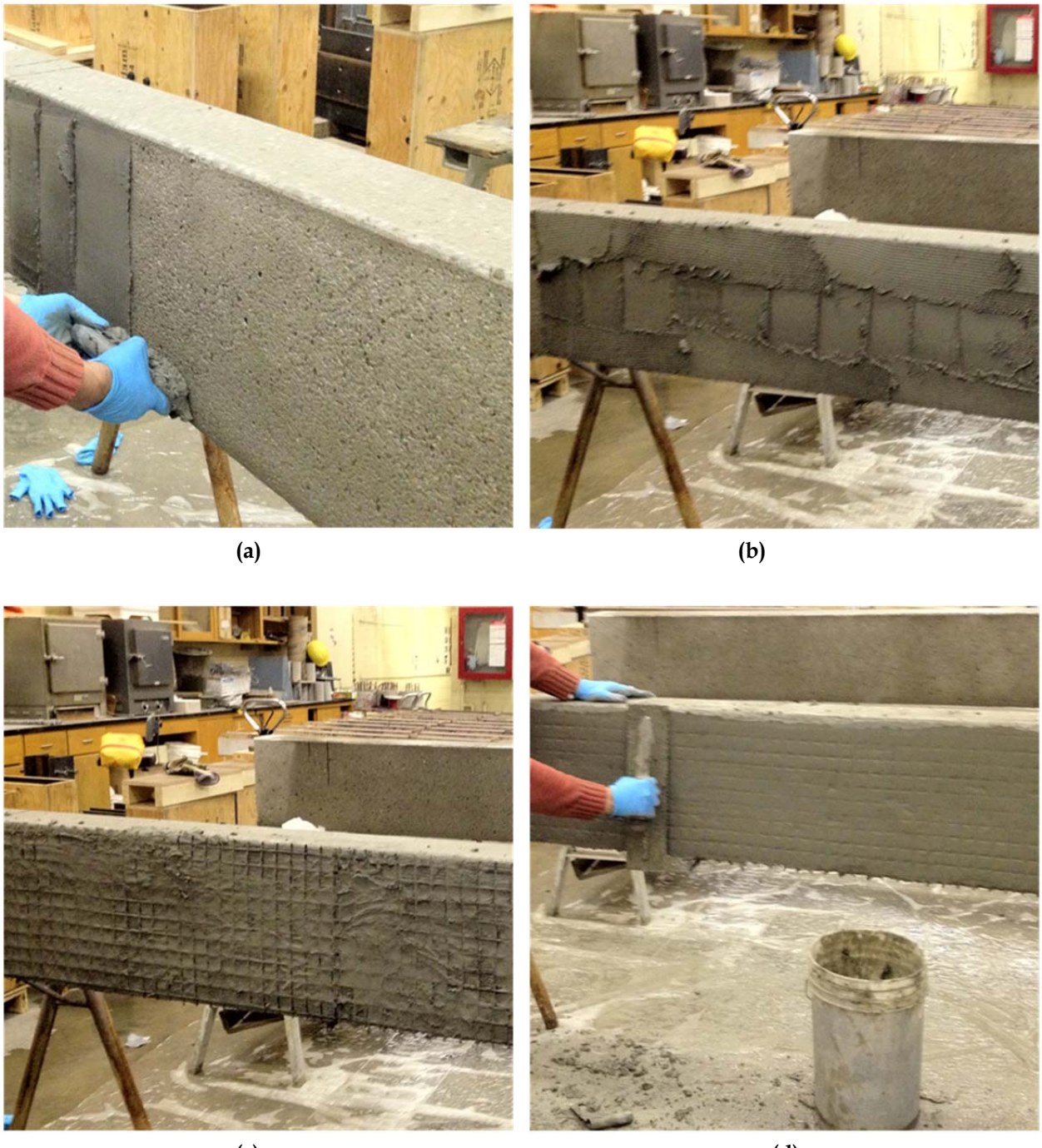

Figure 3.3 : FRCM strengthening procedure (a) application of mortar (b) beam with first layer of mortar (c) beam with grid inserted in mortar (d) finishing after application of second layer of mortar

3.2.4 Instrumentation

All tested beams were instrumented with one strain gauge (5 mm gauge length) mounted on the longitudinal bar at mid span and one strain gauge (60 mm gauge length) mounted on the concrete surface under the loading point. One linear variable differential transducer (LVDT), with a range of 0-25 mm, was placed at mid-span to measure the deflection of the beam. Figure 3.4 shows the layout of the instrumentation.

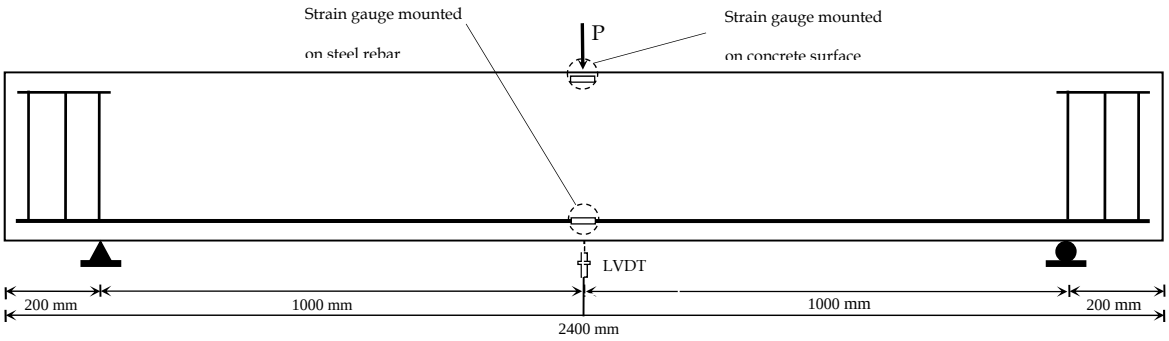

Figure 3.4 : Details of instrumentation

3.2.5 Test Setup and Procedure

The beams were tested in three-point bending with a clear span to depth ratio of 3.25. The beams were simply supported with roller and hinge supports over a clear span of 2000 mm. The load was transferred from the actuator to the beam through a single point loading plate at mid-span. To uniformly distribute the load, the loading plate was potted to the beam using hydro-stone. The test setup is shown in Figure 3.5.

The test procedure was as follows: the beam was placed over the supports, leveled and centered under the point load system. LVDT was mounted at mid-span under the point load. Then the instrumentation (LVDT and strain gauges) was connected to the data acquisition system. The data acquisition system started gathering data before the application of load. The load was increased monotonically at a stroke rate of 0.2 mm/sec using a ramp function generator until failure of the beam. During the test, the initiation and progression of cracks were monitored.

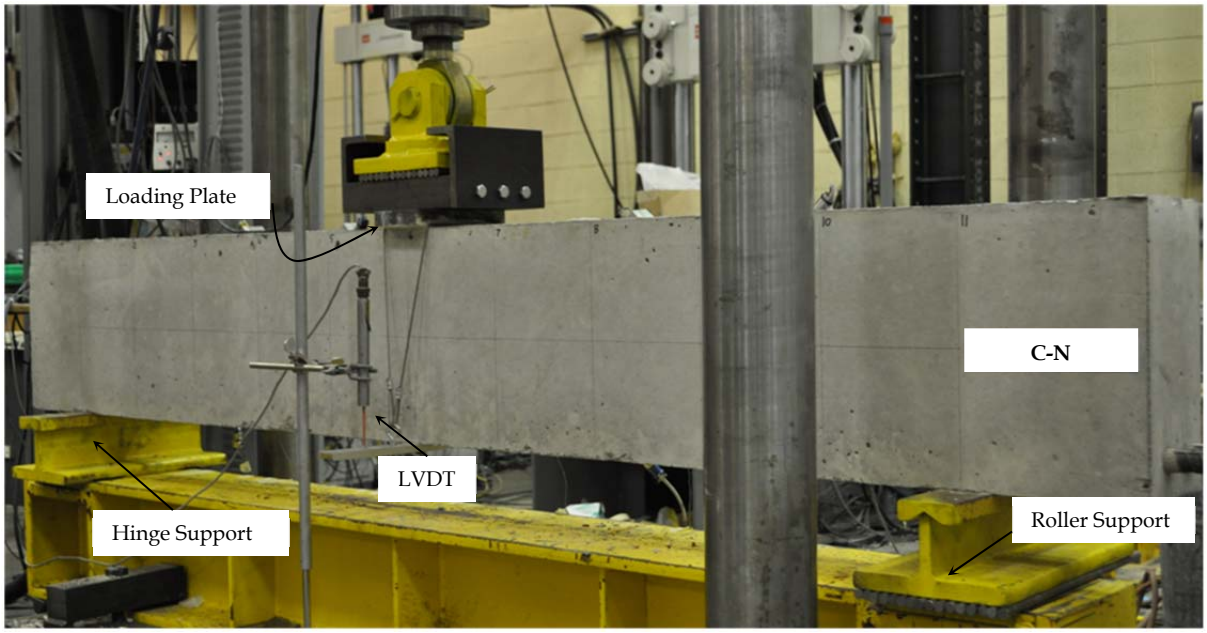

Figure 3.5 : Test setup

3.3 Test Results and Discussion

A summary of test results is given in Table 3.4. In general, the FRCM shear strengthening significantly increased the ultimate load carrying capacity of the shear-

critical RC beams. The increase in ultimate load ranged between 19 to 105% over the control unstrengthened beam. The FRCM shear strengthening significantly increased the deflection at ultimate load of the strengthened beams compared to the control (unstrengthened) beam. The deflection at ultimate load in FRCM strengthened beams ranged between 4.3 mm to 12.6 mm compared to a deflection of 3.9 mm in the control (unstrengthened) beam, representing a maximum increase of 220%. All beams failed in shear as expected, and this can be confirmed by the tensile strain in longitudinal steel bar and compressive strain in concrete; at failure, the strain values in longitudinal steel bar were below the yield strain (2400με) and the strain values in the concrete were below the crushing strain (3500με) in all cases. The structural behavior of the beams is discussed in terms of load-deflection response and failure modes in the following sections.

Table 3.4 : Summary of test results

Beam designation	Tested fc′ (MPa)	Inclined cracking load (kN)	Ultimate load (kN)	Increase in ultimate load (%)	Deflection at ultimate load (mm)	Strain in longitudinal reinforcement at midspan (με)	Concrete strain at midspan (με)	Failure mode
C-N	38	120	123.5	-	3.9	956	778	DT
SB-GT	38	140	146.3	19	4.3	1119	1042	DT
UW-GT	38	135	180.2	46	8.2	1377	1615	DT
SB-CT1	38	144	155.5	26	5.8	1233	1307	DT
UW-CT1	38	138	151.8	23	5.9	1378	2014	DT
SB-CT2	38	154	245.4	99	12.6	2038	2912	SC→DB
UW-CT2	38	154	253.4	105	10.8	2186	2444	SC→DB

Failure mode is specified as DT (diagonal tension) and SC→DB (shear compression-debonding)

3.3.1 Load-Deflection Response

The effects of the FRCM strengthening (material type and strengthening scheme) on the structural behavior of shear-critical RC beams are presented in Figure 3.6 and **Error! Reference source not found.**. In general, the load-deflection response of the FRCM strengthened beams was almost bilinear indicating the brittle nature of shear failure. The FRCM shear strengthening slightly increased the stiffness of the strengthened beams compared to the control (unstrengthened) beams. The maximum increase in stiffness was for beams strengthened with CFRCM-2 (11% increase) followed by beams strengthened with CFRCM-1 (9% increase).

Figure 3.6(a) shows the effect of the type of strengthening material (GFRCM, CFRCM-1 and CFRCM-2) on the load-deflection response of beams strengthened with side bonded FRCM compared to control unstrengthened beam. The control unstrengthened beam exhibited almost linear load-deflection response compared to bilinear load-deflection response in strengthened beams. The load-deflection response of beams strengthened with side bonded GFRCM and CFRCM-1 was bit jagged. The possible reasons for this jagged load-deflection response of these beams are (1) low amount of fibers in these fabrics/textiles and (2) slippage of fabric/textiles tows in mortar. The control (unstrengthened) beam failed at a load of 123.5 kN. The beams that were strengthened with side bonded GFRCM, CFRCM-1 and CFRCM-2 failed at ultimate loads of 146 kN, 156 kN and 245 kN, respectively. This represents an increase in ultimate load of 19%, 26% and 99% in beams strengthened with side bonded GFRCM-1, CFRCM-1 and CFRCM-2, respectively. This was consistent with the strengths of fabric/textiles used in GFRCM, CFRCM-1 and CFRCM-2 of 100kN/m, 135kN/m and 325kN/m, respectively. The beams strengthened with side bonded FRCM experienced higher deflections at ultimate load compared to control unstrengthened beam. The deflection at ultimate load in beams strengthened with side bonded FRCM ranged between 4.3 mm to 12.6 mm compared to a deflection of 3.9 mm in control unstrengthened beam representing an increase of 10% to 220%.

Figure 3.6(b) shows the effect of the type of strengthening material (GFRCM-1, CFRCM-1 and CFRCM-2) on load-deflection response on beams strengthened with u-wrapped FRCM. The load-deflection response of beams strengthened with u-wrapped FRCM was almost similar to the load-deflection response of beams strengthened with side bonded beams. The control (unstrengthened) beam failed at a load of 123.5 kN compared to a failure load of 180 kN, 152 kN and 253 kN in beams strengthened with u-wrapped GFRCM, CFRCM-1 and CFRCM-2, respectively. This corresponds to 46%, 23% and 126% increase in ultimate strength of beams strengthened with u-wrapped GFRCM, CFRCM-1 and CFRCM-2, respectively. This was consistent with the ultimate strengths of fabrics used in these systems except for beam strengthened with u-wrapped GFRCM. This is possibly due to different cracking pattern observed in this beam which resulted in different load carrying mechanism after shear cracking. The beams strengthened with FRCM exhibited higher deflections at ultimate load compared to control unstrengthened beam. The deflection at ultimate load in beams strengthened with u-wrapped FRCM ranged between 5.9 mm to 10.8 mm compared to a deflection of 3.9 mm in control unstrengthened beam representing an increase of 50% to 175%.

Figure 3.7a, b and c show the effect of the strengthening scheme on the load-deflection response of beams strengthened with GFRCM, CFRCM-1 and CFRCM-2, respectively. It was expected that in case of side bonded beams the shorter bond length of a composite layer would result in premature debonding failure of the FRCM composite in these

beams compared to u-wrapped beams. However, none of the FRCM strengthened beams failed by debonding of the composite layer; no major difference in the structural behavior was observed between the two strengthening schemes. This could be attributed to the better bond performance of the FRCM composite to the concrete substrate in comparison to that typically observed for FRP composites. The beam strengthened with u-wrapped CFRCM-1 showed an identical load-deflection behavior to the beam strengthened with side bonded CFRCM-1. The beam u-wrapped with CFRCM-2 experienced a slight increase (6%) in the ultimate load and post shear cracking stiffness compared to the beam with side bonded CFRCM-2. In contrast, the beam with u-wrapped GFRCM had a 26% higher ultimate load and 90% higher ultimate deflection compared to the beam with side bonded GRFCM. The reason is the differences in observed cracking pattern between the beams with u-wrapped vs. side bonded GFRCM which allowed the u-wrapped to carry load long after the appearance of shear cracks. The beams with side bonded GFRCM beams experienced steeper main shear crack which quickly reached load point to cause diagonal tension failure. The beam with U-wrapped GFRCM experienced shallower main shear crack which tend to flatten near load point and hence resulted in higher ultimate load carrying capacity. The beam with U-wrapped GFRCM continued to carry load even after shear cracks were wide enough to disrupt load transfer by aggregate interlock, indicating that the load carrying mechanism had changed to arch action.

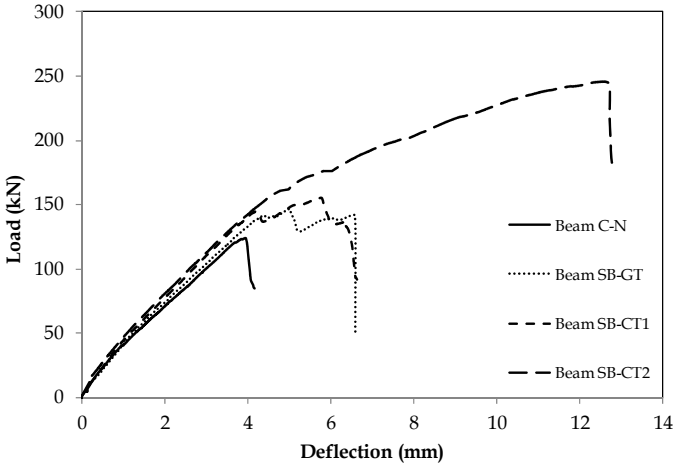

(a)

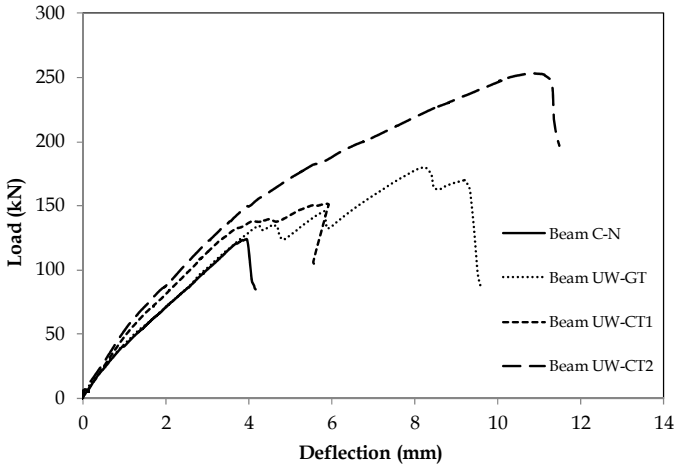

(b)

Figure 3.6 : Effect of strengthening material (a) side bonded specimens (b) u-wrapped specimens

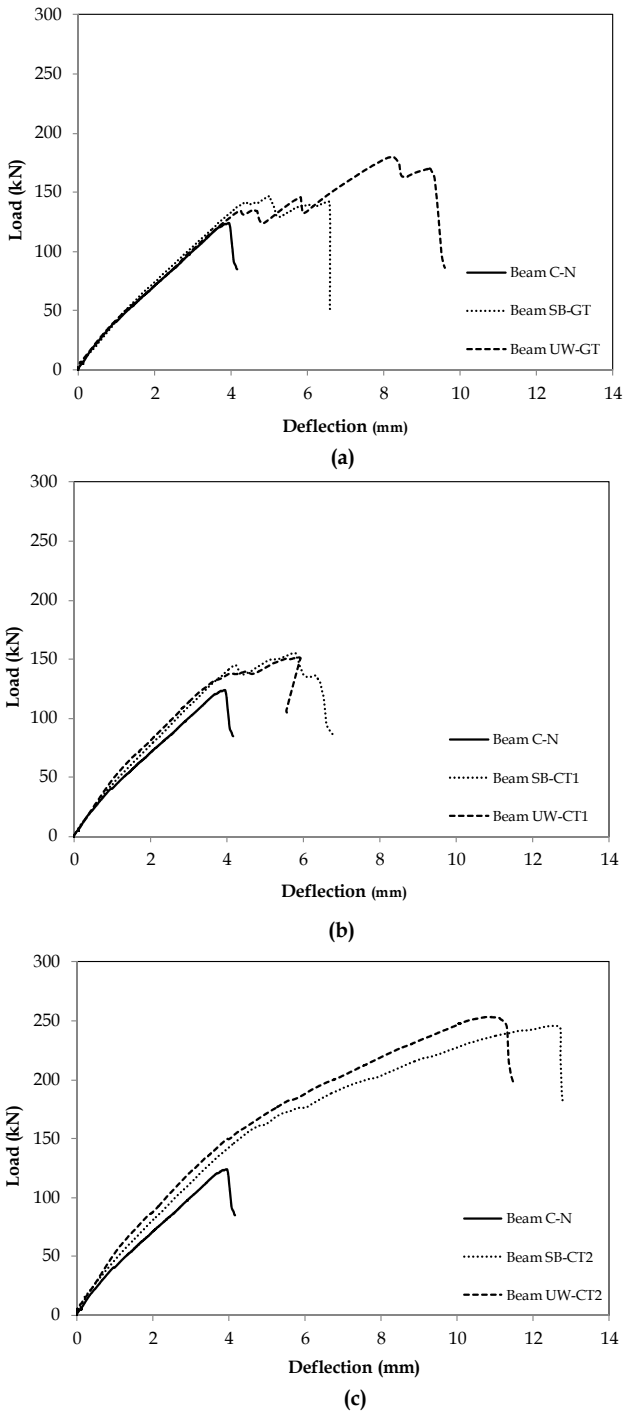

Figure 3.7 : Effect of strengthening scheme (a) beams strengthening with GFRCM (b) beams strengthening with CFRCM-1 (c) beams strengthening with CFRCM-2

3.3.2 Failure Modes

Typical failure modes for all beams are shown in Figure 3.8. The control unstrengthened beam failed by diagonal tension failure as did the beams strengthened with GFRCM and CFRCM-1, while a shear compression-debonding failure was observed in beams strengthened with CFRCM-2. The failure of the control beam by diagonal tension failure is shown in Figure 3.8a. The cracking in the control beam was initiated with the appearance of flexural cracks at mid span under the concentrated load. As the load increased, a single inclined crack appeared in the shear span which progressed towards the load point and support region leading to a diagonal tension failure. The failure mode of beams strengthened with GFRCM and CFRCM-1 are shown in Figure 3.8b and c, respectively. The cracking pattern of these beams was similar to the control beam; the cracking initiated with the appearance of flexural cracks and then a sudden single shear crack resulted in failure of these beams. The beams strengthened with CFRCM-2 failed by shear compression failure as shown in Figure 3.8d. The cracking pattern of these beams was different from the beams strengthened with GFRCM and CFRCM-1 with a number of shear cracks followed by flexural cracks. In addition, the shear cracking load of beams strengthened with CFRCM-2 was higher than that of the beams strengthened with GFRCM and CFRCM-1 (Table 3.4). This may be attributed to higher fiber content in CFRCM-2 compared to CFRCM-1 and GFRCM.

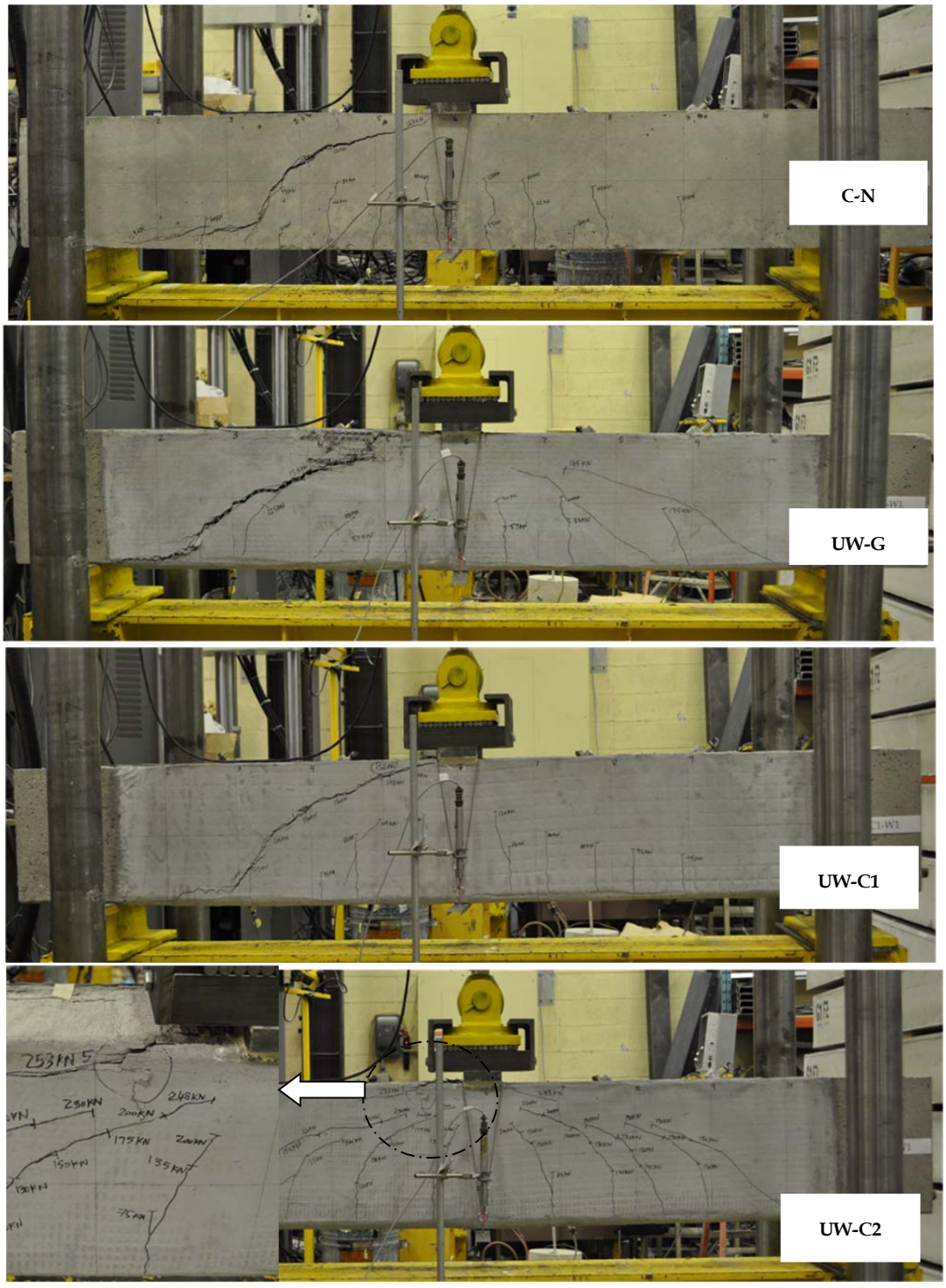

Figure 3.8 : Failure Modes

The failure in the CFRCM-2 strengthened beams was initiated by crushing of the concrete in the compression zone as can be seen in Figure 3.8d. The slippage of the fiber tows of the fabric/textile in mortar resulted in shear crack propagation towards the compression zone, causing crushing of the concrete at the tip of the crack. The crushing of concrete resulted in debonding of the CFRCM-2 composite layer.

3.4 Comparison between Experimental and Analytical Results

The total shear strength of strengthened RC beams is the sum of the shear strength contribution from concrete (V_c), the shear strength contribution from steel stirrups (V_s) and the shear strength contribution from externally bonded strengthening material, FRCM (V_{FRCM}) as follows:

$$V_u = V_c + V_s + V_{FRCM} \qquad \text{Equation 3.1}$$

For simplicity, it is generally assumed that the externally bonded strengthening material does not influence the shear strength contribution from concrete (V_c) and steel (V_s). Hence, the shear strength contribution from concrete (V_c) and steel (V_s) can be calculated using concrete design guidelines such as ACI 318-08, CSA S6-06 and CSA A23.3-04. The shear strength contribution from externally bonded materials (FRP sheets or FRCM) is determined using a similar truss analogy approach to that used for steel stirrups. The only difference is the stress level used in these materials: yield stress is used for the steel stirrups, while the effective stress is used for the FRP and FRCM. The

effective stress for FRP is the lesser of (1) the effective stress based on debonding of FRP sheet, or (2) the effective stress based on the aggregate interlock limit. In the case of FRCM, the effective stress is only dependent on the aggregate interlock limits as debonding of the FRCM layer is not expected. The following sections present different FRP design guidelines along with proposed modifications to predict the shear strength contribution from the FRCM strengthening system.

3.4.1 ACI 440.2R 2008

The ACI 440.2R (2008) provisions to calculate the shear strength contribution from externally bonded FRP are based on a 45˚ truss analogy approach as follows:

$$V_f = \frac{A_f f_{fe} . (sin\alpha + cos\,\alpha) . d_{fv}}{s_f} \qquad \text{Equation 3.2}$$

where $A_f = 2. t_f. w_f =$ cross section area of the FRP sheet ; $f_{fe} = \varepsilon_{fe} E_f$ = effective FRP stress; ε_{fe} is the effective FRP strain; E_f is the elastic tensile modulus of FRP sheet; d_{fv} is the internal level arm; α is the angle of orientation of FRP sheet with longitudinal axis. The effective FRP strain for fully wrapped beams is limited to 0.004 and the effective FRP strain for u-wrapped or side bonded beams is calculated based on FRP to concrete bond mechanism.

Tensile tests on FRCM have revealed that the main failure mode of FRCM is slippage of the fabric tows in the mortar (Arboleda et al. 2012). The bond of mortar with concrete is

stronger than the bond of the fibers in the mortar. As a result, shear-critical RC beams strengthened with FRCM will fail by slippage of the fabric tows in the mortar instead of FRCM debonding. This indicates that the FRP strain limits based on FRP to concrete bond are not applicable for FRCM strengthened shear-critical RC beams. However, the effective FRP strain limit based on aggregate interlock (0.004) is still applicable, and for the current study the shear strength contribution from the FRCM is calculated based on the effective strain limit of 0.004.

3.4.2 CAN/CSA-S6 2006

The CAN/CSA-S6 (2006) provisions to calculate the shear strength contribution from externally bonded FRP are similar to those in ACI 440.2R (2008) except that the CSA S6 provisions are based on the variable angle truss model as follow:

$$V_f = \frac{A_f.E_f.\varepsilon_{fe}.d_f.(cot\theta + cot\alpha).sin\alpha}{s_f} \qquad \text{Equation 3.3}$$

where, θ is the angle of the shear crack measured using general method (based on modified compression filed theory) presented in CSA A23.3-04. In the current study, the effective strain limit of 0.004 based on aggregate interlock was used to calculate the shear strength contribution from FRCM.

3.4.3 Analytical Results

The RC beams in this study did not contain steel stirrups, and hence there was no V_s contribution. The shear contribution from concrete was calculated using CSA A23.3-04. The shear strength contribution from FRCM strengthening was calculated using the ACI 440.2R (2008) and CAN/CSA-S6 (2006) provisions for externally bonded FRP sheets. For analysis purposes, equivalent design thicknesses were calculated for all type of fabrics/textiles based on their ultimate load per width, ultimate strain and tensile modulus. The equivalent design thicknesses for glass textile (GT), carbon textile-1(CT1) and carbon textile-2 (CT2) were 0.0476 mm, 0.0367mm and 0.0883 mm, respectively.

The comparison between the experimental and predicted ultimate loads is presented in Table 3.5. The predicted ultimate load for the control beam correlates very well with the experimental ultimate load with experimental to predicted ultimate load ratio of 1.06. It can be seen from Table 5 that the predicted ultimate loads of the strengthened beams using ACI 440.2R (2008) and CAN/CSA S6 (2006) were in reasonable correlation with experimental ultimate loads. The average ratio of experimental to predicted ultimate load was 1.11 with a coefficient of variation of 0.14. For, CAN/CSA S6 (2006) the average ratio of experimental to predicted ultimate load was 0.97 with a coefficient of variation of 0.15. This analysis shows that the existing FRP design approaches given by ACI 440.2R (2008) and CAN/CSA S6 (2006) can be used to predict the shear contribution from FRCM strengthening with the modification that the effect of

debonding can be neglected when determining the ultimate strain limit for the FRCM system.

Table 3.5 : Comparison between experimental and predicted ultimate loads

Beam designation	Experimental ultimate load, P_{exp} (kN)	Predicted Results								
		CSA A23.3-04 (θ=33)			ACI 440.2R 2008 (θ = 45)			CAN/CSA-S6 2006 (θ=33)		
		V_C (kN)	Ultimate Load, P_{pre}	P_{exp} / P_{pre}	V_{FRCM} (kN)	Ultimate Load, Ppre	P_{exp} / P_{pre}	V_{FRCM} (kN)	Ultimate Load, P_{pre}	P_{exp} / P_{pre}
C-N	123.5	58	116	1.06	-	-	-	-	-	-
SB-GT	146.3	58	-	-	9.0	134.0	1.10	14.0	144	1.02
UW-GT	180.2	58	-	-	9.0	134.0	1.34	14.0	144	1.25
SB-CT1	155.5	58	-	-	21.3	158.6	0.98	32.8	181.6	0.86
UW-CT1	151.8	58	-	-	21.3	158.6	0.96	32.8	181.6	0.84
SB-CT2	245.4	58	-	-	51.2	218.4	1.12	79.0	274	0.90
UW-CT2	253.4	58	-	-	51.2	218.4	1.16	79.0	274	0.92
Mean							1.11			0.97
Coefficient of Variation, %							0.14			0.15

*Predicted ultimate load, $P_{pre} = 2 (V_C + V_{FRCM})$

3.5 Conclusions

The effectiveness of FRCM composite system to strengthen shear-critical RC beams was investigated through testing of seven RC beams. The test variables included the type of FRCM and the strengthening scheme. The experimental results were also compared with theoretical predictions using FRP design guidelines in North America (ACI 440.2R 2008 and CAN/CSA-S6 2006). The main findings of this investigation are summarized as follows:

- The FRCM system significantly enhanced the ultimate load carrying capacity of shear-critical RC beams. The maximum increase in ultimate load was 105% for beams strengthened with u-wrapped CFRCM-2, and the lowest increase in ultimate load was 19% for beams strengthened with side bonded GFRCM.
- The FRCM system slightly increased the stiffness of the strengthened beams compared to the control (unstrengthened) beams. The maximum increase in stiffness was for beams strengthened with CFRCM-2 (11% increase) followed by beams strengthened with CFRCM-1 (9% increase).
- Side bonded vs. u-wrapped FRCM exhibited similar performance in terms of strength and failure modes. This suggests that the bond of the FRCM with the concrete substrate is sufficient that u-wrapping may not be required. This is in contrast to most FRP fabric strengthening systems were u-wrapping is required for adequate bond.

Chapter 4: Strengthening of Shear-Critical RC Beams with CFRCM

This chapter will be submitted to a peer reviewed journal for publication.

The contributing authors are:

Azam, R., Soudki, K. and Jeffrey S. West

Contributors to this chapter include: -

Rizwan Azam: Ph.D. candidate, who researched, analyzed, and wrote the paper.

Khaled Soudki: Supervisor to Rizwan Azam; Deceased September 17, 2013

Jeffrey S. West: Supervisor to Rizwan Azam and assisted with research direction, editing, and general advice.

4.1 Introduction

In recent years, shear strengthening using advanced composite materials such as fiber reinforced polymer (FRP) systems has gained popularity due to the ease of installation and reduced construction time. Fiber reinforced polymer (FRP) systems have been applied to strengthen and repair many reinforced concrete (RC) members worldwide. A number of studies reported in the literature have demonstrated the effectiveness of FRPs to strengthen shear-critical RC members. ACI 440.2R (2008) and Belarbi et al. (2011) are excellent sources of information on shear strengthening using FRPs. The effectiveness of FRPs to strengthen corroded shear-critical RC beams has also been reported in the literature (Azam and Soudki, 2012, Azam and Soudki 2013). In spite of its wide use and effectiveness, the use of epoxy as a bonding agent in FRP strengthening systems may not be optimal for some applications due to poor compatibility with concrete substrate, limited or no moisture diffusion, requirement for special handling/protection equipment for manual workers, and most importantly because of post-repair inspections and assessment of the structure become difficult since the FRP effectively hides the conditions underneath the repair system.

The fabric reinforced cementitious matrix (FRCM) composite system is a relatively new strengthening and rehabilitation system. FRCM has almost all of the same benefits (such as light weight, easy to install and non-corroding characteristics) of typical FRP systems, but overcomes some of the draw backs (such as poor compatibility with

concrete substrate, diffusion tightness, non-applicability on wet surfaces and fire resistance) of using an epoxy as bonding agent in FRP system. The FRCM system replaces the epoxy with cementitious mortar and the fiber sheets with fabric or textile. FRCM has been reported in literature with other names such as textile reinforced concrete (TRC) and textile reinforced mortar (TRM).

A number of studies have been conducted to investigate the effectiveness of FRCM to strengthen shear-critical RC beams (Escrig et al., 2015; Tzoura and Triantafillou 2015; Azam and Soudki 2014a; Al-Salloum et al., 2012; Bruckner et al., 2008; Bruckner et al., 2006; Triantafillou et al., 2006). Different types of FRCMs were used in these studies including carbon fabric reinforced cementitious matrix (CFRCM), glass fabric reinforced cementitious matrix (GFRCM), basalt fabric reinforced cementitious matrix (BFRCM) and polyparaphenylene benzobisoxazole (PBO) fabric reinforced cementitious matrix. The majority of above studies were exploratory studies and mainly focused on effectiveness of the FRCM to enhance ultimate load carrying capacity. Recently, the American Concrete Institute (ACI) has published a new guide for the design and construction of externally bonded FRCMs (ACI 549.4R-13). This document summarizes the majority of research published up to 2013 on the strengthening of RC members using FRCM.

Extensive research has been conducted on shear strengthening of RC beams using FRPs. This research has helped researchers better understand the behaviour of RC beams

strengthened in shear with externally bonded strengthening systems. However, there are still few areas which need further research. For instance, the interaction between the externally bonded shear strengthening system and the internal transverse reinforcement is still not well understood. Chen et al. (2010) found that the stirrups did not yield in beams strengthened with FRPs raising a concern that it might not be safe to assume that the stirrups have yielded when calculating the shear strength of strengthened beams. In addition, a number of researchers have reported a reduction in the shear strength contribution from externally bonded FRP sheets in beams with stirrups (Pellegrino and Modena 2002; Chaallal et al. 2002; Mofidi and Chaallal 2014; Belarbi et al. 2012; Colalillo and Sheikh 2014). Some studies have concluded that the reduction in shear strength contribution from the externally bonded FRP sheets in beams with stirrups is possibly due to reduced bond strength between FRP sheet and concrete substrate (Pellegrino and Modeno 2002; Mofidi and Chaalal 2014). This might not be true for beams strengthened with FRCM, as the FRCM systems generally exhibit better bond performance compared to the FRP system (Azam and Soudki 2014a). This indicates that there is a need to further investigate the interaction between the FRCM and the internal transverse reinforcement in the overall shear capacity of the strengthened beam.

The current research study was designed to investigate the effect of internal transverse reinforcement on behaviour of shear-critical RC beams strengthened with a CFRCM system, in particular to focus on the interaction between the CFRCM and the internal

transverse reinforcement. In order to investigate the interaction between the CFRCM and the internal transverse reinforcement, the shear resistance provided by the CFRCM and the internal transverse reinforcement was calculated using experimentally measured strains in CFRCM and stirrups. The current study will help better understand the interaction between the CFRCM and the internal transverse reinforcement. This study is part of a larger research program on strengthening of reinforced concrete structures using cement-based strengthening systems.

4.2 Experimental Program

In order to examine the structural performance of shear-critical RC beams strengthened with CFRCM, six full scale beams were constructed and tested to failure.

4.2.1 Test Specimens

The details of the beam specimens are presented in Figure 4.1 and Table 4.1. All beams were 250 mm wide, 400 mm deep and 2700 mm long. The longitudinal tensile reinforcement in all of the beams was 6-25M bottom bars and 3-25 top bars. The side and vertical covers to the tension reinforcement were kept at 40 mm for all beams. Three configurations of stirrups were investigated: no stirrups, 6 mm stirrups at 150 mm c/c and 6 mm stirrups at 250 mm c/c. Three additional stirrups were provided in the anchorage zone for the longitudinal reinforcement.

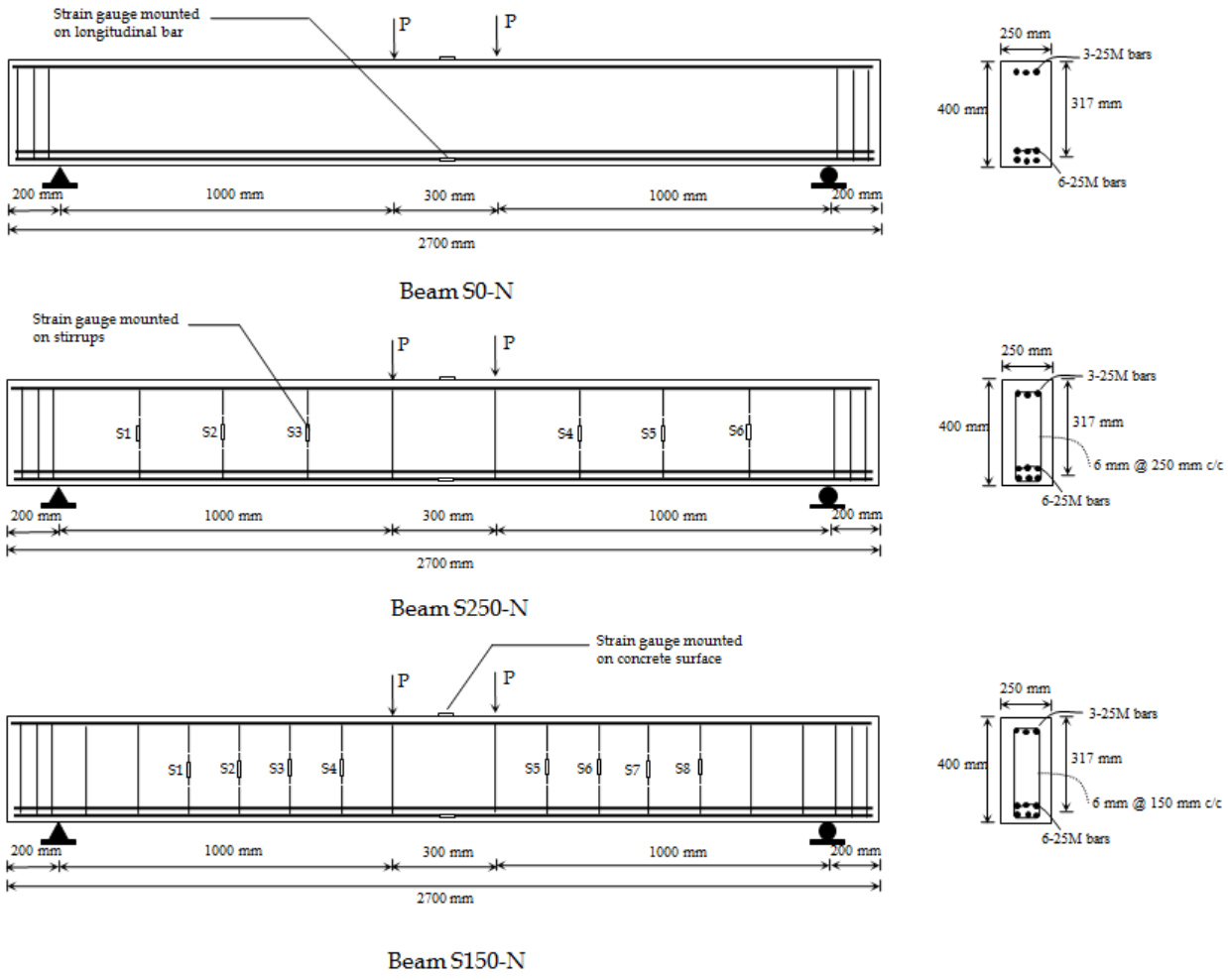

Figure 4.1 : Beam geometry, reinforcement details and layout of strain gauges

Table 4.1 : Details of test specimens

Sr. No.	Beam Designation	Longitudinal Reinforcement			Shear Reinforcement	
		Amount of Rebar	ρ	ρ/ρ_b	Steel Stirrups	External FRCM
1	S0-N	6-25M tension steel and 3-25 compression steel	3.79	0.55	None	None
2	S150-N				6mm @150 mm c/c	None
3	S250-N				6mm @250 mm c/c	None
4	S0-CM				None	CFRCM
5	S150-CM				6mm @150 mm c/c	CFRCM
6	S250-CM				6mm @250 mm c/c e	CFRCM

The beam designation used in this study is as follows: YY-ZZ with YY = steel shear reinforcement and ZZ= strengthening system. The steel shear reinforcement is specified as S0 (beams without stirrups), S150 (beams with 6 mm stirrups @ 150mm c/c) and S250 (beams with 6 mm stirrups @ 250mm c/c) and the strengthening system is specified as N (none) or CM (CFRCM).

4.2.2 Material Properties

The concrete used to fabricate the test beams was supplied by a local ready mix concrete company. The concrete was batched with normal (Type GU) portland cement with a maximum coarse aggregate size of 19 mm and a water-cementing materials ratio of 0.45. Six concrete cylinders (100 mm x 200 mm) were also cast from the same concrete batch. The 28 day compressive strength of the concrete was 63 ± 1 MPa. The longitudinal and transverse steel had a yield strength of 494 MPa and 365 MPa, respectively, as reported by the supplier.

As per the Manufacturer's product data sheet, the carbon fabric used in the CFRCM system had an ultimate strength of 325 kN/m and 250 kN/m in the longitudinal and transverse directions, respectively. The weight of carbon fabric was 609 g/m^2. The orthogonal spacing of fabric tows was 10 x18 mm (Figure 4.2). Sika Monotop 623, polymer modified, one component, and early strength-gaining cementitious mortar was used as the bonding agent in the CFRCM composite layer. The compressive strength of the mortar was measured using 50 mm cubes. The compressive strengths of the mortar at 3, 7 and 28 days were 41±3.3, 45±2.4 and 58±2.8 MPa, respectively.

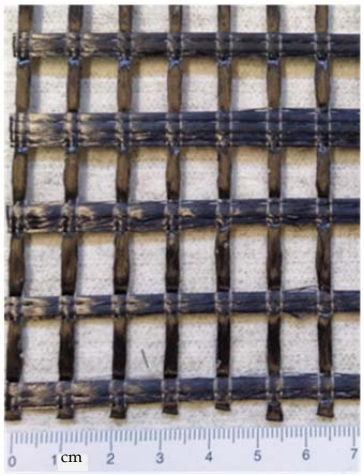

Figure 4.2 : Carbon fabric used in study

4.2.3 CFRCM Strengthening

Three beams were strengthened with CFRCM. The shear spans of beams were strengthened with side bonded CFRCM. The CFRCM strengthening procedure followed the Manufacturer's specifications. The CFRCM strengthening procedure is

presented in detail by Azam and Soudki (2014) and is summarized in the following paragraph.

The concrete surfaces were first sand-blasted to expose the aggregates. Water was sprayed on the dry concrete surfaces of the beams until a saturated surface dry (SSD) condition was achieved. Once the SSD condition was achieved, the first layer of mortar was applied. After the application of the first layer of mortar, the fabric was pressed into the mortar. The fabrics were applied in such a way that the direction of stronger fabric tows was perpendicular to the longitudinal axis of the beam. Then a final layer of mortar was applied to completely cover the fiber textile. Finally, the beam surface was finished with a trowel. The total thickness of the strengthening system was about 6-8 mm.

4.2.4 Instrumentation

All tested beams were instrumented with one strain gauge (5 mm gauge length) mounted on a longitudinal reinforcing bar at mid span and one strain gauge (60 mm gauge length) mounted on the top concrete surface at mid span. Two linear variable differential transformers (LVDTs) with a range of 0-25 mm were placed at mid-span to measure the deflection of the beam. In addition, LVDTs were mounted on the side of the beam in the shear spans to measure diagonal tensile and diagonal compressive displacements. Figure 4.1 and Figure 4.3 show the layout of the instrumentation.

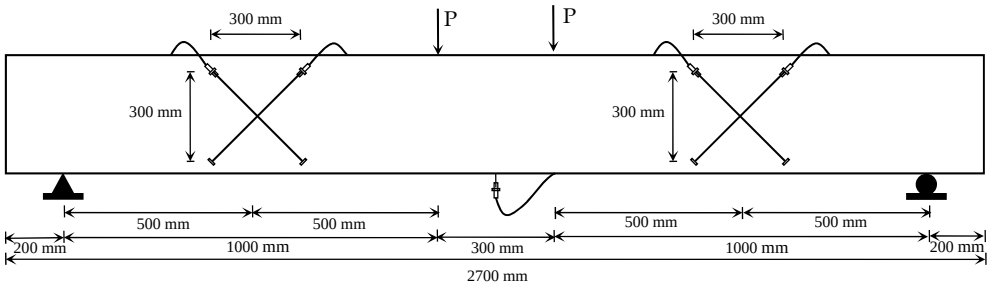

Figure 4.3 : Layout of LVDTs

4.2.5 Test Setup and Procedure

The beams were tested in four-point bending using a closed-loop hydraulic actuator with a 2500 kN capacity in a test frame. The beams were simply supported with roller and hinge supports over a clear span of 2300 mm. The spacing between load points was 300 mm and the shear span was 1000 mm. The load was transferred from the actuator to the beam through two loading plates at mid-span. To uniformly distribute the load, the loading plates were levelled on the beam using hydro-stone. The test setup is shown in Figure 4.4.

The test procedure was as follows: the beam was placed over the supports, leveled and centered. All of the instrumentation (LVDT and strain gauges) was mounted on the beam and connected to the data acquisition system. The data acquisition system started gathering data before the application of load. The load was increased monotonically at a

stroke rate of 0.3 mm/min. using a ramp function generator until failure of the beam. The initiation and progression of cracks were monitored over the duration of the tests.

Figure 4.4 : Test setup

4.3 Experimental Results and Discussion

A summary of the experimental results is given in Table 4.2. The structural behavior of the beams is discussed in terms of load-deflection response, strain in the concrete and longitudinal reinforcement, strain in the stirrups and CFRCM strengthening layer, failure modes, the shear transfer mechanism of CFRCM strengthening layer and interaction between shear components in the following sections.

Table 4.2 : Summary of test results

Beam designation	Inclined cracking load (kN)	Ultimate load (kN)	Increase in ultimate load due to CFRCM (%)	Deflection at ultimate load (mm)	Strain in longitudinal reinforcement at midspan at failure (με)	Concrete strain at midspan at failure (με)	Failure mode
S0-N	287.2	287.2	-	4.0	1073	839	shear
S150-N	300.0	613.9	-	12.7	2595	1984	shear
S250-N	298.0	520.3	-	12.1	1870	2465	shear
S0-CM	350.0	538.3	87.4	12.3	2227	3196	shear
S150-CM	350.0	771.0	25.6	14.0	3021	2386	shear
S250-CM	340.0	678.7	32.2	12.4	2874	2336	shear

4.3.1 Load-Deflection Response

The load-deflection response of all tested beams is shown in Figure 4.5 and Figure 4.6. In general, the load-deflection response of all beams, except (S0-N), was almost bilinear indicating the change of stiffness occurring after the formation of shear cracks. All of the beams failed suddenly, consistent with the brittle nature of shear failure. The load-deflection response of control beam without stirrups (S0-N) was linear as it failed suddenly after formation of a single diagonal shear crack.

The effect of stirrups on the load-deflection response of the control unstrengthened beams is shown in Figure 4.5a. As expected, the presence of stirrups resulted in higher ultimate load and higher deflection at ultimate load in the unstrengthened control beams. The control beam without stirrups (S0-N) failed at a load of 287.2 kN. The control beams with stirrups, S150-N, S250-N, failed at a load of 613.9 kN and 520.3 kN, respectively. This represents an increase in ultimate load of 115% and 81%, respectively.

The deflection in the control beams with stirrups ranged between 12.1 mm to 12.7 mm compared with a deflection of 4.0 mm for the control beam without stirrups, representing an increase of 200% to 218%. The effect of stirrups on the load-deflection response for CFRCM strengthened beams is shown in Figure 4.5b. As expected, the CFRCM strengthened beam with stirrups experienced higher stiffness compared to the CFRCM strengthened beam without stirrups.

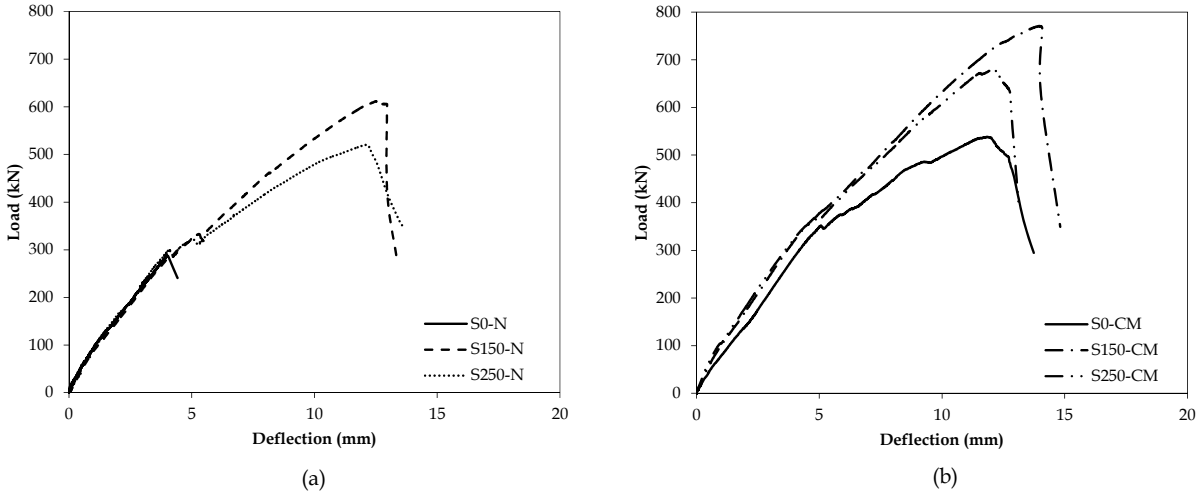

Figure 4.5 : Effect of stirrups on load vs. deflection response (a) control unstrengthened beams (b) strengthened beams

Figure 4.6 (a-c) shows the effect of CFRCM strengthening on the load-deflection response of the beam without stirrups, the beams with stirrups at 250 mm c/c and beams with stirrups at 150 mm c/c, respectively. The largest increase in ultimate load due to the CFRCM strengthening was observed for the beam without stirrups (S0-CM) followed by the beam with stirrups at 250 mm c/c (S250-CM). The smallest increase in

ultimate load due to the CFRCM strengthening was observed for the beam with stirrups at 150 mm c/c (S150-CM). The CFRCM strengthened beams without stirrups (S0-CM) failed at a load of 538.3 kN compared with failure loads of 771 kN and 678.7 kN for the CFRCM strengthened beams with stirrups, S150-CM and S250-CM, respectively (Table 4.2). CFRCM strengthening increased the ultimate load by 87.4% for the beam without stirrups (S0-CM) compared to an increase in ultimate load of 25.6% and 30.4 % for beam with stirrups at 150 mm c/c (LS150-CM) and beam with stirrup at 250 mm c/c (S250-CM), respectively. This indicates that the increase in ultimate load due to CFRCM strengthening decreased with presence of stirrups. The attenuating effect of stirrups on shear strength contribution of shear strengthening is discussed in detail below. The deflection at failure for all strengthened beams ranged between 12.1 to 12.7 mm, similar to that observed for the control beams with stirrups.

These results are consistent with the findings of other researchers (Pellegrino and Modena 2002; Chaallal et al. 2002; Mofidi and Chaallal 2014; Belarbi et al. 2012; Colalillo and Sheikh 2014). Some studies have concluded that the reduction in shear strength contribution from the externally bonded FRP sheets in beams with stirrups is possibly due to reduced bond strength between the FRP sheet and concrete substrate (Pellegrino and Modeno 2002; Mofidi and Chaalal 2014) since a beam with stirrups will experience several shear cracks compared to a single shear crack in beams without stirrups. The increased cracking results in a shorter bond length for FRP sheets which leads to

debonding of FRP sheets at lower loads. The effect of the stirrups on effectiveness of CFRCM strengthening is discussed further following the discussion of the interaction between shear components.

4.3.2 Strain in Concrete and Longitudinal Reinforcement

The compressive and tensile strains measured at failure in the concrete and in the longitudinal reinforcement are presented in Table 4.2. The measured compressive strains at failure in all beams were below the maximum compressive strain of 3500 με normally associated with concrete crushing in flexure. The measured tensile reinforcement strains at failure in three beams (S0-N, S250-N and S0-CM) were below the yield strain of 2500 με, while the strains at failure in the other three beams (S150-N, S150-CM and S250-CM) exceeded the yield strain of 2500 με. As expected, the largest tensile strain in the longitudinal reinforcement (3021 με) was observed for the CFRCM strengthened beam with stirrups at 150 mm c/c (S150-CM). It is important to note that all beams were reinforced with 6-25M bottom rebar placed in two layers, and that the reinforcement strain gauges were mounted on the bottom layer of steel. In all cases, the measured strains were consistent with shear failure and no signs of flexural failure were observed in the beam condition or in the measured load-deflection response.

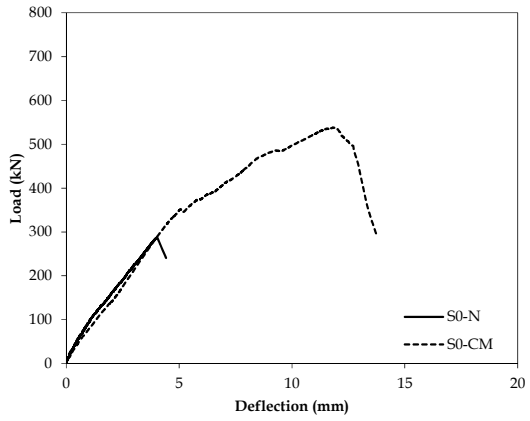

(a)

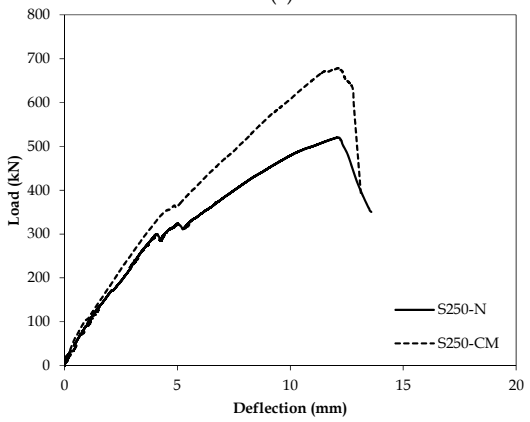

(b)

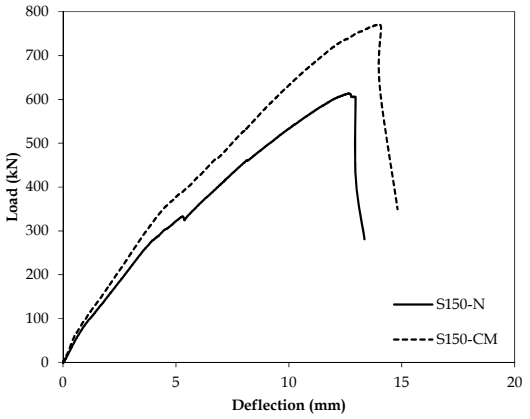

(c)

Figure 4.6 : Effect of CFRCM strengthening on load vs. deflection response of tested beams (a) beams without stirrups (b) beams with stirrups at 250 mm c/c (c) beams with stirrups at 150 mm c/c.

4.3.3 Strain in Stirrups and FRCM Strengthening Layer

Figure 4.7 shows the typical load versus strain in stirrup response for all four stirrups that intersected the main shear crack in the control beam (S150-N). Figure 4.3 shows the location of all stirrups in beam S150-N. As expected, the strain in the stirrups is negligible until formation of a shear crack, followed by a rapid increase in strain after formation of the shear crack as shear force is transferred to the stirrups.

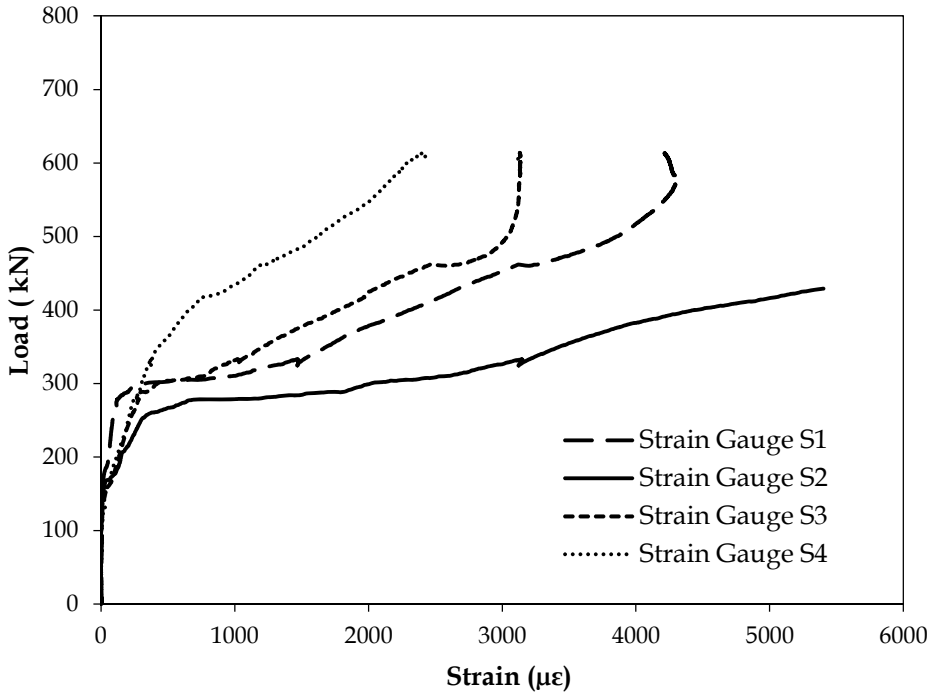

Figure 4.7 : Typical load vs. strain in stirrups (beam S150-N)

The slope of the load versus strain in stirrup curves is different for each stirrup. The main shear crack first appeared at the location of stirrup S2 in beam LS150-N, which resulted in sudden yielding of stirrup S2. This indicates that the 6 mm stirrup at

location S2 was unable to fully control the crack and the shear crack propagated towards stirrup S1 (towards support) and stirrup S3 (towards load point). Stirrup S1 and S3 started taking shear (indicated by increasing strains) until the crack reached stirrup S4. At this point, all stirrups were engaged in carrying shear until failure of the beam occurred.

Figure 4.8 shows the load versus average strain in stirrups response for all tested beams. The average strain in all stirrups that intersected the main shear crack was used to illustrate the effect of the stirrups and the CFRCM strengthening. It can be seen from Figure 4.8 that beams with stirrups at 150 mm c/c (S150-N and S150-CM) exhibited lower strain in the stirrups compared to the beams with stirrups at 250 mm c/c (S250-N, S250-CM). This is mainly due to the increased axial stiffness of the more closely spaced stirrups. Similarly, the CFRCM strengthened beams (S150-CM and S250-CM) exhibited lower strain in the stirrups compared to the control unstrengthened beams (S150-N, S250-N). This demonstrates the load sharing between the stirrups and CFRCM strengthening layer.

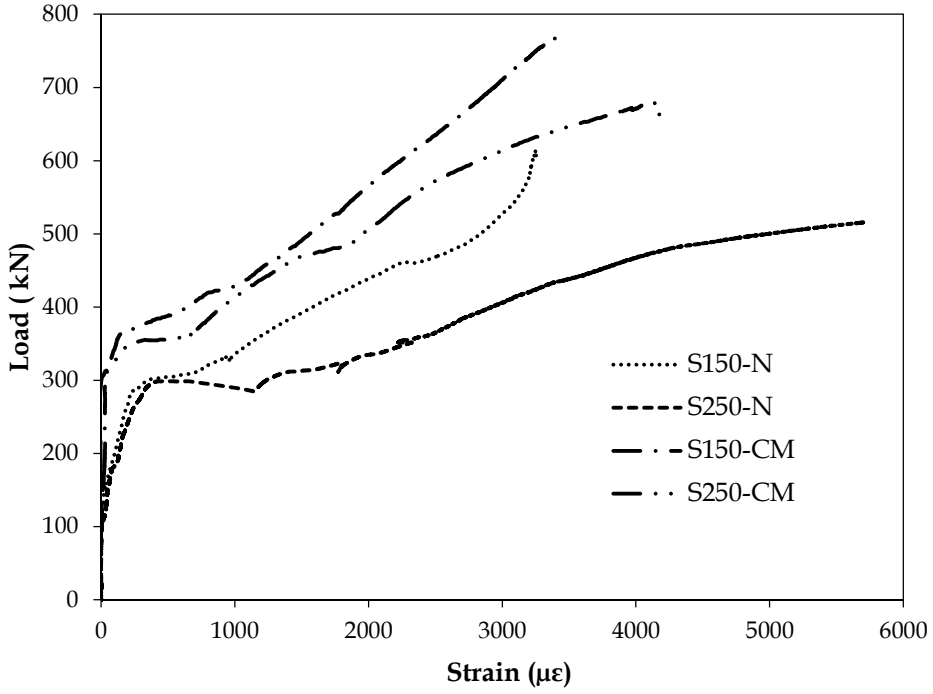

Figure 4.8 : Load vs. average strain in stirrups for all beams

Figure 4.9 shows the strain distribution in the steel stirrups and CFRCM strengthening layer across shear crack in CFRCM strengthened beams (S150-CM and S250-CM) at failure. The strain in the stirrups was measured using strain gauges mounted on stirrups, whereas the vertical strain in the CFRCM strengthening layer was calculated from strain measured using diagonal LVDTs. The strains measured using these two methods showed similar behavior (Fig 9). This indicates that the strain readings measured using strain gauges can be interpreted for strains in the CFRCM strengthening layer. Fig. 9 also includes the average strain across the shear crack at failure. The average strains across shear crack at failure in beams S150-CM and S250-CM were 5436με and 5016με, respectively. The ratio between maximum and average

strain for beams S150-CM and S250-CM were 0.624 and 0.663, respectively. For the CFRCM strengthened beam without stirrups (S0-CM), the vertical strain in the CFRCM was only measured at mid shear span. The average CFRCM strain across shear crack was calculated by multiplying the measured vertical strain in CFRCM by 2/3 assuming that the vertical CFRCM strain measured at mid shear span was maximum CFRCM strain, resulting in an average CFRCM strain of 4799με. The 2/3 ratio between the maximum and average shear strains along an inclined shear crack is based on the assumption of a parabolic distribution of shear stress along the crack length as described by Carolin and Taljsten (2005) and Blanksvard et al. (2009).

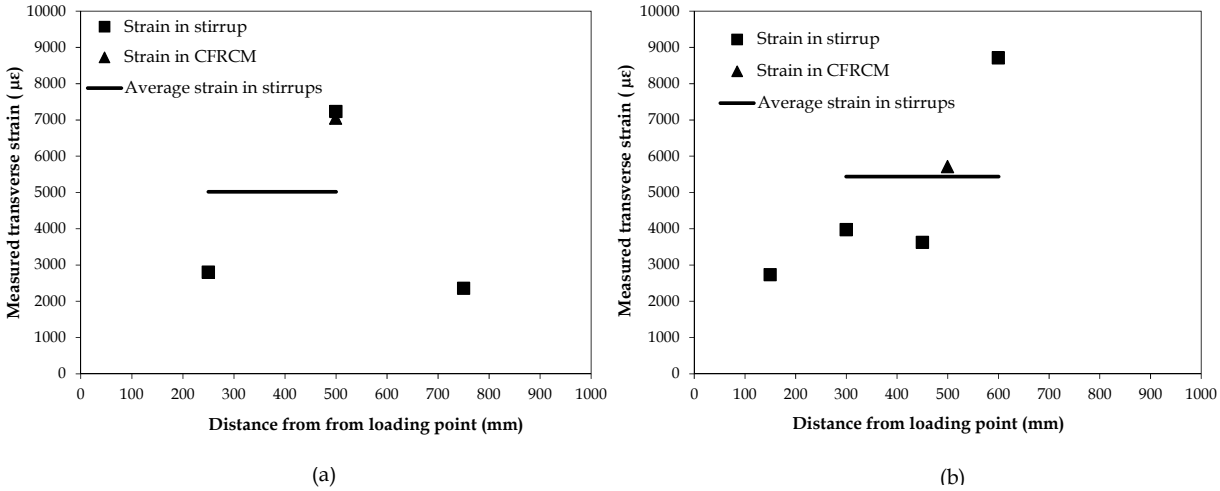

Figure 4.9: : Strain distributions in stirrups and FRCM strengthening layer across shear crack in strengthened beams with stirrups (a) beam S250-CM (b) beam S150-CM

4.3.4 Failure Modes

All of the tested beams failed in shear as shown in Figure 4.10. The cracking in all beams was initiated with the appearance of flexural cracks at mid span. As the load increased, a single inclined crack appeared in the shear span which progressed towards the load point and support region leading to a diagonal tension failure. The control unstrengthened beam without stirrups exhibited single shear crack, while the beams with stirrups and CFRCM strengthened beams exhibited more than one shear crack.

The control unstrengthened beam without stirrups failed suddenly after formation of the diagonal crack, while the control unstrengthened beam with stirrups continued carrying load after formation of the diagonal shear until yielding of stirrups resulted in beam failure. In the CFRCM strengthened beam without stirrups, the shear was carried by the strengthening layer after formation of diagonal cracks until the strengthening layer was unable to control the shear crack propagation, which resulted in beam failure. In the strengthened beams with stirrups, the shear force was simultaneously carried by the stirrups and the strengthening layer until the combined effect of stirrups and strengthening layer was unable to control the shear crack propagation, which resulted in beam failure. The possible shear transfer mechanism of the CFRCM strengthening layer is presented in the following section.

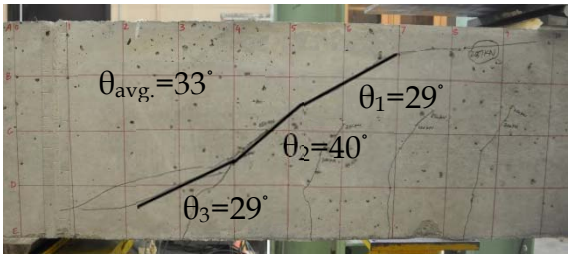

Beam S0-

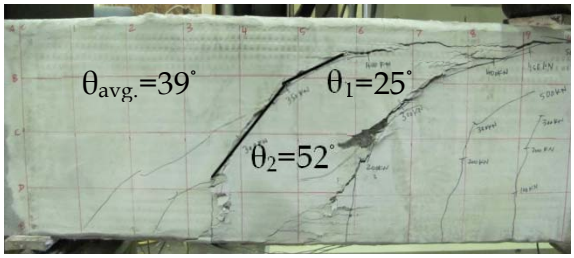

Beam S0-

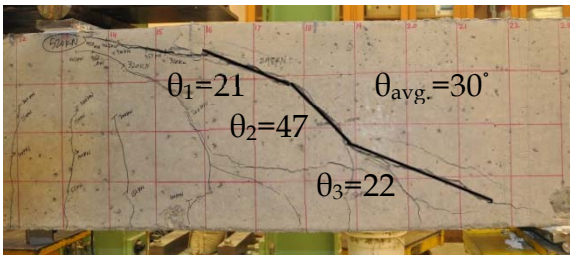

Beam S250-

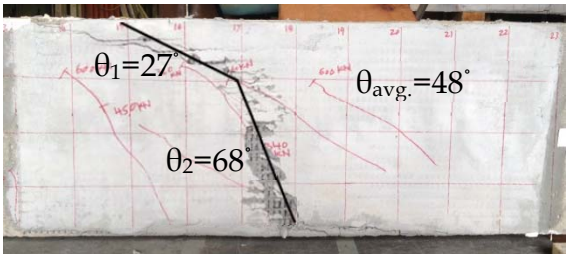

Beam S250-

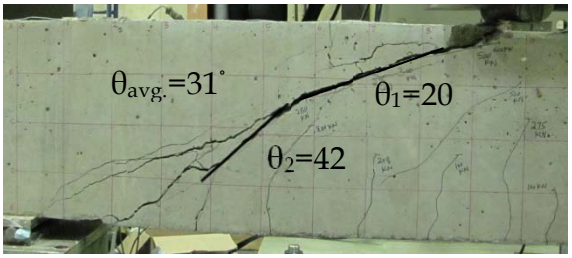

Beam S150-

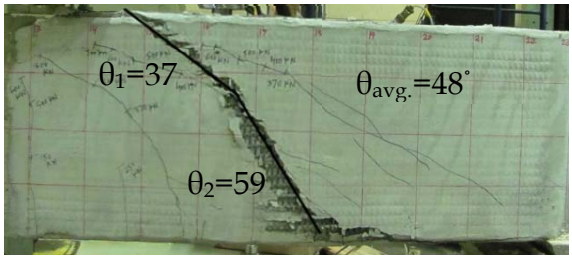

Beam S150-

Figure 4.10 : Failure modes

4.3.5 Shear Transfer Mechanism of CFRCM Strengthening Layer

The FRCM strengthening layer consists of fabric embedded in mortar, where the fabric has tows in two orthogonal directions woven together. When diagonal cracking occurs, the transverse (vertical) tows of the fabric intersect the crack and restrain the crack opening. The effectiveness of transverse tows to control shear cracks depends on the

tensile stiffness of the tows and the shear transfer mechanism between the fabric tows and the original beam concrete surface.

The effect of the tensile stiffness of shear strengthening layer has been studied previously for FRCM shear strengthening (Azam et al. 2016; Escrig et al., 2015; Azam and Soudki 2014a). The tensile stiffness of the fabric depends on the area of fiber tows and the modulus of elasticity of the fabric material. This means that the carbon fabric with high modulus of elasticity will provide better crack control in FRCM compared to glass fabric with a lower modulus of elasticity. Similarly, a heavier fabric with more tow area will provide better crack control compared to lighter fabric with a smaller tow area, assuming that the bond properties between the fabric and the beam surface are constant.

The shear transfer between the fabric tows and the original beam surface have two possible load paths: (1) transverse fabric tows transfer the shear to mortar and mortar transfers the shear to beam surface, or (2) the transverse fabric tows transfer the shear to the longitudinal fabric tows which then transfer the shear to the beam surface through the mortar.

The viability of first load path in which shear is directly transfers from the transverse tows to original beam surface through mortar is dependent on the bond between the fabric tow and the mortar. Tensile testing reported in literature have indicated that the bond between the fabric tows and the mortar is very weak (Arboleda et al. 2012). This

indicates that the first load path is less viable because of limited bond between the fabric tow and mortar.

The viability of second load path mainly depends on the connection between the transverse and longitudinal fabric tows, as in this load path shear is transferred from the transverse tows to the longitudinal tows which act as anchorage for the transverse tows and transfer the vertical shear to the beam surface. Fabric or grid in which the tows in orthogonal directions are strongly connected performs better compared to fabric or grid in which the tows in the two orthogonal directions are weakly connected (Azam and Soudki, 2014b). The other variable that affects the viability of this load path is the anchorage provided by longitudinal tows. The longitudinal fabric tows run along the length of the beam and generally provide sufficient anchorage. However, to achieve proper anchorage of longitudinal tows, the fabric should be covered with enough mortar thickness. Based on observations listed above, it can be concluded that the second load path is more viable compared to first load path.

In the current study, it appears that shear was mainly transferred from the strengthening layer to the beam surface using the second load path explained above. The failure of strengthening layer was initiated by one or both weak links in the second load path: the separation of fabric tows in two orthogonal directions or the loss of anchorage provided by longitudinal tows due to spalling of mortar cover. Figure 4.11 shows a close-up view of the strengthening layer at a failure shear crack. The separated

tows in the two orthogonal directions and mortar cover spall can be seen in Figure 4.11. In addition, the mortar cover spall around the failure crack in the form of band width can also be seen in failure mode of CFRCM strengthened beams (Figure 4.11).

Figure 4.11 : Failure of CFRCM strengthening layer – A closeup view

4.3.6 Interaction between Shear Components

The shear resistance provided by the different component materials (concrete, steel and CFRCM) was calculated in order to investigate the interaction between different shear components. Shear component analysis was performed using free body diagrams (FBDs) drawn for each specimen. Figure 4.12 shows the FBDs for all tested beams. The geometry of the FBDs was based on the shear crack geometry as shown previously in Figure 4.10. The shear resistance provided by stirrups was calculated as:

$$V_s = n.A_v.f_v \qquad \text{Equation 4.1}$$

where V_s is the shear resistance provided by the steel stirrups; n is the number of stirrups crossing the crack; A_v is the cross sectional area of one stirrup and f_v is the average stress in the stirrups crossing the failure crack determined from the experimental stirrup strain measurements. The shear resistance provided by the CFRCM strengthening layer was calculated as:

$$V_{CFRCM} = 2.t_{CFRCM.}E_{CFRCM}.\varepsilon_{CFRCM}.d\ cot\theta \qquad \text{Equation 4.2}$$

where V_{CFRCM} is the shear resistance provided by the CFRCM strengthening layer; t_{CFRCM} is the equivalent design thickness of fabric used in CFRCM strengthening layer; E_{CFRCM} is the tensile modulus of the carbon fabric used in the CFRCM; ε_{CFRCM} is the average measured strain in the CFRCM strengthening layer.; d is effective depth of beam and θ is the experimentally observed average shear crack angle.

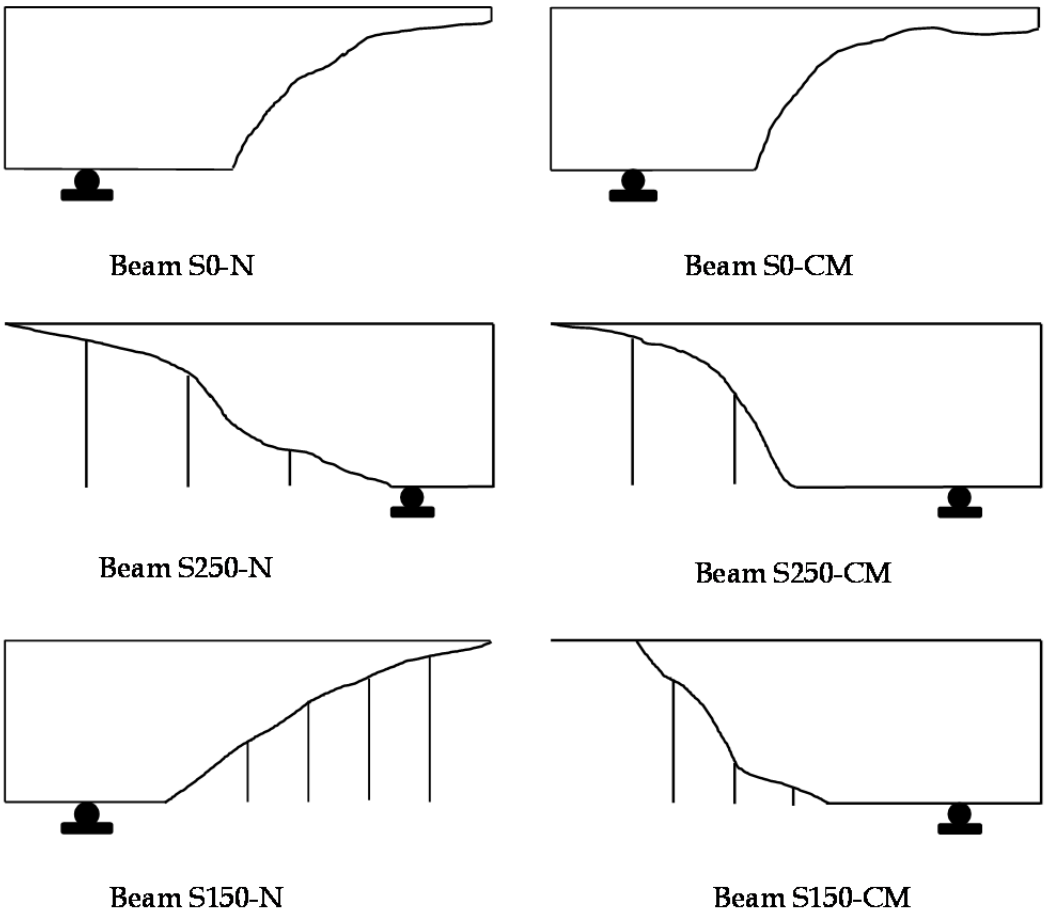

Figure 4.12 : FBDs used for shear component analysis

The shear resistance provided by the concrete was calculated by subtracting the shear resistance provided by the stirrups and strengthening layer from the experimentally observed total shear resistance:

$$V_c = V_{total} - V_s - V_{CFRCM} \qquad \text{Equation 4.3}$$

Figure 4.13 shows the shear component diagrams based on the analysis procedure described above. For the control unstrengthened beams, the shear resistance provided

by the concrete increased with the addition of stirrups since the beams did not fail suddenly after yielding of the stirrups. The shear resistance provided by concrete increased further with the addition of the strengthening layer. Overall, the shear resistance provided by the concrete increased with an increase in total shear reinforcement ratio.

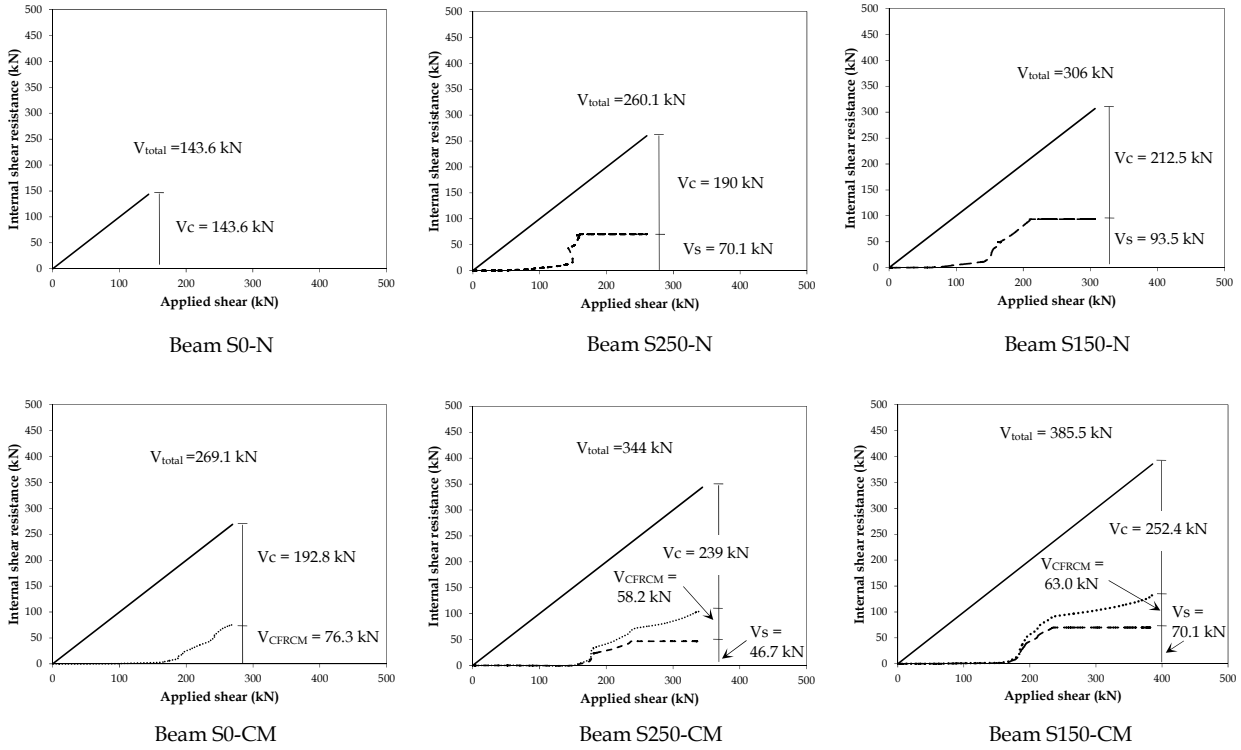

Figure 4.13 : Shear component diagrams for tested beams

The increase in shear resistance provided by the concrete is possibly due to two reasons: 1) the confinement provided by internal and external shear reinforcement, or 2) the shear transfer mechanism changes to arch action, or both.

The shear resistance provided by the steel stirrups decreased with the addition of the strengthening layer due to a change in the diagonal crack angle. The addition of the strengthening layer resulted in steeper diagonal cracking which intersected fewer stirrups (see Figure 4.10 and Figure 4.12) and resulted in a lower overall shear resistance provided by stirrups. Similarly, the shear resistance provided by the CFRCM strengthening layer was slightly higher for beam without stirrups compared to the shear resistance provided by beams with stirrups. As with the addition of stirrups, the total shear reinforcement ratio increased which resulted in steeper diagonal cracks (see Figure 4.10). As a result a shorter length of the CFRCM intersected shear crack ($d\cot\theta$ is decreased; see Eq (2)) which resulted in lower shear resistance provided by the CFRCM strengthening layers for beams with stirrups. Malek and Saadatmanesh (1998) have shown the similar effect of the amount of transverse reinforcement on the diagonal crack angle in RC beams.

4.4 Comparison of Experimental and Predicted CFRCM Shear Strengths

The experimental CFRCM shear strength contributions were estimated by subtracting the capacities of control unstrengthened specimens from those of the respective strengthened specimens: ($V_{CFRCM} = V_{STRENGTHENED} - V_{CONTROL}$). Generally, the shear strength contributions from externally bonded strengthening systems are estimated using this method. However, this method may not provide an accurate estimate as this method does not consider any interaction between the shear resistance components.

Therefore, the CFRCM shear resistance estimated using the experimentally measured CFRCM strain and measured crack angle were also considered. The experimental CFRCM shear strength contributions estimated using both methods are listed in Table 4.3.

Table 4.3 : Comparison between experimental and predicted CFRCM shear contributions

Beam designation	Predicted Results using ACI 549.4R-13	Experimental Results			
		$V_{CFRCM} = 2.t_{CFRCM}.E_{CFRCM}.\varepsilon_{CFRCM}.d\cot\theta$		$V_{CFRCM} = V_{STRENGTHENED} - V_{CONTROL}$	
		V_{CFRCM} (kN)	V_{exp} / V_{pre}	V_{CFRCM} (kN)	V_{exp} / V_{pre}
S0-CM	51.5	76.3	1.48	125.55	2.44
S150-CM	51.5	58.2	1.13	78.55	1.52
S250-CM	51.5	63.0	1.22	79.2	1.54
Mean			1.27		1.83
Coefficient of Variation, %			0.18		0.52

4.4.1 ACI 549.4R-13 Design Equations

The American Concrete Institute (ACI) has recently published ACI 549.4R-13, a new design guide for the design and construction of externally bonded FRCM systems. The ACI 549.4R-13 provisions to calculate the shear strength contribution from externally bonded FRCM are similar to the ACI 440.2R (2008) provisions with some modifications as presented in previous study by Azam and Soudki (2014a). The ACI 549.4R-13

provisions to calculate the shear strength contribution are based on a 45 degree truss analogy and use an effective strain limit of 0.004.

The FRCM shear strength contribution using ACI 549.4R-13 is calculated as:

$$V_f = n \,.\, A_f \,.\, f_{fv} \,.\, d_f \qquad \text{Equation 4.4}$$

Where n is the number of layers of mesh reinforcement; A_f is the area of mesh reinforcement per unit width effective in shear; $f_{fv} = \varepsilon_{fv} E_f$ = design tensile strength of the FRCM shear reinforcement; $\varepsilon_{fv} = \varepsilon_{fu} \leq 0.004$ = design tensile strain of the FRCM shear reinforcement; ε_{fu} = ultimate tensile strain of the FRCM; E_f is the tensile modulus of cracked FRCM and d_f is the effective depth of the FRCM shear reinforcement.

4.4.2 Analytical Results

For analysis purposes, an equivalent design thickness (0.0883 mm) was calculated for the carbon fabric used in this study based on its ultimate load per unit width, ultimate strain and tensile modulus. The mechanical properties of the carbon fabric alone were used in the analysis instead of mechanical properties of CFRCM (fabric embedded in mortar) because the mortar tensile strength is negligible compared to tensile strength of fabric. The role of the mortar in CFRCM is mainly to transfer the stresses from the fabric to the concrete surface of the beam as explained previously.

The experimental and predicted CFRCM shear strength contributions are presented in Table 4.3. The CFRCM shear strength predictions using ACI 549.4R-13 were in good

correlation with experimental CFRCM shear contributions estimated using experimental strain measurements. The average ratio of experimental to predicted CFRCM shear strength contribution was 1.27 with a coefficient of variation of 0.18. However, the CFRCM shear strength predictions using ACI 549.4R-13 were underestimated when compared with the experimental CFRCM shear contributions estimated from capacity subtraction ($V_{FRCM} = V_{STRENGTHENED} - V_{CONTROL}$). The average ratio of experimental to predicted CFRCM shear strength contribution was 1.8 with a coefficient of variation of 0.5. Unlike the experimental strain measurements method, the capacity subtraction method does not take into account the interaction between different shear resisting components. Hence it can be concluded that ACI 549.4R-13 reasonably predicts CFFRCM shear strength contribution. However, the existing methods to calculate the shear contribution from concrete do not account for the effect of strengthening and need to be studied further.

4.5 Discussion of Shear Mechanisms:

The behaviour of strengthened shear-critical RC slender beams is generally described as a beam action mechanism where the shear strength of the beam is commonly determined using a truss analogy approach presented in Section 2.3.3. The total shear strength (V_{total}) of the RC beam is taken as the sum of the shear strength contribution from concrete (V_c), the shear strength contribution from the steel stirrups (V_s) and the shear strength contribution from the strengthening system (V_{CFRCM}) as follows:

$$V_{total} = V_c + V_s + V_{CFRCM} \qquad \text{Equation 4.5}$$

For the stirrups, the truss analogy approach describes the shear strength contribution as the vertical force in the stirrups crossing a typical inclined shear crack, given by the following equation:

$$V_s = n.A_v.f_v \qquad \text{Equation 4.6}$$

where V_s is the shear resistance provided by the steel stirrups; n is the number of stirrups crossing the crack; A_v is the cross sectional area of one stirrup and f_v is the average stress in the stirrups crossing the failure crack determined from the experimental stirrup strain measurements. For design purposes, f_v, is taken as the yield strength of the stirrups. The number of stirrups crossing the crack is taken as the horizontal projected length of the crack divided by the stirrup spacing:

$$n = \frac{z \cdot \cot\theta}{s} \qquad \text{Equation 4.7}$$

where z is the internal lever arm; θ is the crack angle and s is the spacing of stirrups. The ACI Building Code for Structural Concrete (ACI 318-14) assumes a 45˚ truss model so that Equation 4.6 reduces to $\frac{z}{s}$.

The Canadian design code approach (CSA A23.3-04) considers a variable angle truss model where the crack angle (θ) increases as the transverse reinforcement ratio is

increased. However, the crack angle (θ) defined in the General Method in CSA A23.3-04 shows only a minor increase in crack angle with the addition of stirrups. The Simplified Method in CSA A23.3-04 suggests that a crack angle of 35˚ can be assumed in lieu of more rigorous calculations.

The truss analogy approach defines the shear resistance provided by the strengthening layer in a similar manner as follows:

$$V_{CFRCM} = 2.t_{CFRCM.}E_{CFRCM}.\varepsilon_{CFRCM}.d\ cot\theta \qquad \text{Equation 4.8}$$

where V_{CFRCM} is the shear resistance provided by the CFRCM strengthening layer; t_{CFRCM} is the equivalent design thickness of fabric used in CFRCM strengthening layer; E_{CFRCM} is the tensile modulus of the carbon fabric used in the CFRCM; ε_{CFRCM} is the average measured strain in the CFRCM strengthening layer.; d is effective depth of beam and θ is the experimentally observed average shear crack angle. Note that $d\ cot\theta$ is the horizontal projected length of an inclined shear crack crossed by the strengthening system.

The mechanics of the shear strength contribution from the concrete are more complicated than those of the shear reinforcement. The influence of the reinforcement on the concrete shear contribution is not addressed consistently by different shear design approaches, and V_c is commonly taken as the ultimate shear strength of slender beams without stirrups. For example, the ACI Building Code for Structural Concrete

(ACI 318-14) assumes that the shear strength contribution from concrete is the same for beams with or without stirrups and is taken as the shear causing significant cracking. Similar to ACI 318-14, the CSA A23.3-04 considers that the shear strength contribution for concrete for beams with or without stirrups is the same for beams with an effective shear depth of 300 mm or less. For beams with an effective shear depth greater than 300 mm, the V_c is increased for beams with stirrups in comparison to the same beam without stirrups. However, the increase is not a function of the amount of transverse reinforcement (assuming that at least the minimum specified shear reinforcement is provided).

The mechanics of the shear strength contributions from the stirrups and strengthening system are straightforward if the strains and crack geometry are known. For design purposes, these parameters are assumed or specified empirically as described in Section 2.3.3. From a behaviour perspective, the shear strength contributions from the stirrups and strengthening system in the beams tested in this study were determined using the experimentally observed crack angles and measured strains in the stirrups and strengthening system. Using values of V_s and V_{frcm} determined in this manner, the concrete contribution, V_c, was estimated by subtracting the stirrup and strengthening system shear contributions from the applied shear loading on the beams. These results were presented previously in Section 4.3.6. This type of shear component analysis is

useful to understand the mechanics of the strengthened beams as discussed in the following sections.

4.5.1 Stirrup Shear Contribution

As expected, the strains in the stirrups consistently exceeded the yield strain of the steel, confirming the assumption of yielding at ultimate. The strain in the stirrups reached yielding prior to failure of the beams in shear for both the unstrengthened and strengthened beams. This indicates that both V_c and V_{CFRCM} continued to increase after V_s reached an upper bound due to yielding of the steel stirrups (note that the measured strains in the stirrups were not large enough to be consistent with strain hardening).

4.5.2 CFRCM Strengthening System Contribution

The strains in the CFRCM system continued to increase up to failure of the beams in shear. This indicates that V_{CFRCM} continues to increase up to failure of the beam, as the CFRCM system was able to control the diagonal cracks even after the stirrups had yielded.

The average measured strain in the CFRCM system at ultimate exceeded 0.004 in all cases. This suggests that the assumption of a maximum FRCM strain of 0.004 at ultimate is reasonable for design purposes.

4.5.3 Inclined Shear Crack Angle

As shown in Figure 4.10, the experimentally observed average shear crack angles varied between 30˚ to 48˚, and indicated that the inclined crack angle increased as the transverse reinforcement ratio increased. A similar effect of the amount of transverse reinforcement on the diagonal crack angle in RC beams has been reported in the literature by Malek and Saadatmanesh (1998).

The crack angle predictions for the beams according to the CSA A23.3-04 General Method showed a minor increase with the addition of transverse reinforcement, ranging between 33˚ to 35˚. The crack angle predictions by CSA A23.3-04 were comparable to the values observed for the unstrengthened beams in this study. However, the crack angle predictions were significantly (37%) lower than the observed angles for the strengthened beams. This suggests that the shear strength contributions from stirrups (V_s) and strengthening system (V_{CFRCM}) based on crack angles predicted by CSA A23.3-04 will be over predicted. The experimentally observed crack angles for strengthened beams were comparable to the assumed crack angle of 45˚ in ACI 318-14. However, the experimentally observed crack angles for unstrengthened beams were 36% lower compared to the assumed crack angle of 45˚ in ACI 318-14. This suggests that the shear strength contributions from the stirrups and strengthening system based on 45˚ truss analogy will be comparable to experimentally observed contributions for the strengthened beams. However, the predicted shear strength contribution from the

stirrups based on a 45˚ truss analogy will be significantly under predicted for the unstrengthened beam.

4.5.4 Concrete Shear Contribution

The concrete shear contribution estimated experimentally (by subtracting V_s and V_{CFRCM} from the applied shear load up to failure) indicates that V_c increased as the amount of shear reinforcement (internal and external) increased. The observed increases are inconsistent with the ACI 318 assumption that V_c is not a function of shear reinforcement. Furthermore, the observed increases in V_c with increase in transverse reinforcement ratio were in contrast to the decrease in V_c with increase in transverse reinforcement suggested by the CSA A23.3 shear provisions for beams with stirrups. Note that the effective shear depth of beams tested in current study was 288 mm and As per CSA A23.3-04 for beams with effective shear depth less than 300, the shear strength contribution for beams with or without stirrups is essentially the same.

In general, the estimated concrete shear contributions were consistently larger than the predicted values of V_c. Although the current shear design provisions for V_c appear to be conservative, these results suggest that interaction between the shear contributions is more complex than is assumed by the commonly accepted shear mechanism of the plastic truss analogy. As discussed in Section 4.3.6, the increase in shear resistance provided by the concrete is possibly due to the confinement of the concrete by internal

and external shear reinforcement, or because the shear transfer mechanism changes to arch action, or some combination of these effects.

As described in Section 2.2, shear in reinforced concrete beams can be transferred by two load transfer mechanism: beam action and arch action. The beam action is generally associated with slender beams while arch action is associated with deep beams. For beam action to exist, equilibrium requires the presence of shear flow across any horizontal plane between the reinforcement and the compression zone. If shear flow does not exist or is interrupted, then shear is transferred by arch action. This may occur when an inclined shear crack is wide enough such that the shear flow can no longer be transmitted in the concrete, or when the longitudinal reinforcing bars are de-bonded.

In the current study, the control beam without stirrups failed suddenly after the formation of diagonal cracks indicating that the beam transferred the shear by beam action only. In contrast, the beams with stirrups continued to carry increasing load even after the stirrups had yielded and the cracks were wide enough to disrupt the shear flow, suggesting that the shear mechanism changed from beam action to arch action. Similarly, the strengthened beams (with or without stirrups) also continued to carry increasing load even after the inclined cracks were wide enough that the shear flow would have been disrupted, indicating the transfer of load by arch action in strengthened beams as the beams approached failure in shear.

4.5.5 Conclusion: Shear Mechanisms

In conclusion, even though the existing shear strength prediction methods appear to be conservative, the mechanics behind the predictions do not appear to be completely consistent with the observed load transfer mechanisms up to failure. The existing prediction and design approach for slender beams is based on the concept that shear is transferred by beam action, but the experimental results appear to indicate that a portion of shear is transferred by arch action once the inclined shear cracks begin to disrupt shear flow in the beam section. This concept needs to be investigated further in future studies. In addition, new prediction approaches should be explored to better account for the interaction between the different shear resting components.

4.6 Conclusions

The structural performance of shear-critical RC beams strengthened with CFRCM was investigated experimentally in this study. A total of six full scale RC beams were tested. Test variables included the amount of internal shear reinforcement and the use of CFRCM strengthening. In addition, the shear strength contribution from the CFRCM was predicted using ACI 549.4R-13. Based on results of this study, the following conclusions can be drawn:

- CFRCM strengthening is effective in enhancing the load-carrying capacity of shear-critical RC beams. The maximum increase in the ultimate load (87.4%) was observed for beams without stirrups.
- An increase in the amount of transverse reinforcement (internal and/or external) results in steeper diagonal crack angles. As the total transverse reinforcement ratio is increased, the crack angle could be greater than 45˚. Therefore, the shear strength predictions of strengthened beams with an assumed crack angle smaller than 45˚ may lead to an overestimation of the shear strength contribution from the strengthening system.
- CFRCM strengthening reduces the shear strength contribution from stirrups. The CFRCM strengthened beams with stirrups exhibited steeper shear cracks compared to control unstrengthened beams with stirrups. The steeper shear cracks intersect fewer stirrups, resulting in reduced shear strength contribution from stirrups in strengthened beams. Similarly, the presence of stirrups reduces the shear strength contribution from CFRCM strengthening. Again, the addition of stirrups results in steeper shear cracks which intersect fewer fibers tows in the CFRCM system which results in a reduced shear strength contribution from CFRCM strengthening layer.
- CFRCM strengthening resulted in lower strains in the internal shear reinforcement (stirrups) at a given load level. However, the stirrups in all beams tested yielded

before beam failure. Therefore, it is safe to assume that the stirrups are yielded while calculating the shear strength of strengthened beams.

- The average CFRCM strain across shear crack at failure for all specimens was 5083 με; with a coefficient of variation of 6%. Thus, it appears that the CFRCM strain limit of 4000με specified in ACI 549.4R-13 is adequate for design.
- Based on the observed shear transfer mechanism of the CFRCM strengthening layer, it can be concluded that shear in the transverse (vertical) tows of the fabric is mainly transferred to the concrete surface through the longitudinal tows which act as anchorage for the transverse tows. Therefore, to achieve better performance of the CFRCM strengthening layer, a fabric in which the tows are strongly connected in orthogonal directions should be used.
- The CFRCM shear strength predictions using ACI 549.4R-13 were in good correlation with experimental CFRCM shear contributions estimated using experimental strain measurements.

Chapter 5: CFRP Grid Embedded in Mortar for Strengthening of Shear-Critical RC Beams

This chapter will be submitted to a peer reviewed journal for publication.

The contributing authors are:

Azam, R., Soudki, K. and Jeffrey S. West

Contributors to this chapter include: -

Rizwan Azam: Ph.D. candidate, who researched, analyzed, and wrote the paper.

Khaled Soudki: Supervisor to Rizwan Azam; Deceased September 17, 2013

Jeffrey S. West: Supervisor to Rizwan Azam and assisted with research direction, editing, and general advice.

5.1 Introduction

Fibre reinforced polymer (FRP) systems have been used to strengthen and repair many reinforced concrete (RC) members worldwide. A number of studies reported in the literature have demonstrated the effectiveness of FRPs to strengthen shear-critical RC members; ACI 440.2R (2008) and Belarbi et al. (2011) are excellent sources of information on shear strengthening using FRPs. In spite of its wide use and effectiveness, the use of epoxy as a bonding agent in FRP strengthening systems may not be optimal for some applications due to poor compatibility with concrete substrate, limited or no moisture diffusion, requirement for special handling/protection equipment for manual workers, and most importantly because post-repair inspections and assessment of the structure is difficult since the FRP effectively hides the conditions underneath the repair system.

Cement-based composites are a relatively new strengthening and rehabilitation system. They have almost all of the same benefits of typical FRP systems such as low weight, ease of installation and non-corroding properties, but overcome some of the drawbacks of using epoxy as bonding agent such as poor compatibility with the concrete substrate, lack of vapour permeability and fire resistance. A cement-based composite system replaces the epoxy with cementitious mortar, and the fibre sheets are replaced with fabrics or FRP grids.

Two types of cement-based systems have been reported in the literature. The first type of cement-based composite system consists of an open-weaved fabric and mortar. This type of cement-based system has been referred to in the literature as fabric reinforced cementitious matrix (FRCM), textile reinforced concrete (TRC), and textile reinforced mortar (TRM). The majority of the studies on the strengthening of shear-critical RC beams with cement-based systems have been conducted using this type system (Escrig et al., 2015; Tzoura and Triantafillou 2015; Azam and Soudki 2016; Azam and Soudki 2014a; Al-Salloum et al., 2012; Bruckner et al., 2008; Bruckner et al., 2006; Triantafillou et al., 2006). The second type of cement-based composite system consists of FRP grid and mortar. This type of system has been referred to in the literature as mineral-based composites (MBC) systems. Only one study has been reported in the literature to date to investigate the behaviour of shear-critical RC beams strengthened with this type of strengthening system (Blanksvard et al., 2009).

Recently, a pilot study was conducted to compare the effectiveness of these two types of cement-based systems for strengthening of shear-critical RC beams (Azam and Soudki, 2014b). The results of the pilot study indicated that the MBC system (CFRP grid embedded in mortar) is a promising strengthening system, and in some cases may perform better compared to other types of cement-based systems.

The literature review revealed that CFRP grid embedded in mortar (CGM) is a promising strengthening technique. However, very limited research has been

conducted on this topic. Therefore, a need exists for further investigation of the effectiveness of CGM strengthening for shear-critical RC beams.

Recent studies on shear strengthening of RC beams with FRPs have indicated that the interaction between the externally bonded shear strengthening system (FRPs) and the internal transverse reinforcement is still not well understood. Chen et al. (2010) found that the stirrups did not yield in beams strengthened with FRPs raising a concern that it might not be safe to assume that the stirrups have yielded when calculating the shear strength of strengthened beams. In addition, a number of researchers have reported a reduction in the shear strength contribution from externally bonded FRP sheets in beams with stirrups (Pellegrino and Modena 2002; Chaallal et al. 2002; Mofidi and Chaallal 2014; Belarbi et al. 2012; Colalillo and Sheikh 2014).This indicates that there is a need to further investigate the interaction between externally bonded system and the internal transverse reinforcement in the overall shear capacity of the strengthened beam.

The current research study was designed to investigate the effect of internal transverse reinforcement on behaviour of shear-critical RC beams strengthened with a CGM system, in particular to focus on the interaction between the CGM and the internal transverse reinforcement. In order to investigate the interaction between the CGM and the internal transverse reinforcement, the shear resistance provided by the CGM and the internal transverse reinforcement was calculated using experimentally measured

strains in CGM and stirrups. The current study will help better understand the interaction between the CGM and the internal transverse reinforcement. This study is part of a larger research program on strengthening of reinforced concrete structures using cement-based strengthening systems.

5.2 Research Program

In order to examine the structural performance of shear-critical RC beams strengthened with CFRP grid embedded in mortar, six full scale beams were fabricated and tested to failure.

5.2.1 Test Specimens

The details of the beam specimens are presented in Figure 5.1 and Table 5.1. All beams were 250 mm wide, 400 mm deep and 2700 mm long. The longitudinal tensile reinforcement in all of the beams was 6-25M bottom bars and 3-25M top bars. The side and vertical covers to the tension reinforcement were kept at 40 mm for all beams. The internal transverse steel reinforcement was provided in three configurations: no stirrups, 6 mm stirrups @ 150 mm c/c, and 6 mm stirrups @ 250 mm c/c. Three additional stirrups were provided in the anchorage zone for the longitudinal reinforcement in all beams.

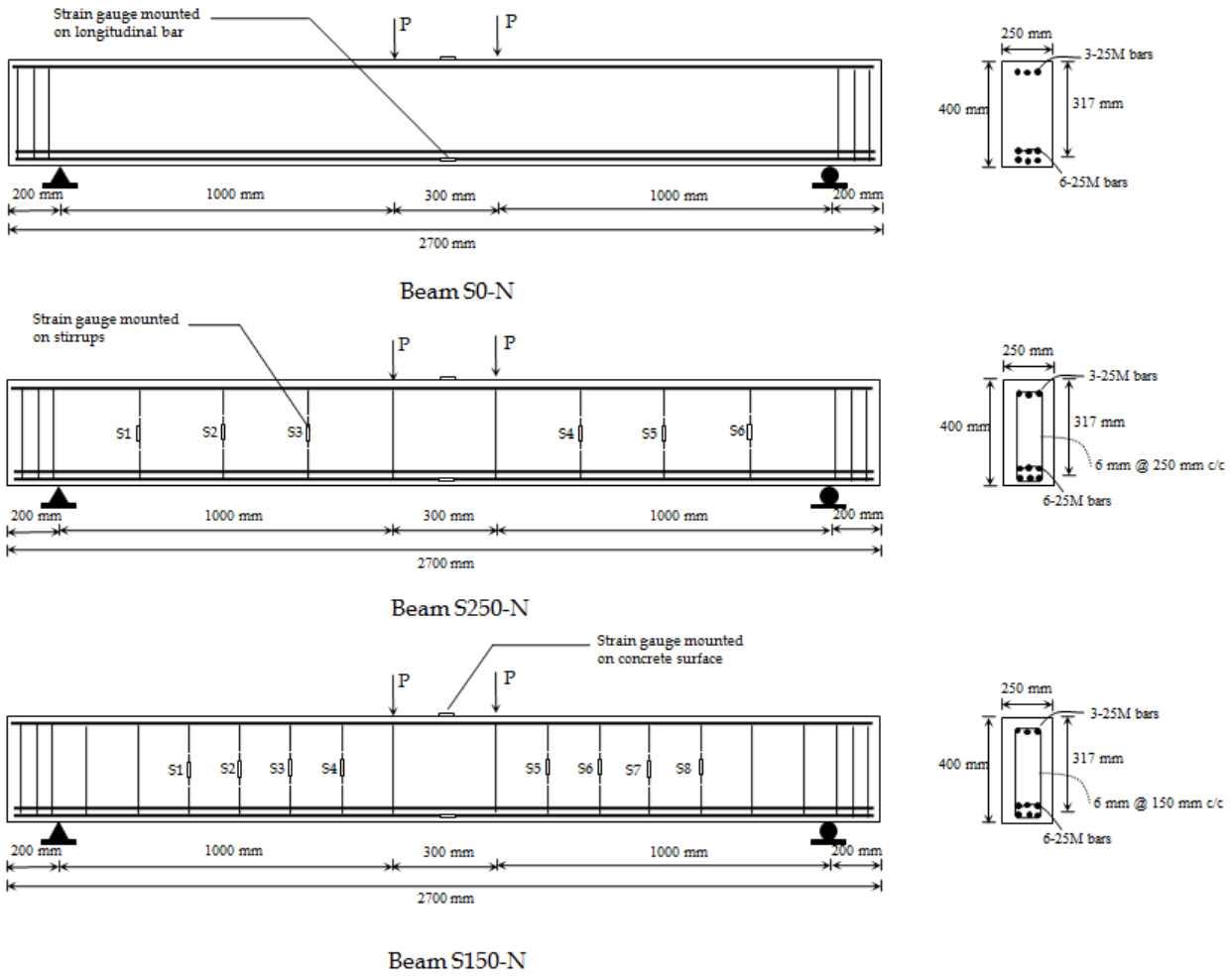

Figure 5.1 : Beam geometry, reinforcement details and layout of strain gauges

Table 5.1 : Details of test specimens

Sr. No.	Beam Designation	Longitudinal Reinforcement			Shear Reinforcement	
		Amount of Rebar	ρ	ρ / ρb	Internal Steel Stirrups	External Strengthening
1	S0-N	6-25M (T) + 3-25M (C)	3.79	0.55	None	None
2	S150-N				6mm @150 mm c/c	None
3	S250-N				6mm @250 mm c/c	None
4	S0-CGM				None	CGM
5	S150-CGM				6mm @150 mm c/c	CGM
6	S250-CGM				6mm @250 mm c/c	CGM

The beam designation used in this study is as follows: YY-ZZ with YY = steel reinforcement and ZZ= strengthening system. The steel reinforcement is specified as S0 (beams without stirrups), S150 (beams with 6 mm stirrups @ 150mm c/c) and S250 (beams with 6 mm stirrups @ 250mm c/c) and the strengthening system is specified as N (none) and CGM (CFRP grid embedded in mortar).

5.2.2 Material Properties

The concrete used to fabricate the test beams was supplied by a local ready-mix concrete supplier. The concrete was batched with Type GU portland cement and had a maximum coarse aggregate size of 19 mm and a water cementing-material ratio of 0.45. Six concrete cylinders (100 mm x 200 mm) were also cast from the same concrete batch. The 28 day compressive strength of the concrete was 63 ± 1 MPa. The longitudinal and transverse steel had a yield strength of 494MPa and 365 MPa, respectively, as reported by the supplier.

The CFRP grid had tensile modulus of 234.5 GPa and elongation at rupture of 0.76%. The CFRP grid had an ultimate strength of 80 kN/m in both directions. The orthogonal spacing of CFRP grid was 41 x 46 mm (Figure 5.2). Note that all properties of the CFRP grid are as reported by the Manufacturer. Sika Monotop 623, polymer modified, one component, and early strength-gaining cementitious mortar was used as the bonding agent in the CGM composite layer. The compressive strength of the mortar was measured using 50 mm cubes. The compressive strengths of the mortar at 3, 7 and 28 days were 41±3.3, 45±2.4 and 58±2.8 MPa, respectively.

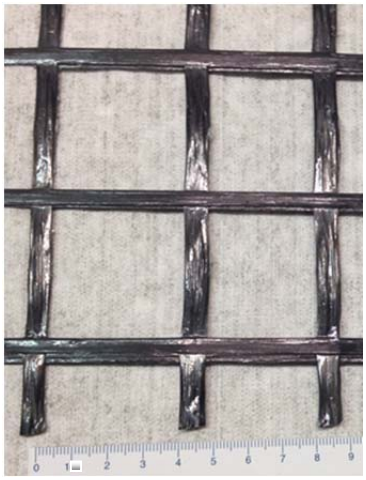

Figure 5.2 : CFRP grid used in study

5.2.3 Cement-Based Composite Strengthening

Three beams were strengthened with CFRP grid embedded in mortar (CGM) installed on the shear spans of the beams. The strengthening procedure is presented in detail by Azam and Soudki (2014a) and is summarized below.

The concrete surfaces were first sand-blasted to expose the aggregates. Water was sprayed on the dry concrete surfaces of the beams until the saturated surface dry (SSD) condition was achieved. Once the SSD condition was achieved, the first layer of mortar was applied. After the application of the first layer of mortar, the CFRP grid was pressed into the mortar. Then a final layer of mortar was applied to completely cover the CFRP grid. Finally, the beam surface was finished with a trowel. The total thickness of the strengthening system was about 8-12 mm.

5.2.4 Instrumentation

All of the tested beams were instrumented with one strain gauge (5 mm gauge length) mounted at midspan on one of the longitudinal bars in the bottom layer of reinforcement, and one strain gauge (60 mm gauge length) mounted on the concrete compression surface under the loading point. Two linear variable differential transducers (LVDTs), with a range of 0 to 25 mm, were placed at mid-span to measure the deflection of the beam. Figure 5.1 and Figure 5.3 show the layout of instrumentation.

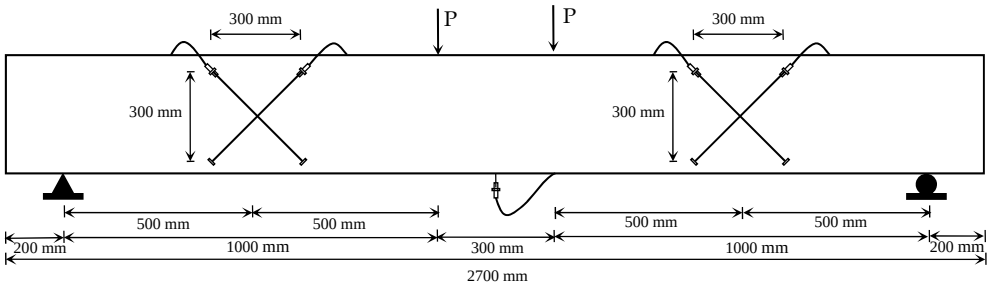

Figure 5.3 : Layout of LVDTs

5.2.5 Test Setup and Procedure

The beams were tested in four-point bending using a large portal frame equipped with a 2500 kN closed-loop hydraulic actuator. The beams were simply supported with roller and hinge supports over a clear span of 2300 mm. The spacing between load points was 300 mm and shear span was 1000 mm. The load was transferred from the actuator to the beam through two loading plates at mid-span. To uniformly distribute the load on concrete surface, the loading plates were levelled on the beam using hydro-stone. The test setup is shown in Figure 5.4.

Figure 5.4 : Test Setup

The test procedure was as follows: the beam was placed over the supports, leveled and centered. All of the instrumentation (LVDT and strain gauges) was mounted on the beam and connected to the data acquisition system. The data acquisition system started gathering data before the application of load. The load was increased monotonically at a stroke rate of 0.3 mm/min. using a ramp function generator until failure of the beam. During the test, the initiation and progression of cracks were monitored.

5.3 Test Results and Discussion

5.3.1 General Behaviour

A summary of test results is given in Table 5.2. In general, the CGM (CFRP grid embedded in mortar) shear strengthening was effective in enhancing the load carrying

capacity of shear-critical RC beams. The increase in ultimate load ranged between 10% and 45% in comparison to the control (unstrengthened) beams. The CGM shear strengthening significantly increased the deflection at failure of the strengthened beam without stirrups by 165% (from 4.0 mm to 10.6 mm) compared to the control (unstrengthened) beam without stirrups. The deflection at ultimate load in control (unstrengthened) and strengthened beams with stirrups ranged between 11.3 mm and 12.9 mm. This indicates that there was almost no effect of the strengthening systems on the deflection at ultimate load in beams with stirrups. All of the beams failed in shear as expected, as confirmed by the shear cracking and limited ductility in the load-deflection response. In addition, the measured steel and concrete strains were consistent with shear failure rather than flexural failure; the measured concrete compressive strains at failure in all beams were below the maximum compressive strain of 3500 με normally associated with concrete crushing at flexure, and the measured tensile strains were below the yield strain of 2500 με with the exception of beam (S150-CGM). It is important to note that all beams were reinforced with 6-25M bottom rebar placed in two layers and strain gauges were mounted on the bottom layer of steel.

Table 5.2 : Summary of test results

Beam designation	Ultimate load (kN)	Increase in ultimate load due to Strengthening (%)	Deflection at ultimate load (mm)	Strain in longitudinal reinforcement at midspan at ultimate load (με)	Concrete strain at midspan at ultimate load (με)	Failure mode
S0-N	287.2	-	4.0	1073	839	shear
S150-N	613.9	-	12.7	2595	1984	shear
S250-N	520.3	-	12.1	1870	2465	shear
S0-CGM	423.5	47.5	10.6	1573	1407	shear
S150-CGM	677.4	10.3	12.9	2657	2399	shear
S250-CGM	570.6	10.0	11.3	2352	1883	shear

5.3.2 Failure Modes

All of the tested beams failed in shear by diagonal tension failure. The failure modes for all beams are shown in Figure 5.5. The cracking in all beams was initiated with the appearance of flexural cracks at midspan. As the load increased, a single, more inclined crack appeared in the shear span which progressed towards the load point and the support region, eventually leading to a diagonal tension failure. The control unstrengthened beam without stirrups exhibited a single shear crack, while the beams with stirrups and strengthened beams exhibited more than one shear crack.

The control unstrengthened beam without stirrups failed suddenly after formation of a single diagonal crack, while the control unstrengthened beam with stirrups continued carrying load after formation of the diagonal shear cracks until yielding of the stirrups resulted in beam failure. In the strengthened beams without stirrups, the shear force was carried by the strengthening layer after formation of the diagonal cracking until the

strengthening layer was unable to control the shear crack propagation, which resulted in beam failure. In the strengthened beams with stirrups, the shear force was simultaneously carried by the stirrups and the strengthening layer until the combined effect of stirrups and strengthening layer was unable to control the shear crack propagation, which resulted in beam failure. The possible shear transverse mechanism of the CGM (CFRP grid embedded in mortar) strengthening layer is described below.

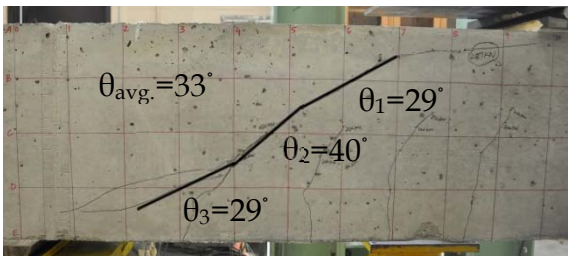

Beam S0-

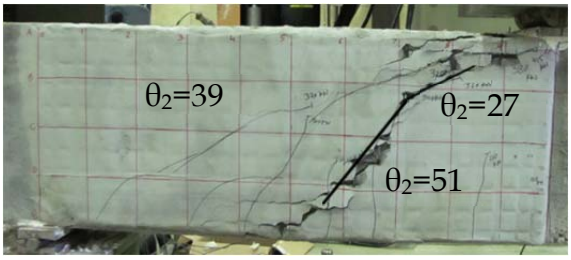

Beam S0-

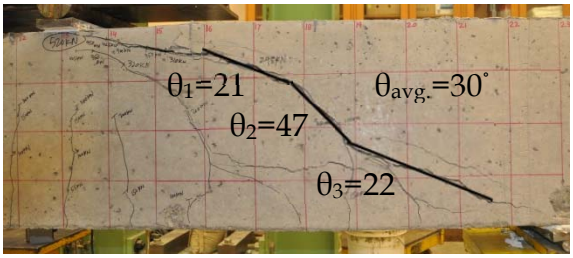

Beam S250-

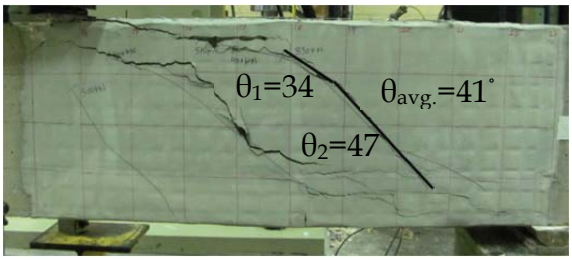

Beam S250-CGM

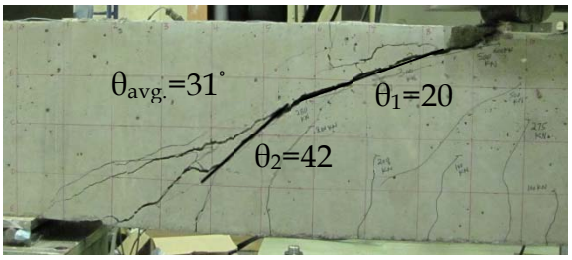

Beam S150-

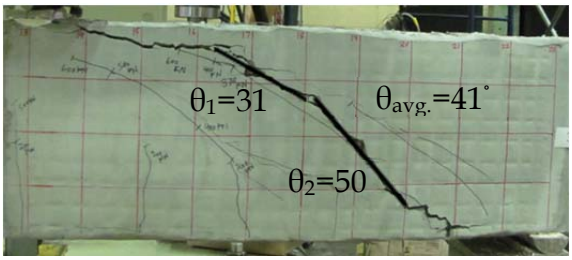

Beam S150-

Figure 5.5 : Failure modes

At the onset of diagonal cracking, the transverse tows of the CFRP grid intersect the crack and restrain the crack opening. The shear force carried by the transverse tows of the CFRP grid is transferred to the longitudinal tows which act as anchorage to the transverse tows. In this shear transfer mechanism, a failure could happen at two locations: firstly, when shear is transferred from the traverse tows to the longitudinal tows if the orthogonal connection between the tows is broken, and secondly when the shear is transferred from the longitudinal tows to the mortar if the longitudinal tows do not have enough mortar cover and fail by peeling or cover spalling. In the current study, the failure of the strengthening layer was caused by one or both of these mechanisms. Figure 5.6 shows a close-up of the strengthening layer at failure shear cracks where the separated tows in the orthogonal directions and mortar cover spall are visible.

Figure 5.6 : Failure of strengthening layer – A close-up view

5.3.3 Strain in Stirrups and CGM Strengthening Layer

Figure 5.7 shows the typical load versus strain behaviour for all four stirrups that intersected the main shear crack in the strengthened beam (S150-CGM). Figure 1 shows the location of all stirrups in beam S150-CGM. As expected, the strain in the stirrups is negligible until formation of the shear crack, and the strains increased rapidly after formation of shear cracking.

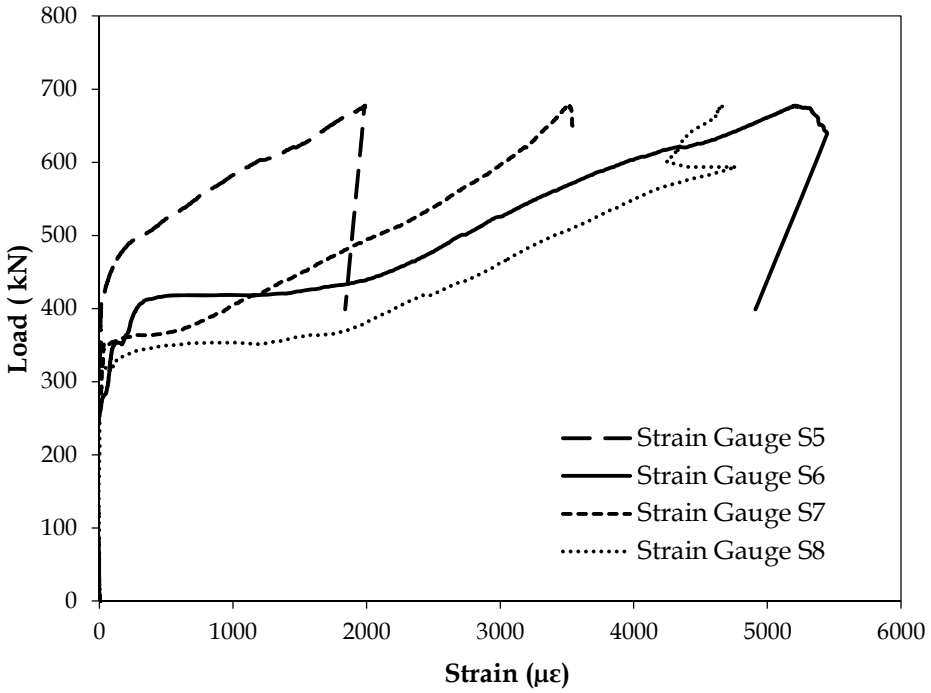

Figure 5.7 : Typical load vs. strain in stirrups (beam S150-CGM)

The main shear crack appeared at location of stirrup S8 in beam S150-CGM. As the applied load increased, the shear crack propagated towards stirrups S6 and S7 (towards the load point). With further increases in load, the shear crack intersected stirrup S5,

after which all stirrups carried shear force until failure of the beam. The shear crack pattern is consistent with the strain in the stirrups as shown in Figure 5.5. All stirrups reached or exceeded the yield strain of 1825 με prior to failure of the beam.

Figure 5.8 shows the load versus average stirrup strain behavior for all tested beams. The average strain in all stirrups that intersected the main shear crack was used to illustrate the effect of amount of stirrups on the contribution from the CFRP grid embedded in mortar (CGM) strengthening. As shown in Figure 5.8, beams with more closely spaced stirrups (S150-N and S150-CGM) exhibited a lower average strain in the stirrups compared to beams with fewer stirrups (S250-N, S250-CGM). This is mainly attributed to the increased axial stiffness of the more closely spaced stirrups. Similarly, the strengthened beams (S150-CGM and S250-CGM) showed a lower average strain in the stirrups compared to the control unstrengthened beams (S150-N, S250-N). This reduction in strain for strengthened beams is due to the fact that shear force is simultaneously carried by the stirrups and the strengthening layer in this situation.

Figure 5.9 shows the strain distribution in the steel stirrups and CGM strengthening layer across shear crack in the strengthened beams (S150-CGM and S250-CGM) at failure. The strain in the stirrups was measured using strain gauges mounted on stirrups; whereas the vertical strain in the CGM strengthening layer was calculated from strain measured using diagonal LVDTs. The strains measured using strain gauges mounted on the stirrups were lower compared to strain measured using diagonal

LVDTs (Figure 5.9). It is important to note that the strain in the stirrups at particular section depends on the proximity of strain gauge to shear crack, whereas LVDTs measured the average strain across the shear crack. As well, the vertical strain in the CGM using LVDTs was only measured at mid-shear span. The average CGM strain across shear crack was calculated by multiplying the measured vertical strain in CGM by 2/3 assuming that the vertical CGM strain measured at mid shear span was maximum CGM strain. The 2/3 ratio between the maximum and average shear strains along an inclined shear crack is based on the assumption of a parabolic distribution of shear stress along the crack length as described by Carolin and Taljsten (2005) and Blanksvard et al. (2009). The average strains across shear crack at failure in beams S150-CGM, S250-CGM and S0-CGM were 4673με, 4960με and 4385με, respectively.

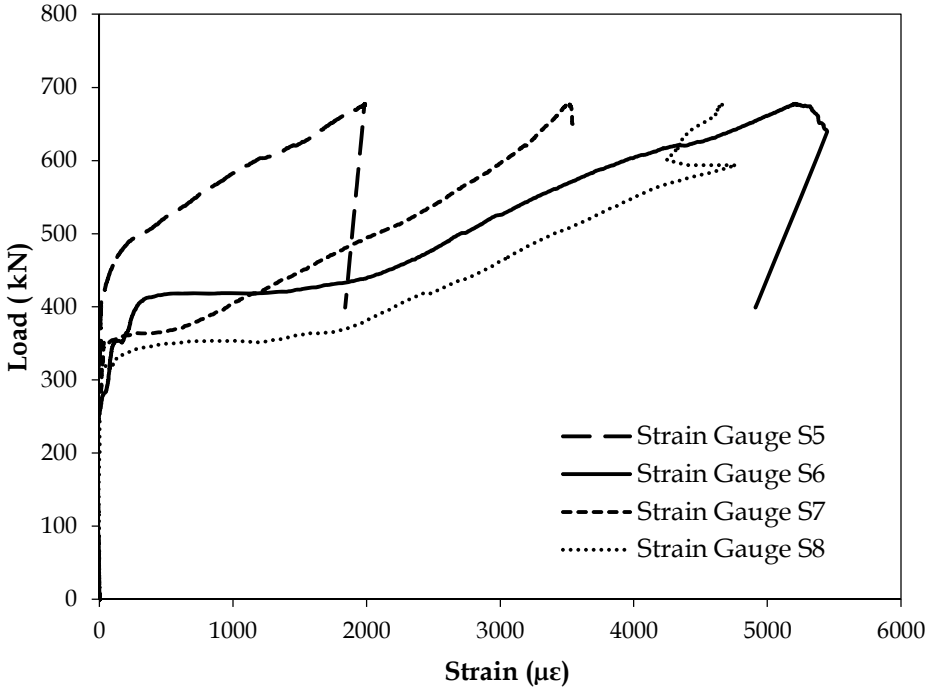

Figure 5.8 : Load vs. average strain in stirrups for all beams

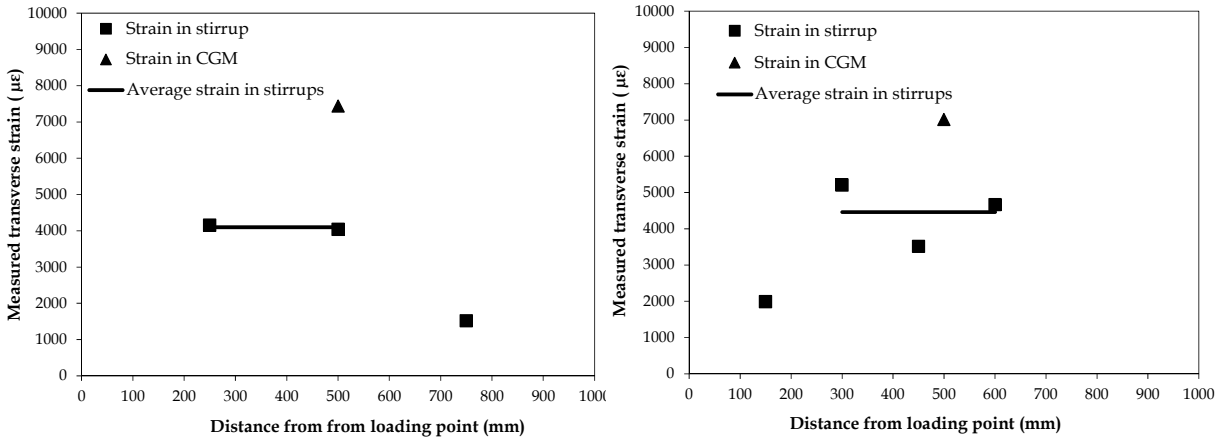

Figure 5.9 : : Strain distributions in stirrups and FRCM strengthening layer across shear crack in strengthened beams with stirrups (a) beam S250-CGM (b) beam S150-CGM

5.3.4 Load-Deflection Response

The load-deflection response for all of the beams is shown in Figure 5.10 and Figure 5.11. In general, the load-deflection response of all beams, except (S0-N), was almost bilinear with no ductility indicating the brittle nature of shear failure. A change in stiffness is noted coincident with the formation of shear cracking. The load-deflection response of the control beam without stirrups (S0-N) was essentially linear as it failed suddenly after formation of the first diagonal shear crack.

Effect of Strengthening: The effect of CGM (CFRP grid embedded in mortar) strengthening on the load-deflection response of the beams is shown in Figure 5.10 (a-c). The control unstrengthened beam without stirrups (S0-N) failed at a load of 287.2 kN, while the control unstrengthened beams with stirrups, SI50-N and S250-N failed at loads of 613.9 kN and 520.3 kN, respectively. The strengthened beams without stirrups (S0-CGM) failed at a load of 423.5 kN compared with the failure loads of 677.4 kN and 570.6 kN, for strengthened beams with stirrups (S150-CGM and S250-CGM), respectively. The CGM (CFRP grid embedded in mortar) strengthening system increased the ultimate load by 47.5 % for beam without stirrups (L-CGM) compared with the increase in ultimate load of 10.3% and 10.0% for beams with stirrups at 150 mm c/c (S150-CGM) and beams with stirrups 250 mm c/c (S250-CGM), respectively. The attenuating effect of stirrups on shear strength contribution of shear strengthening is discussed in detail below. The minimum deflection of 4.0 mm at failure was observed

for control unstrengthened beam without stirrups (L-N). The deflection at failure for all other beams ranged between 10.6 to 12.9 mm. The CGM strengthening slightly increased the stiffness of the strengthened beams compared to the control unstrengthened beam.

The attenuating effect of stirrups on shear strength contribution of shear strengthening has been reported by other researchers (Pellegrino and Modena 2002; Chaallal et al. 2002; Mofidi and Chaallal 2014; Belarbi et al. 2012; Colalillo and Sheikh 2014). Some researchers have concluded that the reduced bond strength between the FRP sheet and concrete in beams with stirrups is the main cause for the reduction in shear strength contribution from the externally bonded FRP sheets in beams with stirrups (Pellegrino and Modeno 2002; Mofidi and Chaalal 2014) since a beam with stirrups will experience several shear cracks compared to a single shear crack in beams without stirrups. The increased cracking results in a shorter bond length for FRP sheets which leads to debonding of FRP sheets at lower loads.

The effect of the stirrups on effectiveness of CGM strengthening is discussed further following the discussion of the interaction between shear components.

Effect of Stirrups: The effect of the stirrups on the load-deflection response of the beams is shown in Figure 5.11 (a-b). As expected, the beams with stirrups experienced higher stiffness compared to the beams without stirrups. Figure 5.11a shows the effect of stirrups on the load-deflection response of the control unstrengthened beams. The

presence of stirrups resulted in higher ultimate load and higher deflection at ultimate load in the control unstrengthened beams (Table 5.2); the control beam without stirrups (S0-N) failed at a load of 287.2 kN, while the control beams with stirrups, S150-N, S250-N, failed at loads of 613.9 kN and 520.3 kN, respectively. This represents an increase in ultimate load of 115% and 81%, respectively. The deflection at ultimate load in the control beams with stirrups ranged between 12.1 mm to 12.7 mm compared with a deflection of 4.0 mm in control beam without stirrups, representing an increase of 200% to 218%. Figure 5.11b shows the effect of stirrups on the load-deflection response of the CGM strengthened beams. The presence of stirrups resulted in 60% and 35% increase in ultimate load for the strengthened beams with stirrups (S150-CGM and S250-CGM, respectively) compared to the strengthened beam without stirrups, S0-CGM (Table2).

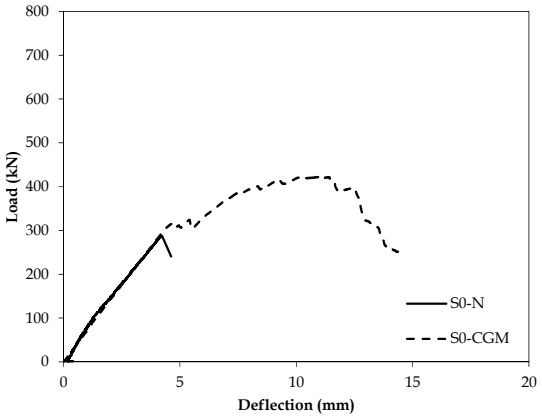

(a)

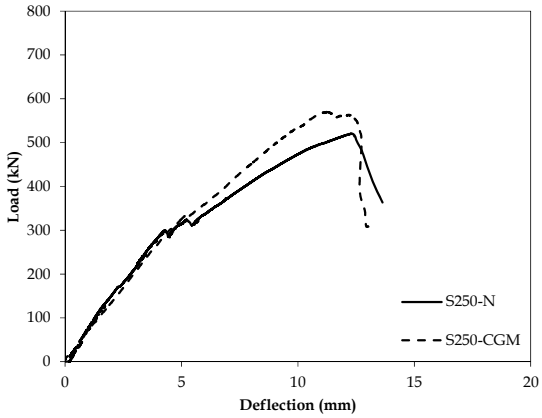

(b)

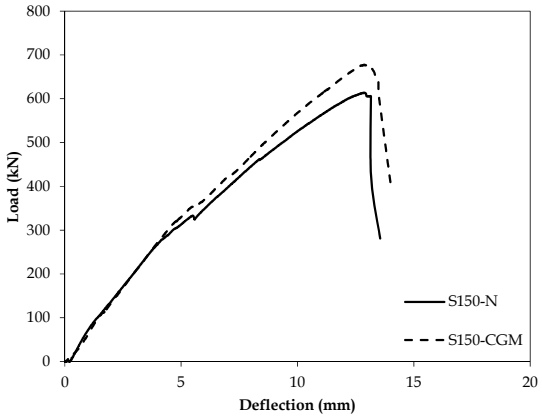

(c)

Figure 5.10 : Effect of strengthening on load vs. deflection response of tested beams (a) beams without stirrups (b) beams with stirrups at 250 mm c/c (c) beams with stirrups at 150 mm c/c.

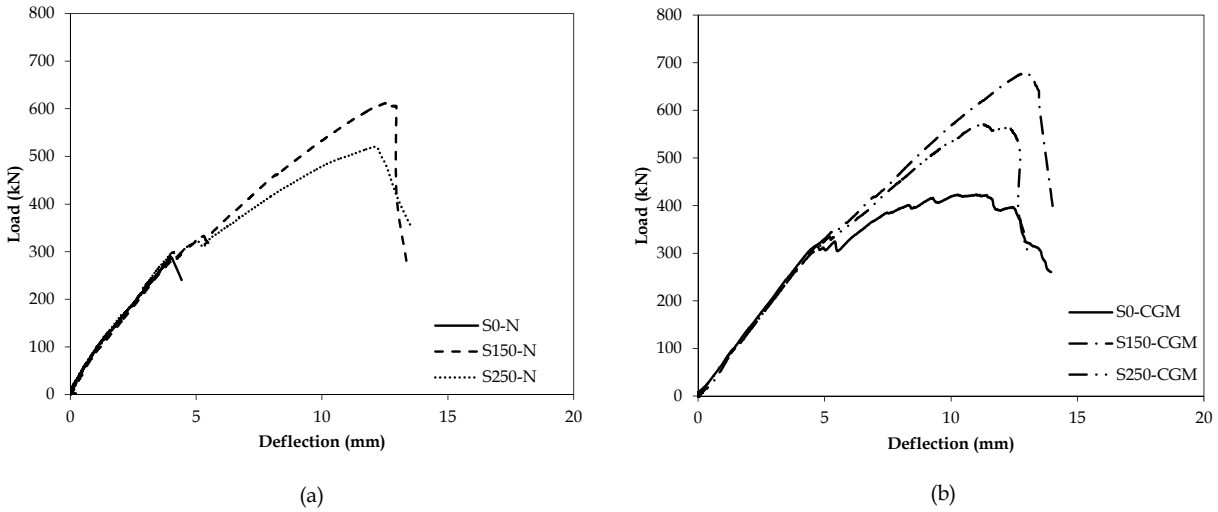

Figure 5.11 : Effect of stirrups on load vs. deflection response (a) control unstrengthened beams (b) strengthened beams

5.3.5 Interaction between Shear Components

The shear resistance provided by the different component materials (concrete, steel and CGM) was calculated in order to investigate the interaction between the different shear components. A shear component analysis was performed using free body diagrams (FBDs) drawn for each specimen at failure (**Error! Reference source not found.**). The geometry of the FBDs was based on the shear crack geometry as shown previously in Fig. 5. The shear resistance provided by the stirrups crossing the shear crack was calculated as:

$$V_s = n.A_v.f_v \qquad \text{Equation 5.1}$$

Where V_s is the shear resistance provided by the steel stirrups; n is the number of stirrups crossing the crack; A_v is the cross sectional area of one stirrup and f_v is the

average stress in the stirrups crossing the failure crack determined from the experimental stirrup strain measurements. The shear resistance provided by the CGM strengthening layer was calculated as:

$$V_{CGM} = 2.t_{CGM.}E_{CGM}.\varepsilon_{CGM}.d\ cot\theta \qquad \text{Equation 5.2}$$

where V_{CGM} is the shear resistance provided by the CGM strengthening layer; t_{CGM} is the equivalent design thickness of CFRP grid used in CGM strengthening layer; E_{CGM} is the tensile modulus of the CFRP GRID used in the CGM; ε_{CGM} is the average measured strain in the CGM strengthening layer.; d is effective depth of beam and θ is the experimentally observed average shear crack angle.

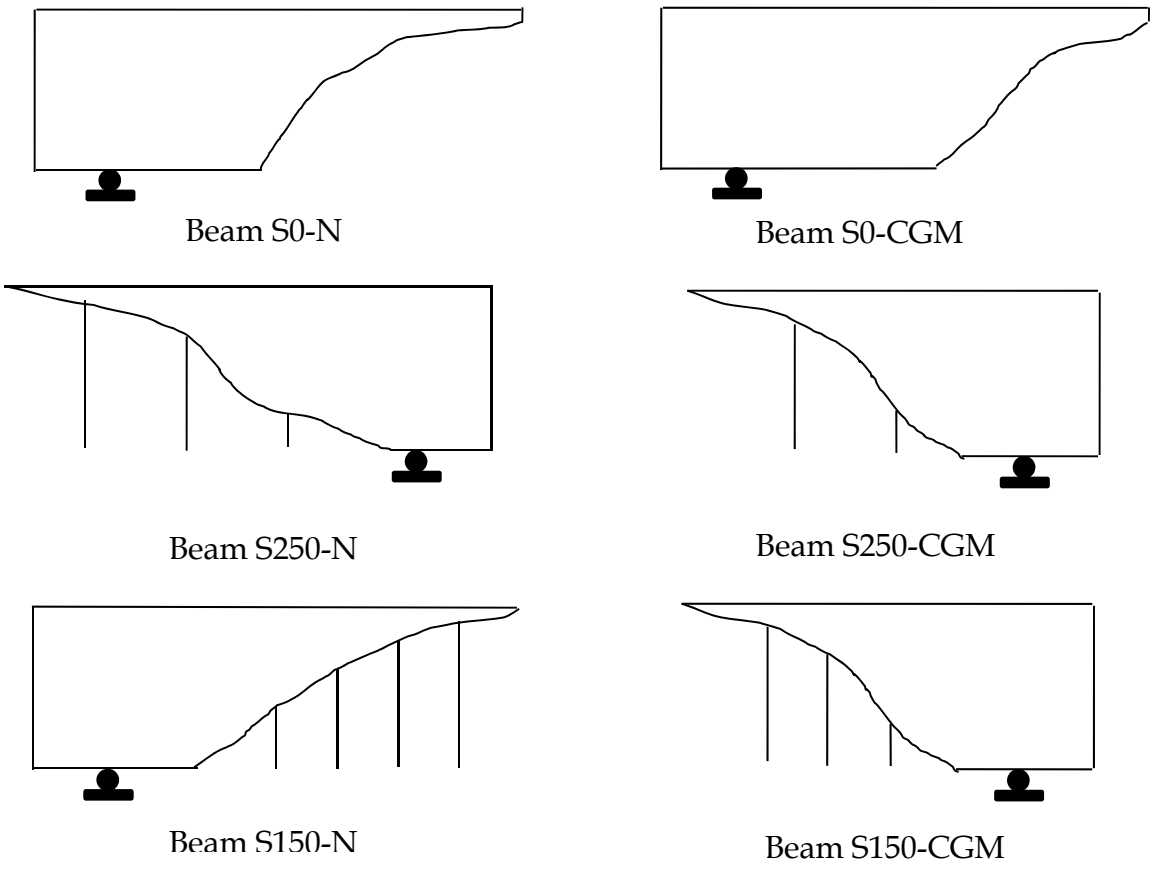

Figure 5.12 : FBDs used for shear component analysis

The shear resistance provided by the concrete was calculated by subtracting the shear resistance provided by the stirrups and strengthening layer from the experimentally observed total shear resistance:

$$V_c = V_{total} - V_s - V_{CGM} \qquad \text{Equation 5.3}$$

where V_{total} is the shear force in the beam shear span at failure. Figure 5.13 shows the shear component diagrams based on the analysis procedure described above. For the control unstrengthened beams, the shear resistance provided by the concrete increased

with the addition of stirrups since the beams did not fail suddenly after yielding of the stirrups. The shear resistance provided by concrete increased further with the addition of the strengthening layer. Overall, the shear resistance provided by the concrete increased with an increase in total shear reinforcement ratio. The increase in shear resistance provided by the concrete is possibly due to two reasons: 1) the confinement provided by internal and external shear reinforcement, or 2) the shear transfer mechanism changes to arch action, or both.

The shear resistance provided by the steel stirrups decreased with the addition of the strengthening layer due to a change in the diagonal crack angle. The addition of the strengthening layer resulted in steeper diagonal cracking which intersected fewer stirrups (see Figure 5.5) and resulted in a lower overall shear resistance provided by stirrups. Malek and Saadatmanesh (1998) have shown the similar effect of the amount of transverse reinforcement on the diagonal crack angle in RC beams.

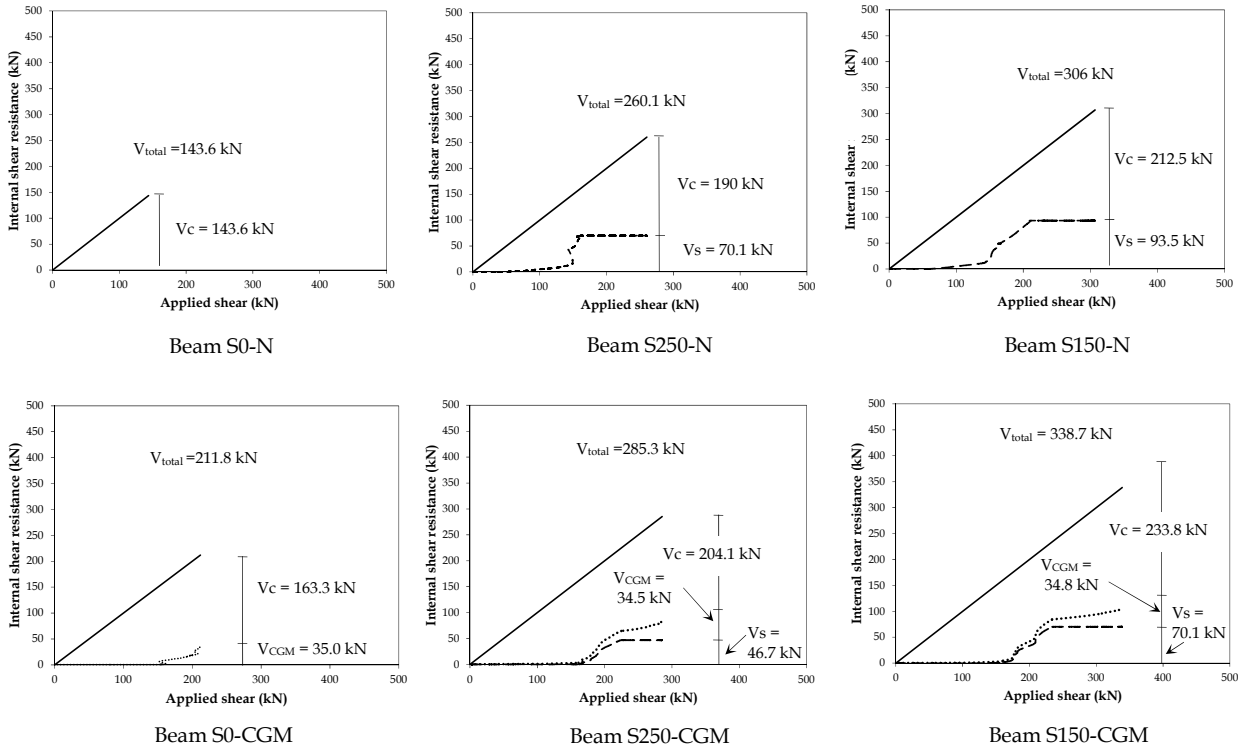

Figure 5.13 : Shear component diagrams for tested beams

5.4 Comparison of Experimental and Predicted CGM Shear Strength Contributions

The contribution of an externally bonded strengthening systems to the shear strength of a beam is commonly estimated by subtracting the failure load of the control unstrengthened beam from that of the companion strengthened beam: ($V_{CGM} = V_{STRENGTHENED} - V_{CONTROL}$). However, this method may not provide an accurate estimate of the actual shear force carried by the external strengthening system as this method does not consider any interaction between the shear resistance components. Therefore,

the CGM shear resistance estimated using the experimentally measured CGM strain and measured crack angle were also considered as presented in the preceding section. The experimental CGM shear strength contributions estimated using both methods are listed in Table 5.3 and discussed in detail below.

Table 5.3 : Comparison between experimental and predicted shear contributions for CFRP Grid in mortar

Beam designation	Experimental		Predicted								
			ACI 440.2R (2008)			CAN/CSA–S6 (2006)			Blanksvard et al. (2009)		
			θ = 45			θ = 33-35			θ = 33-35		
	V_{CGM} (exp-1) = $V_{STRENGTHENED}$ – $V_{CONTROL}$ (kN	V_{CGM} (exp-2) = 2.t_{CGM}.E_{CGM}.ε_{CGM}.dcotθ	V_{CGM} (kN)	V_{exp-1} / V_{pre}	V_{exp-2} / V_{pre}	V_{CGM} (kN)	V_{exp-1} / V_{pre}	V_{exp-2} / V_{pre}	V_{CGM} (kN)	V_{exp-1} / V_{pre}	V_{exp-2} / V_{pre}
S0-CGM	68.15	35.0	18.2	3.74	1.92	28.1	2.42	1.24	73.05	0.93	0.48
S150-CGM	31.75	34.8	18.2	1.74	1.91	27.3	1.16	1.27	71.15	0.45	0.49
S250-CGM	25.1	34.5	18.2	1.38	1.90	26.8	0.94	1.29	69.25	0.36	0.50
Mean				2.30	1.91		1.50	1.27		0.58	0.49
Coefficient of Variation, %				1.30	0.01		0.80	0.03		0.30	0.01

Note: Angles used are as per these design approaches

The shear strength contribution from externally bonded materials such as FRP sheets or FRP grid embedded in mortar is generally predicted using a truss analogy approach similar to that used for steel stirrups. The only difference is the stress level at ultimate used in these materials: yield stress is used for the steel stirrups, while the effective stress is used for externally bonded FRP sheets. The following sections present different

FRP design guidelines along with proposed modifications to predict the shear strength contribution from the CFRP grid embedded in mortar. The following sections present different design methods used to predict the shear strength contribution from the CGM strengthening system.

5.4.1 ACI 440.2R-08

The ACI 440.2R-08 (2008) provisions to calculate the shear strength contribution from externally bonded FRP sheets are based on a 45˚ truss analogy approach as follows:

$$V_f = \frac{A_f f_{fe} . (sin\alpha + cos\,\alpha) . d_{fv}}{s_f} \qquad \text{Equation 5.4}$$

where $A_f = 2. t_f. w_f =$ cross section area of the FRP sheet ; $f_{fe} = \varepsilon_{fe} E_f$ = effective FRP stress; ε_{fe} is the effective FRP strain; E_f is the elastic tensile modulus of the FRP sheet; d_{fv} is the internal lever arm; α is the angle of orientation of the FRP sheet with respect to the longitudinal axis of the beam and s_f is the spacing of FRP shear reinforcement. The effective FRP strain for fully wrapped beams is limited to 0.004 based on loss of aggregate interlock in concrete by ACI 440.2R-08, and the effective FRP strain for u-wrapped or side bonded beams is calculated based on the FRP to concrete bond mechanism.

Debonding of the strengthening layer was not observed in the current study, and therefore, the FRP strain limits based on FRP to concrete bond were not used in the

current study. However, the effective FRP strain limit based on aggregate interlock (0.004) is still applicable, and was used to estimate the shear strength contribution from the strengthening layer in the current study.

5.4.2 CAN/CSA-S6 2006

The CAN/CSA-S6 (2006) provisions to calculate the shear strength contribution from externally bonded FRP are similar to those in ACI 440.2R (2008) except that the CSA S6 provisions are based on the variable angle truss model as follow:

$$V_f = \frac{A_f . E_f . \varepsilon_{fe} . d_f . (cot\theta + cot\alpha) . sin\alpha}{s_f} \qquad \text{Equation 5.5}$$

where, θ is the angle of the shear crack estimated using the General Method (based on modified compression field theory) as presented in CSA A23.3-04 (all other variables as defined previously for ACI 440.2R-08 approach). In the current study, the effective strain limit of 0.004 based on aggregate interlock was used to calculate the shear strength contribution from the strengthening layer.

5.4.3 Blanksvard et al. (2009)

Blanksvard et al. (2009) proposed a simple approach to calculate the shear strength contribution from CGM as presented in Equation 5.6 to Equation 5.9.

$$V_{CGM} = V_{CFRP\ GRID} + V_{MORTAR} \qquad \text{Equation 5.6}$$

where V_{CGM} is the shear strength contribution for CGM, $V_{CFRP\ GRID}$ is the shear strength contribution from the CFRP grid alone and V_{MORTAR} is the shear strength contribution from the mortar. The shear strength contribution from the CFRP grid is given in Equation 5.7:

$$V_{CFRP\ GRID} = \frac{2.\varepsilon_{ver,ef}.E_{ver}.A_{ver}.h_{ef}.cot\theta}{S_{ver}} \qquad \text{Equation 5.7}$$

$$\varepsilon_{ver,ef} = \frac{2}{3}.\varepsilon_{ver,ult} \qquad \text{Equation 5.8}$$

where $\varepsilon_{ver,ef}$ is the effective strain of the fiber grid tows in the vertical direction; E_{ver} is the elastic modulus of the vertical CFRP grid tow; A_{ver} is the area of one fiber tow in the vertical direction; h_{ef} is the effective height of the section; S_{ver} is the spacing of vertical FRP grid tows; θ is the angle between shear crack and member axis; $\varepsilon_{ver,ult}$ is the ultimate strain of the fiber grid tows in the vertical direction. The shear strength contribution from mortar is given in Equation 5.9:

$$V_{MORTAR} = \frac{1}{3}t_{MBA,tot}.h_{ef}.f_{MBA,t} \qquad \text{Equation 5.9}$$

where $t_{MBA,\ tot}$ is the total thickness of the mineral-based bonding agent (mortar); h_{ef} is the effective height of the section and $f_{MBA,t}$ is the tensile strength of the mineral-based bonding agent (mortar).

In the current study, h_{ef} is equal to the height of the beam (400 mm). The total thickness of the mortar is 16 mm and the tensile strength of the mortar is 3.5 MPa as reported in the Manufacturer's product data.

5.4.4 Discussion of Analytical Results

For analysis purposes, an equivalent design thickness of 0.0436 mm was calculated for the CFRP grid used in this study based on its ultimate strength per unit width, ultimate strain and tensile modulus. The predicted shear strength contributions for the strengthened beams are presented in Table 3 for each of the three design methods. The experimentally determined shear strength contributions for the CGM system are also listed in Table 5.3 for both approaches described previously (i.e., based on measured strains and based on capacity subtraction).

The experimental shear strength contribution estimated from capacity subtraction ($V_{CGM} = V_{STRENGTHENED} - V_{CONTROL}$) indicates that a reduction in the shear strength contribution from the CGM strengthening system occurs in beams with stirrups. In contrast, the experimental CGM shear strength estimated using experimental strain measurements suggests that the shear strength contribution from the CGM strengthening system remains essentially constant for the beams with stirrups since the measured CGM strains at failure of the beams were similar, and since there was no significant change in the angle of inclination of the shear crack. In fact, the V_{CGM}

values for all three CGM strengthened beams in this study were approximately 35 kN regardless of the internal shear reinforcement (see Table 3).

The CGM shear strength predictions using CAN/CSA-S6 (2006) were in good correlation with the experimental CGM shear contributions estimated using experimental strain measurements. The average ratio of experimental to predicted CGM shear strength contribution was 1.27 with a coefficient of variation of 0.03. In contrast, the CGM shear strength predictions using CAN/CSA-S6 (2006) were underestimated when compared with the experimental CGM shear contributions estimated from capacity subtraction ($V_{CGM} = V_{STRENGTHENED} - V_{CONTROL}$). The average ratio of experimental to predicted CGM shear strength contribution was 1.5 with a coefficient of variation of 0.8.

A comparison of the CGM shear strength predictions with experimental estimates suggests that the ACI 440.2R 2008 underestimated the shear strength contribution from CGM strengthening layer. The average ratio of experimental to predicted CGM shear strength contribution was 2.3 with a coefficient of variation of 1.3 when experimental CGM shear strength estimated from capacity subtraction ($V_{FRCM} = V_{STRENGTHENED} - V_{CONTROL}$). The average ratio of experimental to predicted CGM shear strength contribution was 1.91 with a coefficient of variation of 0.01 when experimental CGM shear strength estimated using experimental strain measurements.

In contrast to the CAN/CSA S6 and ACI 40.2R-08 predictions, the CGM shear strength predictions using the design method by Blanksvard et al. (2009) overestimated the shear strength contribution from CGM strengthening layer. The average ratio of experimental to predicted CGM shear strength contribution was 0.58 with a coefficient of variation of 0.3 when experimental CGM shear strength estimated from capacity subtraction ($V_{CGM} = V_{STRENGTHENED} - V_{CONTROL}$). The ratio of experimental to predicted shear strength was 0.93 for beams without stirrups and 0.45-0.36 for beams with stirrups. It is important to mention that Blanksvard et al. (2009) validated their design method using beams without stirrups, which may explain why the experimental to predicted shear strength ratio correlates relatively well for the beam without stirrups but significantly over predicts the strength contribution from the CGM system when stirrups are present. Overall, the design method by Blanksvard significantly over predicted the shear strength contribution from the CGM strengthening layer. This is mainly due to the higher strain limit of 0.0057 ($\varepsilon_{ver,ef} = \frac{2}{3}.\varepsilon_{ver,ult}$) used in the design method by Blanksvard et al. (2009).

5.5 Discussion of Shear Mechanisms:

The behaviour of strengthened shear-critical RC slender beams is generally described as a beam action mechanism where the shear strength of the beam is commonly determined using a truss analogy approach presented in Section 2.3.3. The total shear

strength (V_{total}) of the RC beam is taken as the sum of the shear strength contribution from concrete (V_c), the shear strength contribution from the steel stirrups (V_s) and the shear strength contribution from the strengthening system (V_{CGM}) as follows:

$$V_{total} = V_c + V_s + V_{CGM} \qquad \text{Equation 5.10}$$

For the stirrups, the truss analogy approach describes the shear strength contribution as the vertical force in the stirrups crossing a typical inclined shear crack, given by the following equation:

$$V_s = n.A_v.f_v \qquad \text{Equation 5.11}$$

where V_s is the shear resistance provided by the steel stirrups; n is the number of stirrups crossing the crack; A_v is the cross sectional area of one stirrup and f_v is the average stress in the stirrups crossing the failure crack determined from the experimental stirrup strain measurements. For design purposes, f_v, is taken as the yield strength of the stirrups. The number of stirrups crossing the crack is taken as the horizontal projected length of the crack divided by the stirrup spacing:

$$n = \frac{z \cdot \cot\theta}{s} \qquad \text{Equation 5.12}$$

where z is the internal lever arm; θ is the crack angle and s is the spacing of stirrups. The ACI Building Code for Structural Concrete (ACI 318-14) assumes a 45˚ truss model so that Equation 5.12 reduces to $\frac{z}{s}$.

The Canadian design code approach (CSA A23.3-04) considers a variable angle truss model where the crack angle (θ) increases as the transverse reinforcement ratio is increased. However, the crack angle (θ) defined in the General Method in CSA A23.3-04 shows only a minor increase in crack angle with the addition of stirrups. The Simplified Method in CSA A23.3-04 suggests that a crack angle of 35˚ can be assumed in lieu of more rigorous calculations.

The truss analogy approach defines the shear resistance provided by the strengthening layer in a similar manner as follows:

$$V_{CGM} = 2.t_{CGM.}E_{CGM}.\varepsilon_{CGM}.d\ cot\theta \qquad \text{Equation 5.13}$$

where V_{CGM} is the shear resistance provided by the CGM strengthening layer; t_{CGM} is the equivalent design thickness of CFRP grid used in CGM strengthening layer; E_{CGM} is the tensile modulus of the CFRP grid used in the CGM; ε_{CGM} is the average measured strain in the CGM strengthening layer; d is effective depth of beam and θ is the experimentally observed average shear crack angle. Note that $d\ cot\theta$ is the horizontal projected length of an inclined shear crack crossed by the strengthening system.

The mechanics of the shear strength contribution from the concrete are more complicated than those of the shear reinforcement. The influence of the reinforcement on the concrete shear contribution is not addressed consistently by different shear design approaches, and V_c is commonly taken as the ultimate shear strength of slender beams without stirrups. For example, the ACI Building Code for Structural Concrete (ACI 318-14) assumes that the shear strength contribution from concrete is the same for beams with or without stirrups and is taken as the shear causing significant cracking. Similar to ACI 318-14, the CSA A23.3-04 considers that the shear strength contribution for concrete for beams with or without stirrups is the same for beams with an effective shear depth of 300 mm or less. For beams with an effective shear depth greater than 300 mm, the V_c is increased for beams with stirrups in comparison to the same beam without stirrups. However, the increase is not a function of the amount of transverse reinforcement (assuming that at least the minimum specified shear reinforcement is provided).

The mechanics of the shear strength contributions from the stirrups and strengthening system are straightforward if the strains and crack geometry are known. For design purposes, these parameters are assumed or specified empirically as described in Section 2.3.3. From a behaviour perspective, the shear strength contributions from the stirrups and strengthening system in the beams tested in this study were determined using the experimentally observed crack angles and measured strains in the stirrups and

strengthening system. Using values of V_s and V_{CGM} determined in this manner, the concrete contribution, V_c, was estimated by subtracting the stirrup and strengthening system shear contributions from the applied shear loading on the beams. These results were presented previously in Section 5.3.5. This type of shear component analysis is useful to understand the mechanics of the strengthened beams as discussed in the following sections.

5.5.1 Stirrup Shear Contribution

As expected, the strains in the stirrups consistently exceeded the yield strain of the steel, confirming the assumption of yielding at ultimate. The strain in the stirrups reached yielding prior to failure of the beams in shear for both the unstrengthened and strengthened beams. This indicates that both V_c and V_{CGM} continued to increase after V_s reached an upper bound due to yielding of the steel stirrups (note that the measured strains in the stirrups were not large enough to be consistent with strain hardening).

5.5.2 CGM Strengthening System Contribution

The strains in the CGM system continued to increase up to failure of the beams in shear. This indicates that V_{CGM} continues to increase up to failure of the beam, as the CGM system was able to control the diagonal cracks even after the stirrups had yielded.

The average measured strain in the CGM system at ultimate exceeded 0.004 in all cases. This suggests that the assumption of a maximum CGM strain of 0.004 at ultimate is reasonable for design purposes.

5.5.3 Inclined Shear Crack Angle

As shown in Figure 5.5, the experimentally observed average shear crack angles varied between 30˚ to 41˚, and indicated that the inclined crack angle increased as the transverse reinforcement ratio increased. A similar effect of the amount of transverse reinforcement on the diagonal crack angle in RC beams has been reported in the literature by Malek and Saadatmanesh (1998).

The crack angle predictions for the beams according to the CSA A23.3-04 General Method showed a minor increase with the addition of transverse reinforcement, ranging between 33˚ to 34˚. The crack angle predictions by CSA A23.3-04 were comparable to the values observed for the unstrengthened beams in this study. However, the crack angle predictions were significantly (20%) lower than the observed angles for the strengthened beams. This suggests that the shear strength contributions from stirrups (V_s) and strengthening system (V_{CGM}) based on crack angles predicted by CSA A23.3-04 will be over predicted. The experimentally observed crack angles for unstrengthened and strengthened beams were 10% lower compared to the assumed crack angle of 45˚ in ACI 318-14. This suggests that the shear strength contributions

from the stirrups and strengthening system based on 45˚ truss analogy will be under predicted for the unstrengthened and the strengthened beam.

5.5.4 Concrete Shear Contribution

The concrete shear contribution estimated experimentally (by subtracting V_s and V_{CGM} from the applied shear load up to failure) indicates that V_c increased as the amount of shear reinforcement (internal and external) increased. The observed increases are inconsistent with the ACI 318 assumption that V_c is not a function of shear reinforcement. Furthermore, the observed increases in V_c with increase in transverse reinforcement ratio were in contrast to the decrease in V_c with increase in transverse reinforcement suggested by the CSA A23.3 shear provisions for beams with stirrups. Note that the effective shear depth of beams tested in current study was 288 mm and As per CSA A23.3-04 for beams with effective shear depth less than 300, the shear strength contribution for beams with or without stirrups is essentially the same.

In general, the estimated concrete shear contributions were consistently larger than the predicted values of V_c. Although the current shear design provisions for V_c appear to be conservative, these results suggest that interaction between the shear contributions is more complex than is assumed by the commonly accepted shear mechanism of the plastic truss analogy. As discussed in Section 5.3.5, the increase in shear resistance provided by the concrete is possibly due to the confinement of the concrete by internal

and external shear reinforcement, or because the shear transfer mechanism changes to arch action, or some combination of these effects.

As described in Section 2.2, shear in reinforced concrete beams can be transferred by two load transfer mechanism: beam action and arch action. The beam action is generally associated with slender beams while arch action is associated with deep beams. For beam action to exist, equilibrium requires the presence of shear flow across any horizontal plane between the reinforcement and the compression zone. If shear flow does not exist or is interrupted, then shear is transferred by arch action. This may occur when an inclined shear crack is wide enough such that the shear flow can no longer be transmitted in the concrete, or when the longitudinal reinforcing bars are de-bonded.

In the current study, the control beam without stirrups failed suddenly after the formation of diagonal cracks indicating that the beam transferred the shear by beam action only. In contrast, the beams with stirrups continued to carry increasing load even after the stirrups had yielded and the cracks were wide enough to disrupt the shear flow, suggesting that the shear mechanism changed from beam action to arch action. Similarly, the strengthened beams (with or without stirrups) also continued to carry increasing load even after the inclined cracks were wide enough that the shear flow would have been disrupted, indicating the transfer of load by arch action in strengthened beams as the beams approached failure in shear.

5.5.5 Conclusion: Shear Mechanisms

In conclusion, even though the existing shear strength prediction methods appear to be conservative, the mechanics behind the predictions do not appear to be completely consistent with the observed load transfer mechanisms up to failure. The existing prediction and design approach for slender beams is based on the concept that shear is transferred by beam action, but the experimental results appear to indicate that a portion of shear is transferred by arch action once the inclined shear cracks begin to disrupt shear flow in the beam section. This concept needs to be investigated further in future studies. In addition, new prediction approaches should be explored to better account for the interaction between the different shear resting components.

5.6 Conclusions

An experimental study was conducted to investigate the effectiveness of CFRP grid embedded in mortar as a shear strengthening system for concrete beams. In addition, the shear strength contribution from the strengthening system (CFRP grid embedded in mortar) was predicted using design guidelines for FRP strengthening systems (ACI 440.2R (2008) and CAN/CSA S6 (2006)) as well as the design method developed by Blanksvard et al. (2009). Based on results of this study, the following conclusions can be drawn:

- CFRP grid embedded in mortar (CGM) is effective in enhancing the load carrying capacity of shear-critical RC beams. Based on measured strains, the strength contribution from the CGM was similar for all beams tested (independent of internal reinforcement amount). However, based on capacity subtraction, the increase in ultimate load of the strengthened beams without stirrups was 47.5%, while the strength enhancement was lower for strengthened beams with stirrups where the average strength increase was 10.2 %.
- CGM strengthening reduces the shear strength contribution from stirrups. The CGM strengthened beams with stirrups exhibited steeper shear cracks compared to control unstrengthened beams with stirrups. The steeper shear cracks intersected fewer stirrups, resulting in reduction in the shear strength contribution from the stirrups in the strengthened beams.
- The average CGM strain across shear crack at failure for all specimens was 4672 με; with a coefficient of variation of 6%. Thus, it appears that the strain limit of 4000με specified in FRP design guidelines in North America (ACI 440.2R (2008) and CAN/CSA S6 (2006)) is appropriate for use with the CGM strengthening used in this study.
- Based on the observed shear transfer mechanism of the CGM strengthening layer, it can be concluded that the failure of the strengthening layer is caused by the CFRP grid rupture provided that the CFRP grid is covered with enough mortar cover. To

ensure the CFRP grid rupture failure, a thicker layer of mortar should be used in CGM strengthening layer in future studies.

- The CGM shear strength predictions using CAN/CSA S6 (2006) were in good correlation with experimental CGM shear contributions estimated using experimental strain measurements.

Chapter 6: Strengthening of Shear-Critical RC Beams: Alternatives to Existing Externally Bonded CFRP Sheets

This chapter will be submitted to a peer reviewed journal for publication.

The contributing authors are:

Azam, R., Soudki, K. and Jeffrey S. West

Contributors to this chapter include: -

Rizwan Azam: Ph.D. candidate, who researched, analyzed, and wrote the paper.

Khaled Soudki: Supervisor to Rizwan Azam; Deceased September 17, 2013

Jeffrey S. West: Supervisor to Rizwan Azam and assisted with research direction, editing, and general advice.

6.1 Introduction

Fibre reinforced polymer (FRP) systems have been used to strengthen and repair many reinforced concrete (RC) members worldwide. A number of studies reported in the literature have demonstrated the effectiveness of FRPs to strengthen shear-critical RC members. ACI 440.2R (2008) and Belarbi et al. (2011) are excellent sources of information on shear strengthening using FRPs. In spite of its wide use and effectiveness, the use of epoxy as a bonding agent in FRP strengthening systems may not be optimal for some applications due to poor compatibility with the concrete substrate, limited or no moisture diffusion, requirement for special handling/protection equipment for manual workers, and most importantly because post-repair inspections and assessment of the structure become difficult since FRP effectively hides the conditions underneath the repair system.

Cement-based composites are a relatively new strengthening and rehabilitation system. They have almost all of the same benefits of typical FRP systems such as low weight, ease of installation and non-corroding properties, but overcome some of the drawbacks such as poor compatibility with concrete substrate, lack of vapour permeability and fire resistance of using epoxy as bonding agent in FRP systems. A cement-based composite system replaces the epoxy with cementitious mortar and the fibre sheets are replaced with fabrics or FRP grids.

Two types of cement-based systems have been reported in the literature. The first type of cement-based composite system consists of fabric and mortar. This type of cement-based system has been referred to in the literature as fabric reinforced cementitious matrix (FRCM), textile reinforced concrete (TRC), and textile reinforced mortar (TRM). The majority of the studies on the strengthening of shear-critical RC beams have been conducted using this type of cement-based system (Escrig et al., 2015; Tzoura and Triantafillou 2015; Azam and Soudki 2016; Azam and Soudki 2014; Al-Salloum et al., 2012; Bruckner et al., 2008; Bruckner et al., 2006; Triantafillou et al., 2006). The second type of cement-based composite system consists of FRP grid and mortar. This type of system has been referred to in the literature as mineral-based composites (MBC) systems. Only one study has been reported in literature to date to investigate the behaviour of shear-critical RC beams strengthened with this type of strengthening system (Blanksvard et al., 2009).

A few studies have been reported in the literature to investigate the effectiveness of cement-based strengthening systems in comparison to existing epoxy-based system to strengthen shear-critical RC beams (Tzoura and Triantafillou 2015; Blanksvard et al., 2009; Triantafillou et al., 2006). These studies have reported contradictory results: Tzoura and Triantafillou (2015) and Triantifillou and Papanicolaou (2006) found that a cement-based composite system was less effective compared to FRP, while Blanksvard et al. (2009) found that cement-based composite system was more effective than FRP. It

is important to note that different types of cement-based systems were used in these studies. Tzoura and Triantafillou (2015) and Triantifillou and Papanicolaou (2006) used dry carbon fabric/ textile embedded in mortar, whereas Blanksvard et al. (2009) used CFRP grid embedded in mortar. The different types of cement-based systems could have been the source of the contradictory results. This indicates that further studies are required to investigate the effectiveness of the cement-based systems in comparison to the epoxy-based system.

The current study is designed to investigate the effectiveness of both types of cement-based composite systems in comparison to the epoxy-based system to strengthen shear-critical RC beams. The effectiveness of cement-based shear strengthening systems in comparison to the existing epoxy-based system is evaluated based on several performance criteria including the load-deflection response; the ability to control diagonal or shear crack width; the internal stirrup strain response and the overall efficiency of strengthening systems. This study is part of a larger research program on strengthening of reinforced concrete structures using cement-based strengthening systems.

6.2 Experimental Program

A total of twelve reinforced concrete beams were tested. The test matrix is given in Table 6.1.The variables included three strengthening systems (CFRP grid embedded in

mortar, CFRCM and CFRP sheet) and the amount of internal transverse shear reinforcement. The test beams were divided into three series: series S0 (beams without stirrups), series S150 (beams with 6mm stirrups @ 150 mm c/c) and series S250 (beams with 6mm stirrups @ 250 mm c/c). Each series contained four beams: one control unstrengthened beam and three strengthened beams.

Table 6.1 : Test matrix

Strengthening System	Amount of Transverse Reinforcement		
	Series S0	Series S150	Series S250
None	S0-N	S150-N	S250-N
CFRP grid in Mortar	S0-CGM	S150-CGM	S250-CGM
CFRCM	S0-CM	S150-CM	S2-CM
CFRP Sheet	S0-CP	S150-CP	S250-CP

6.2.1 Test Specimens

The details of the test specimens are presented in Table 6.2 and Figure 6.1. All beams were 250 mm wide, 400 mm deep and 2700 mm long. The longitudinal tensile reinforcement in all of the beams was 6-25M bottom bars and 3-25 top bars. The side and vertical covers to the tension reinforcement were kept at 40 mm for all beams. The internal transverse steel reinforcement used was 6 mm stirrups 150 mm c/c and 6 mm stirrups @ 250 mm c/c. Three additional stirrups were provided in the anchorage zone for the longitudinal reinforcement.

The beam designation used in this study is as follows: YY-ZZ with YY = steel reinforcement and ZZ= strengthening system. The steel reinforcement is specified as S0 (beams without stirrups), S150 (beams with 6 mm stirrups @ 150mm c/c) and S250 (beams with 6 mm stirrups @ 250mm c/c) and the strengthening system is specified as N (none), CGM (CFRP grid embedded in mortar), CM (CFRCM) and CP (CFRP sheet).

Table 6.2 : Details of specimens

Sr. No.	Beam Designation	Longitudinal Reinforcement			Shear Reinforcement	
		Amount of Rebar	ρ (%)	ρ/ ρb (%)	Internal Steel Stirrups	External Strengthening System
1	S0-N	6-25M (T) + 3-25M (C)	3.79	0.55	None	None
2	S150-N				6mm @150 mm c/c	None
3	S250-N				6mm @250 mm c/c	None
4	S0-CGM				None	CFRP grid in mortar
5	S150-CGM				6mm @150 mm c/c	CFRP grid in mortar
6	S250-CGM				6mm @250 mm c/c	CFRP grid in mortar
7	S0-CM				None	CFRCM
8	S150-CM				6mm @150 mm c/c	CFRCM
6	S250-CM				6mm @250 mm c/c	CFRCM
10	S0-CP				None	CFRP sheet
11	S150-CP				6mm @150 mm c/c	CFRP sheet
12	S250-CP				6mm @250 mm c/c	CFRP sheet

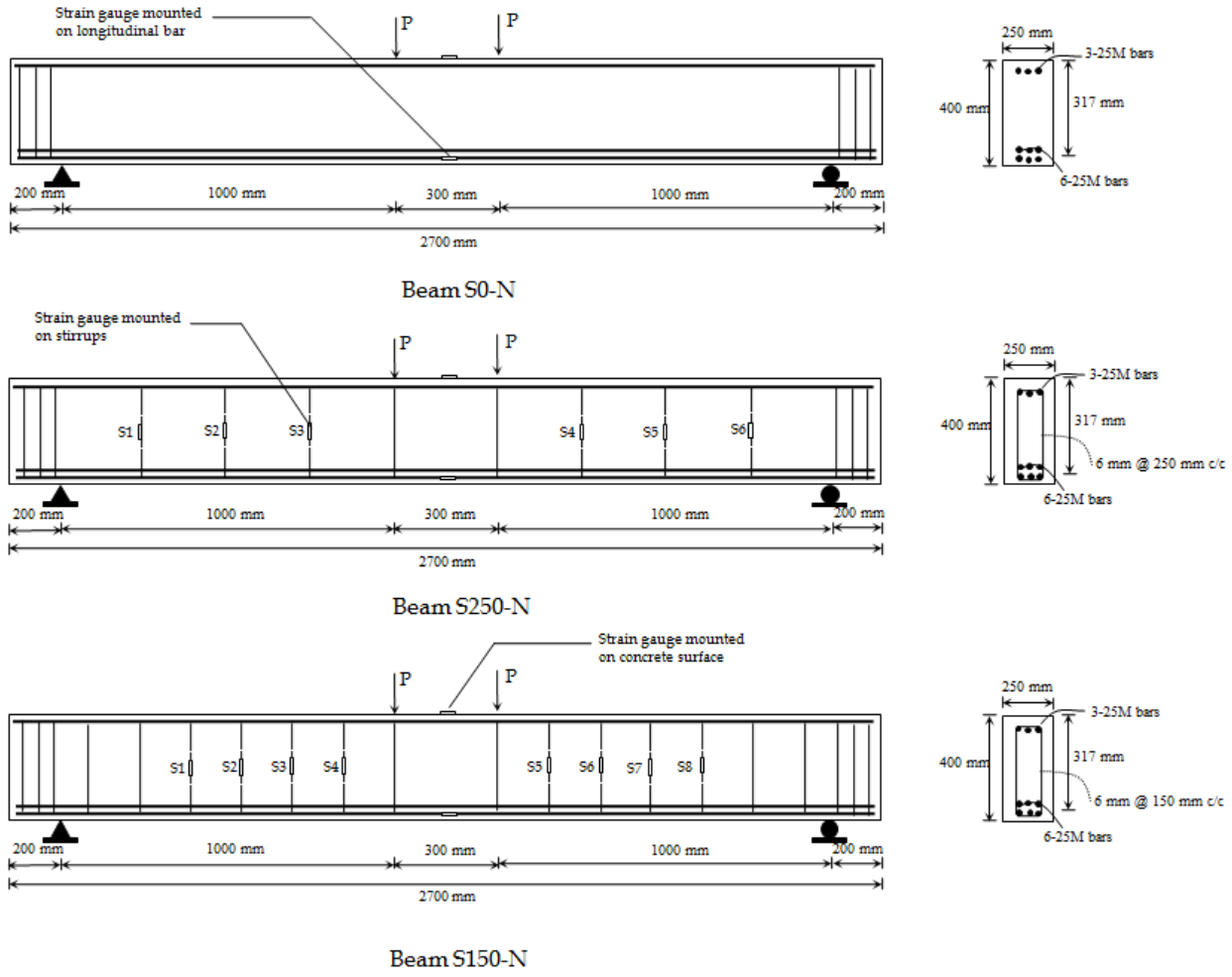

Figure 6.1 : Beam geometry, reinforcement details and layout of strain gauges

6.2.2 Material Properties

The concrete used to fabricate the test beams was supplied by a local ready-mix concrete company. The concrete was batched with Type GU portland cement and had a maximum coarse aggregate size of 19 mm and a water-cementing material ratio of 0.45. The 28 day compressive strength of the concrete was 63 ± 1 MPa. The longitudinal and transverse steel had a yield strength of 494MPa and 365 MPa, respectively, as reported by the supplier.

The CFRP grid had tensile modulus of 234.5 GPa and elongation at rupture of 0.76%. The CFRP grid had an ultimate strength of 80 kN/m in both directions. The orthogonal spacing of CFRP grid was 41 x 46 mm (Figure 6.2). The carbon fibers used to make carbon fabric (used in CFRCM) had tensile modulus of 230 GPa and elongation at rupture of 1.6%. The carbon fabric had an ultimate strength of 325 kN/m and 250 kN/m in longitudinal and transverse direction, respectively. The orthogonal spacing of fabric tows was 10 x 18 mm (Figure 6.2). Note that the properties of the CFRP grid and the carbon fabric listed above are as reported by the respective material Manufacturers. Sika Monotop 623, polymer modified, one component, and early strength-gaining cementitious mortar was used as the bonding agent in the strengthening layer. The compressive strength of the mortar was measured using 50 mm cubes. The compressive strengths of the mortar at 3, 7 and 28 days were 41±3.3, 45±2.4 and 58±2.8 MPa, respectively.

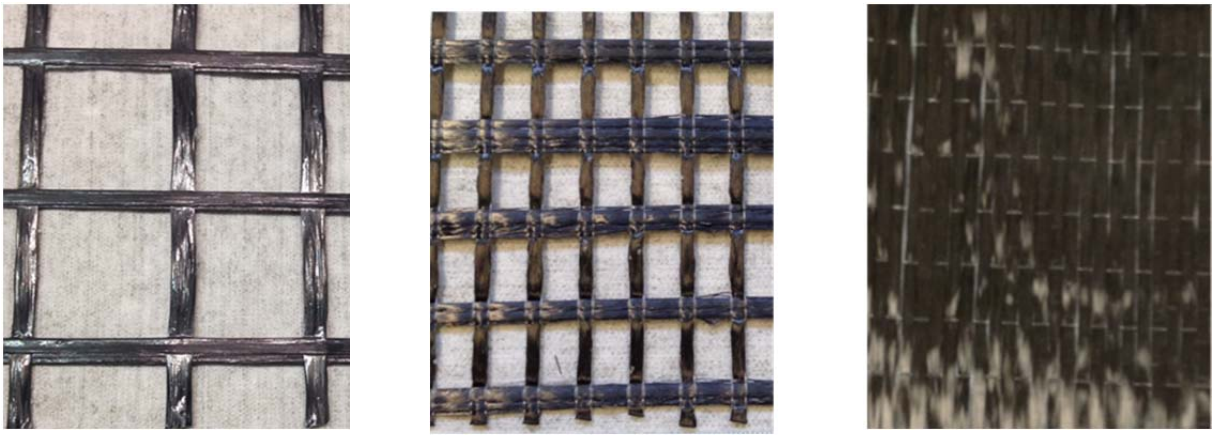

(a) (b) (c)

Figure 6.2: Fabric/grid/sheet used in study (a) CFRP grid (b) carbon fabric (c) carbon sheet

SikaWrap Hex 230C carbon fiber sheets and Sikadur 330 epoxy resin were used in the CFRP strengthening sustem (Figure 6.2). The dry carbon fibers used in the CFRP sheet had a tensile modulus of 230 GPa and elongation at rupture of 1.5%. The cured CFRP had tensile modulus of 65.4 GPa and an elongation at rupture of 1.33% (as reported by Manufacturer).

6.2.3 Installation of Strengthening Systems

Nine beams were strengthened with the three strengthening systems described in the previous section: three beams were strengthened with each type of strengthening system. The shear spans of beams were strengthened using side-bonded strengthening. The strengthening procedure for cement-based strengthening systems is presented in detail by Azam and Soudki (2014a).

The application of the epoxy-based system (CFRP sheet) followed the Manufacturer's specifications. The concrete surfaces were sand-blasted to expose the aggregates. Epoxy resin was then applied to concrete surface. Then dry fiber sheets were placed by hand on the epoxy-coated surface. A steel roller was used to apply pressure on the fiber sheets to remove air pockets.

6.2.4 Instrumentation

All beams were instrumented with one strain gauge (5 mm gauge length) mounted on one of the longitudinal (tension) bars at mid span and one strain gauge (60 mm gauge length) mounted on the concrete compression surface under the loading point. Two linear variable differential transformers (LVDTs), with a range of 0 to 25 mm, were placed at mid-span to measure the deflection of the beam. In addition, LVDT's were placed on the side of the beams in the shear spans to measure diagonal tensile and diagonal compressive displacements (average strains). Figure 6.1 and Figure 6.3 show the layout of instrumentation.

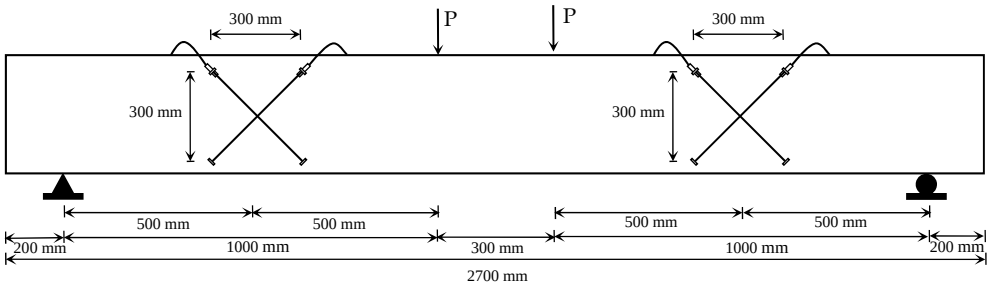

Figure 6.3: Layout of LVDTs used to measure diagonal displacement in shear span

6.2.5 Test Setup and Procedure

The beams were tested in four-point bending in a test frame using a closed-loop hydraulic actuator with a 2500 kN capacity. The beams were simply supported with roller and hinge supports over a clear span of 2300 mm. The spacing between load points was 300 mm and the shear span was 1000 mm. The load was transferred from the actuator to the beam through two loading plates at mid-span. To uniformly distribute the load, the loading plates were levelled on the beam using hydro-stone. The test setup is shown in Figure 6.4.

Figure 6.4 : Test setup

The test procedure was as follows: the beam was placed over the supports, leveled and centered. All of the instrumentation (LVDT and strain gauges) was mounted on the beam and connected to the data acquisition system. The data acquisition system started gathering data before the application of load. The load was increased monotonically at a stroke rate of 0.3 mm/sec using a ramp function generator until failure of the beam. During the test, the initiation and progression of cracks were monitored and marked.

6.3 Test Results and Discussion

A summary of test results is given in Table 6.3. In general, all three types of strengthening systems were effective in enhancing the load carrying capacity of shear-critical RC beams. The increase in ultimate load ranged between 10% and 87.4% in

comparison to the control (unstrengthened) beams. All of the beams failed in shear as evidenced by significant shear cracking and sudden failure. Furthermore, the tensile strain in the longitudinal reinforcement and compressive strain in concrete did not indicate that flexural failure had occurred; the measured compressive strains at failure in all beams were below maximum compressive strain of 3500 με normally associated with the failure in flexure for design purposes. Similarly, the measured tensile strains at failure in six beams were below yield strain of 2500 με. The measured tensile strains at failure in other six beams exceeded the yield strain of 2500 με. It is important to note that all beams were reinforced with 6-25M bottom rebar placed in two layers and strain gauges were mounted on bottom layer of steel. In addition, no signs of flexural failure were observed in load-deflection curves.

Typical failure modes of the control and strengthened beams are shown in Figure 6.5. It is important to mention here that the appearance and propagation of cracks in beams strengthened with cement-based systems can be readily observed, which gives an indication of failure. In contract to this, the cracks were not visible in the beams strengthened with CFRP sheets and the beams failed suddenly without any indication of failure.

Table 6.3 : Summary of test results

Beam designation	Ultimate load (kN)	Increase in ultimate load (%)	Deflection at ultimate load (mm)	Strain in longitudinal reinforcement at midspan at ultimate load (με)	Concrete strain at midspan at ultimate load (με)	Failure mode
S0-N	287.2	-	4.0	1073	839	shear
S150-N	613.9	-	12.7	2595	1984	shear
S250-N	520.3	-	12.1	1870	2465	shear
S0-CGM	423.5	47.5	10.66	1570	1407	shear
S150-CGM	677.4	10.3	12.9	2657	2399	shear
S250-CGM	570.6	10.0	11.3	2352	1883	shear
S0-CM	538.3	87.4	12.3	2227	3196	shear
S150-CM	771.0	25.6	14.0	3021	2386	shear
S250-CM	678.7	30.4	12.4	2874	2336	shear
S0-CP	530.9	84.8	10.0	2414	2566	shear
S150-CP	757.1	23.3	15.25	2980	2527	shear
S250-CP	713.6	37.1	13.25	2703	2076	shear

The cracking patterns and failure modes of the beams strengthened with cement-based systems are presented in chapter 4 and 5. In addition, the shear transfer mechanics of the cement-based composite strengthening layer and shear strength predictions from strengthening layer are described in chapter 4 and 5.

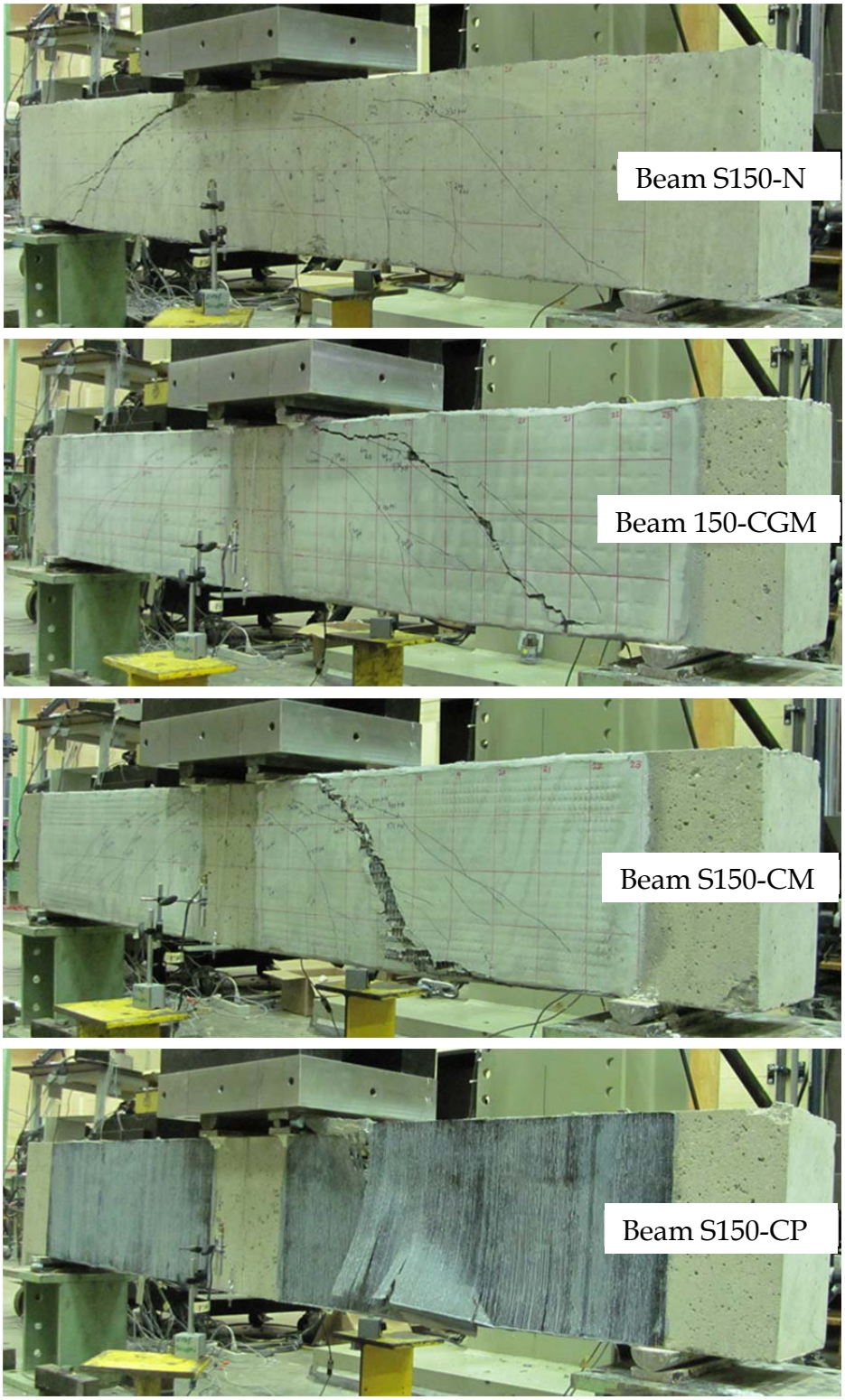

Figure 6.5 : Typical Failure Modes

The performance of cement-based systems in comparison to the epoxy-based system is evaluated in terms of the load-deflection response, the diagonal tensile displacement, strain in the stirrups and the overall efficiency of strengthening systems in the following sections.

6.3.1 Effect of Strengthening System on Load-Deflection Response

In general, the load-deflection response of all beams, except (S0-N), was almost bilinear indicating the change of stiffness occurring after the formation of shear cracks. All of the beams failed suddenly, consistent with the brittle nature of shear failure. The load-deflection response of control beam without stirrups (S0-N) was linear as it failed suddenly after formation of a single diagonal shear crack. The shear strengthening slightly increased the stiffness of the strengthened beams compared with the control unstrengthened beam.

The effect of the strengthening system on the load-deflection response of beams is shown in Figure 6.6 a-c. Figure 6.6 a shows the load versus deflection response for series S0 beams (beams without stirrups). The control unstrengthened beam without stirrups failed at a load of 287.2 kN. The beams that were strengthened with CFRP grid in mortar, CFRCM and CFRP sheet failed at ultimate load of 423.5 kN, 538.3 kN and 530.9 kN, respectively. This represent an increase in ultimate load of 47.5, 87.4 and 84.8% in beams strengthened with CFRP grid in mortar, CFRCM and CFRP sheet, respectively.

The strengthened beams experienced a larger deflection at ultimate load compared to the control (unstrengthened) beam; the deflection at ultimate load in strengthened beams ranged between 10 mm and 12.3 mm compared with a deflection of 4.0 mm for the control (unstrengthened) beam, representing an increase of 150% to 208%.

Figure 6.6b shows the load versus deflection response for the beams in series S250 (beams with 6 mm stirrups @ 250mm c/c). The control unstrengthened beam with stirrups failed at a load of 520.3 kN. The beams strengthened with CFRP grid in mortar, CFRCM and CFRP sheet failed at ultimate loads of 570.6 kN, 678.7 kN and 713.6 kN, respectively. This shows an increase of 10.0%, 30.4% and 37.1% in beams strengthened with CFRP grid in mortar, CFRCM and CFRP sheet, respectively. The deflection at ultimate load in control (unstrengthened) and strengthened beams with stirrups ranged between 10 mm and 15.3 mm.

Figure 6.6c shows the load versus deflection response for the beams in series S150 (beams with 6 mm stirrups @150mm c/c). The control unstrengthened beam with stirrups failed at a load of 613.9 kN. The beams strengthened with CFRP grid in mortar, CFRCM and CFRP sheet failed at ultimate loads of 677.4 kN, 771.0 kN and 757.1 kN, respectively. This corresponds to a 10.3%, 25.6% and 23.3% increase in ultimate strength of beams strengthened with CFRP grid in mortar, CFRCM and CFRP sheet, respectively.

The beams that were strengthened with the CFRP sheet showed almost twice the increase in ultimate load compared to the increase in ultimate load in the beams strengthened with the CFRP grid in mortar. The ultimate strength of the CFRP sheets (440.5 kN/m) was five times higher than the ultimate strength of CFRP grid (80 kN/m).

Taking into account the relative ultimate strength of the CFRP sheet and the CFRP grid it can be concluded that the CFRP grid in mortar performed more efficiently compared to the CFRP sheet. The beams that were strengthened with CFRCM and the CFRP sheet showed almost the same increase in ultimate load (Table 6.3). It is important to note that the carbon fabric used in the CFRCM has ultimate strength of 325 kN/m compared to 440.5 kN/m ultimate strength of the carbon sheet used in the CFRP system. This indicates that the CFRCM also performed more efficiently than the CFRP sheet, offering a similar increase in shear capacity in spite of the lower ultimate strength of the material. Overall, the cement-based systems (CFRP grid in mortar and CFRCM) performed more efficiently compared to the epoxy-based system (CFRP sheet).

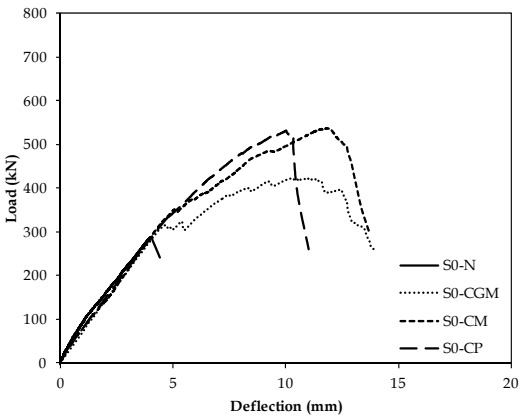

(a)

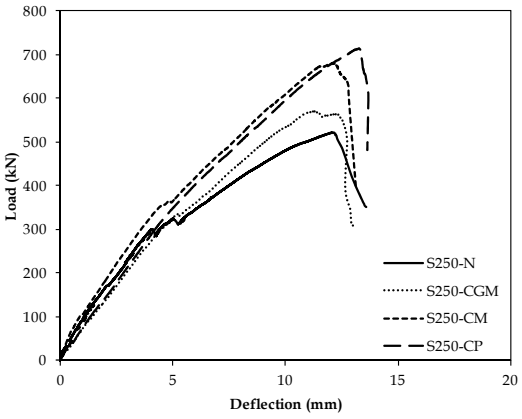

(b)

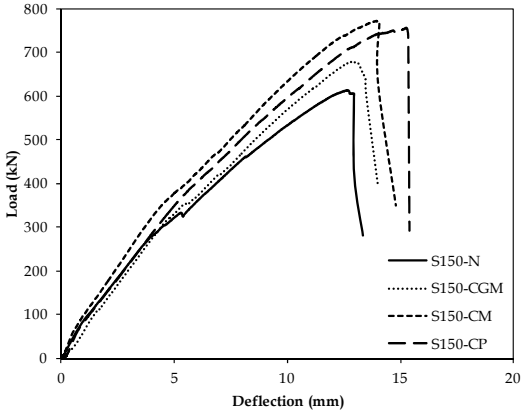

(c)

Figure 6.6 : Effect of strengthening system on load vs. deflection response of beams (a) beams without stirrups (b) beams with stirrups at 250 mm c/c (c) beams with stirrups at 150 mm c/c.

6.3.2 Effect of Strengthening System on Diagonal Tensile Displacements

Figure 6.7a-c shows the load versus diagonal tensile displacement curves of beams. In general, all of the strengthening systems were effective in controlling the diagonal tensile displacement for beams with or without stirrups. In order to quantify the relative effectiveness of different strengthening systems to control the diagonal cracks, the diagonal tensile displacement corresponding to the maximum load in the control beam was compared with the diagonal tensile displacement at same load level in the beams with the different strengthening systems. This quantitative analysis was only performed on beams with stirrups as the control beam without stirrups failed suddenly after formation of the diagonal crack.

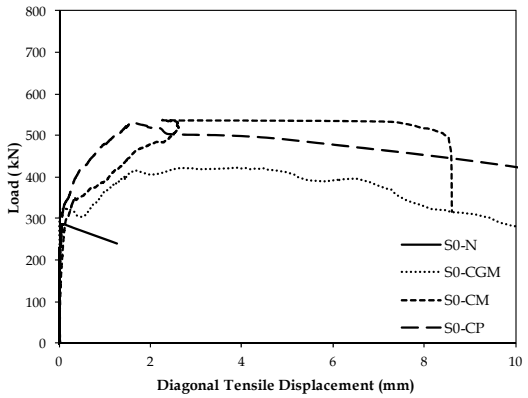

(a)

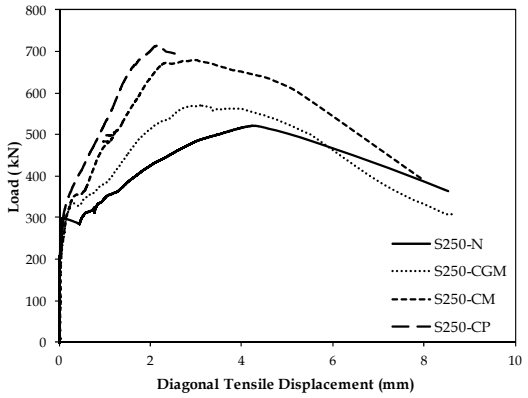

(b)

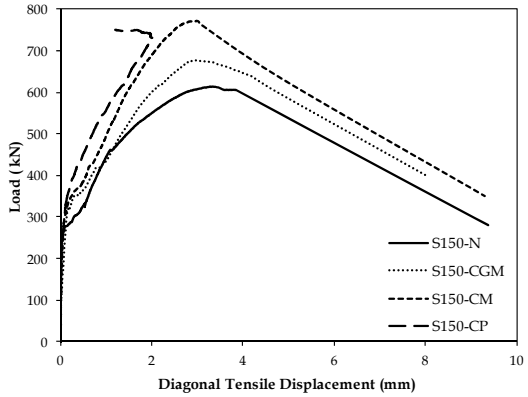

(c)

Figure 6.7 :Effect of strengthening system on load vs. diagonal tensile displacement (a) beams without stirrups (b) beams with stirrups at 250 mm c/c (c) beams with stirrups at 150 mm c/c.

Figure 6.7b shows the load versus diagonal tensile displacement curves of series S250 beams. The diagonal tensile displacement at maximum load in control beam (S250-N) was 4.23 mm compared a diagonal tensile displacement of 2.1 mm, 1.34 mm and 1.0 mm in beams strengthened with CFRP grid in mortar, CFRCM and CFRP sheet, respectively. This corresponds to a 50%, 68% and 76% decrease in the diagonal tensile displacement for the beams strengthened with CFRP grid in mortar, CFRCM and CFRP sheet, respectively. Figure 6.7c shows the load versus diagonal tensile displacement curves for the series S150 beams. The diagonal tensile displacement at maximum load in the control beam (S150-N) was 3.31 mm compared a diagonal tensile displacement of 2.13 mm, 1.54 mm and 1.34 mm in the beams strengthened with CFRP grid in mortar, CFRCM and CFRP sheet, respectively. This corresponds to a decrease of 36%, 54% and 60% for the beams strengthened with CFRP grid in mortar, CFRCM and CFRP sheet, respectively. On average, the diagonal tensile displacements in the beams strengthened with CFRP grid in mortar, CFRCM and CFRP sheet were reduced by 43%, 61% and 68%, respectively.

When diagonal cracking occurs in a strengthened beam, the strengthening system intersects the crack and restrains the crack opening. The effectiveness of strengthening system to control shear cracks depends on the tensile stiffness of the strengthening system and the bond between the strengthening system and the original beam concrete surface. The effect of the tensile stiffness of shear strengthening layer has been studied

previously for FRCM shear strengthening (Azam et al. 2016; Escrig et al., 2015; Azam and Soudki 2014a). The tensile stiffness of the fabric primarily depends on the area of the fiber tows and the modulus of elasticity of the fabric material. This means that the carbon fabric with high modulus of elasticity will provide better crack control in FRCM compared to glass fabric with a lower modulus of elasticity (assuming that the area of fibre tows is similar and that bond is adequate). Similarly, a heavier fabric with more tow area will provide better crack control compared to lighter fabric with a smaller tow area, assuming that the bond properties between the fabric and the beam surface are constant.

In the current study, the modulus of elasticity of the CFRP grid, carbon fabric and carbon fiber sheet was essentially equivalent at 230 GPa. However, the area of dry fiber or grid used was different in the three strengthening systems. The area of dry fiber or grid per meter shear span was 87.2 mm^2, 176.6 mm^2 and 255.6 mm^2, respectively, for the CFRP grid in mortar, CFRCM and CFRP sheet systems. This indicates that the CFRP sheets have a tensile stiffness that is almost 200% higher than that of the CFRP grid in mortar and 45% higher than the CFRCM. In contrast, the CFRP sheet was only 58% more effective in controlling the diagonal crack width compared to the CFRP grid in mortar (on average, the beams strengthened with CFRP sheets exhibited 60% reduction in diagonal crack width compared with a 43% reduction in beams strengthened with CFRP grid embedded in mortar). The CFRP sheets exhibited only 11% better

performance compared to the CFRCM, in spite of the 45% higher tensile stiffness of the CFRP sheet compared to the CFRCM. Considering the relative tensile stiffness of the CFRP sheet and the cement-based systems (CFRCM and CFRP grid in mortar), it can be concluded that the cement-based systems were more efficient in terms of controlling the diagonal tensile displacements. This appears to be primarily due to the better bond performance of cement-based systems compared to the epoxy-based systems. This is explained further following the discussion of the efficiency of strengthening systems.

6.3.3 Effect of Strengthening System on Strain in Stirrups

Figure 6.8a and Figure 6.8b shows the load versus average strain measurements in the stirrups for all tested beams in series S250 and S150, respectively. The average strain in all stirrups that intersected the main shear crack was used to illustrate the effect of the strengthening system on the shear response of the beam. As expected, the strengthened beams exhibited smaller strains in the stirrups compared to the control unstrengthened beams. This reduction in strain in the stirrups for strengthened beams is due to load sharing between the stirrups and the strengthening layer.

The yielding of stirrups was delayed in the strengthened beams compared to unstrengthened beams. However, the stirrups yielded before shear failure in all of the beams in this study which is in consistent with the assumption of yielding used in all shear design provisions.

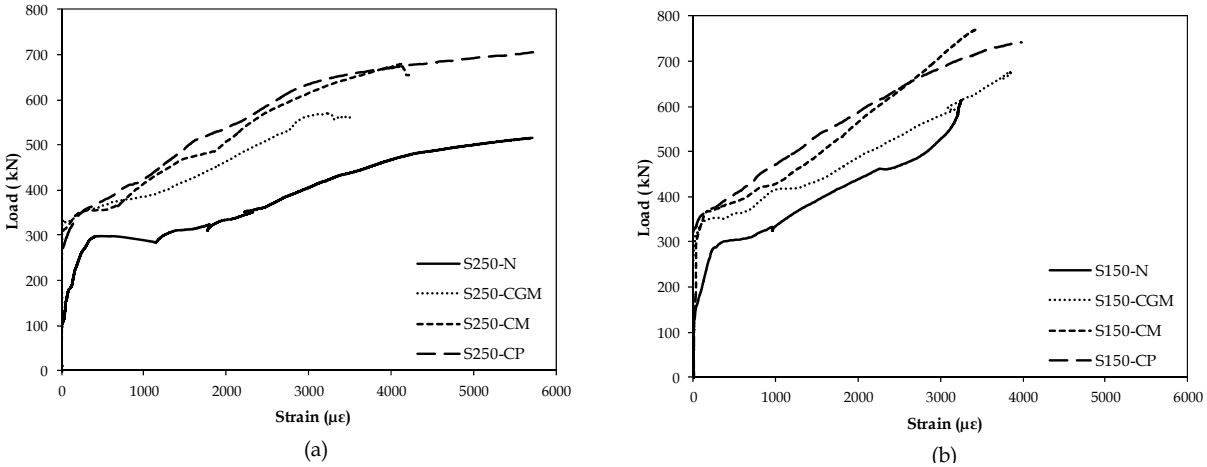

Figure 6.8 : Effect of strengthening system on load vs. average strain in stirrups (a) beams with stirrups at 250 mm c/c (b) beams with stirrups at 150 mm c/c.

6.3.4 Efficiency of Strengthening Systems

The performance of the two types of cement-based systems (CFRP grid in mortar and CFRCM) in comparison to the epoxy-based system (CFRP sheet) is illustrated by considering the efficiency of the strengthening systems. The efficiency is defined as the shear strength contribution from the strengthening system for each specimen divided by the ultimate tensile capacity per unit length of the strengthening system. The shear strength contribution from the different strengthening system is assumed to be equal to difference between the ultimate load of the companion strengthened and control beams. The tensile properties of the strengthening system are taken as the strength of the sheet, fabric or grid without the contribution of the bonding agent (without epoxy for CFRP sheet and without mortar for CFRCM and CFRP grid embedded in mortar). The

ultimate tensile capacities of the fiber strengthening systems in the beams strengthened with CFRP grid in mortar, CFRCM and CFRP were equal to 160 kN/m, 650 kN/m and 881 kN/m, respectively. Figure 6.9 and Table 6.4 present the efficiency of the different strengthening systems used. It is evident from Figure 6.9 that the CFRP grid embedded in mortar is the most efficient strengthening system followed by the CFRCM system. The CFRP sheet is the least efficient strengthening system among the three strengthening systems investigated in current study.

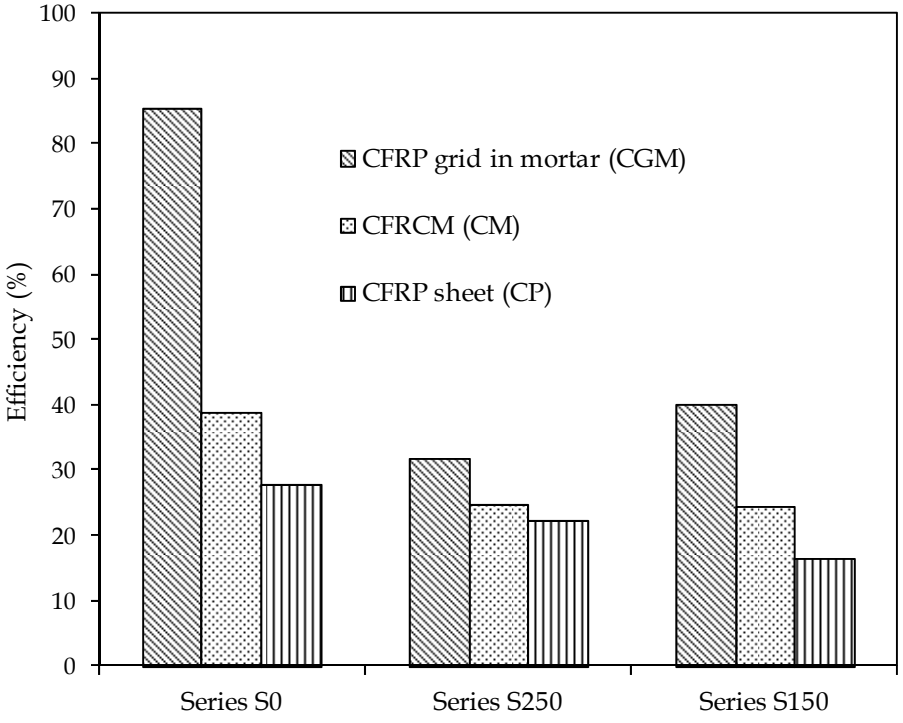

Figure 6.9 : Efficiency of cement-based shear strengthening systems in comparison to CFRP sheets

In general, shear-critical RC beams with a span to depth ratio (a/d) greater than 2.5 fail in shear by an inclined diagonal crack that penetrates through the compression zone

(diagonal tension failure). The transverse reinforcement (internal stirrups and/or external strengthening system) within the shear spans controls the diagonal crack width and delays or prevents such a failure. The ability of the transverse reinforcement to control the diagonal crack width depends on the properties of the transverse reinforcement (effective strength and stiffness) as well as the bond behaviour of the transverse reinforcement with the concrete. In the published literature, a few researchers have reported the effect of bond between steel stirrups and the concrete on behaviour of shear-critical RC beams. Potisuk et al. (2011) concluded that the loss of bond between steel stirrups and the concrete due to corrosion results in a significant reduction in ultimate load carrying capacity of shear-critical RC beams. Azam and Soudki (2013) reported that the use of smooth stirrups in shear-critical RC beams could result in a reduced ultimate load carrying capacity due to weak bond between the smooth stirrups and the concrete. Similarly, a strengthening system with excellent bond to the concrete will perform better to control the diagonal crack width, and hence will result in a higher ultimate load carrying capacity. Previous research on the bond of cement-based systems is limited. Azam and Soudki 2014a reported that the cement-based systems have excellent bond with the concrete substrate. Blanksvard et al. (2009) did not observe bond failures in tests of beams strengthened with a cement-based CFRP grid system. These previous studies are consistent with findings of the current study as

the cement-based systems have shown better efficiency compared to the epoxy-based system as discussed in previous section.

The apparent higher efficiency of the cement-based systems is mainly attributed to the better bond performance of the cement-based systems compared to the epoxy-based system. In the case of the cement-based systems, the bond between the vertical (transverse) fibers of the strengthening system and the concrete appears to be significantly enhanced by the anchorage provided by the orthogonal (horizontal or longitudinal) tows of the fabric or grid. This distributes the bond stresses over a much larger area than in the CFRP sheet systems where bond of the vertical fibers to the concrete is provided by the epoxy over a more localized region. The shear transfer mechanism of the cement-based composite strengthening layer is presented in chapter 4 and 5.

Table 6.4 : Efficiency of different strengthening systems

Strengthening System	Beam Designation	Ultimate Tensile Capacity per unit length/shear span (kN)	Increase in Shear Strength due to strengthening (kN)	Efficiency of Strengthening System (%)
CFRP grid in mortar	S0-CGM	160	136.3	85.2
	S150-CGM	160	63.5	39.7
	S250-CGM	160	50.3	31.4
CFRCM	S0-CM	650	251.1	38.6
	S150-CM	650	157.1	24.2
	S250-CM	650	158.4	24.4
CFRP	S0-CP	881	243.7	27.6
	S150-CP	881	143.2	16.2
	S250-CP	881	193.3	21.9

The enhanced bond provided by the orthogonal tows in the cement-based systems is even more pronounced in the CFRP grid in mortar in comparison to the CFRCM since the orthogonal tows in the CFRP grid are strongly connected (woven and epoxy-bonded) compared to the orthogonal tows of carbon fabric used in CFRCM which are weakly connected (woven or tied with string). The more strongly connected tows of the CFRP grid in more appear to further enhance the anchorage of the vertical tows, thus improving shear resistance and system efficiency.

6.4 Conclusions

An experimental study was conducted to investigate the effectiveness of cement-based composite systems in comparison to an existing epoxy-based system (carbon fiber

reinforced polymer, CFRP) to strengthen shear-critical RC beams. Based on results of this study, the following conclusions can be drawn:

- Cement-based composite systems performed better than the epoxy-based strengthening system to strengthen shear-critical RC beams, offering a similar increase in shear capacity in spite of the lower ultimate strength of the material: the increase in ultimate load carrying capacity of beams without stirrups strengthened with CFRCM was 87.4% compared to an increase of 84.8% in beams without stirrups strengthened with CFRP sheet.
- Cement-based systems exhibited a better ability to control diagonal (shear) crack widths compared to the epoxy-based systems, providing a greater reduction in diagonal crack width despite the relative lower ultimate strength and stiffness of the cement-based systems.

  CFRP grid embedded in mortar is the most efficient shear strengthening system in terms of shear strength increase relative to system strength. This efficiency appears to be due to improved bond between the strengthening system and concrete substrate provided by anchorage of the vertical tows of the grid by the longitudinal tows.

Chapter 7: Shear Strengthening of RC Deep Beams with Cement-Based Composites

This chapter will be submitted to a peer reviewed journal for publication.

The contributing authors are:

Azam, R., Soudki, K. and Jeffrey S. West

Contributors to this chapter include: -

Rizwan Azam: Ph.D. candidate, who researched, analyzed, and wrote the paper.

Khaled Soudki: Supervisor to Rizwan Azam; Deceased September 17, 2013

Jeffrey S. West: Supervisor to Rizwan Azam and assisted with research direction, editing, and general advice.

7.1 Introduction

In general, the shear mechanism and failure mode of reinforced concrete beams depends on the shear span to depth ratio (a/d). Beams with a shear span to depth ratio greater than 2.5 are considered to be slender beams, and beams with a shear span to depth ratio less than 2.5 are considered to be deep beams. Slender beams transfer vertical loading to the support through beam action (combined bending & shear) whereas the deep beams transfer the load directly to the supports through compressive stresses by arch action. Because of their different failure mechanisms, deep and slender beams are studied separately.

Fiber reinforced polymer (FRP) systems have been applied to strengthen and repair many reinforced concrete (RC) members worldwide. A number of studies reported in the literature have demonstrated the effectiveness of FRPs to strengthen shear-critical RC members. ACI 440.2R-08 (2008) and Belarbi et al. (2011) are excellent sources of information on shear strengthening using FRPs. The effectiveness of FRPs to strengthen corroded shear-critical RC beams has also been reported in the literature (Azam and Soudki 2012, Azam and Soudki 2013). In spite of its wide use and effectiveness, the use of epoxy as a bonding agent in FRP strengthening systems may not be optimal for some applications due to poor compatibility with concrete substrate, limited or no moisture diffusion, requirement for special handling/protection equipment for manual workers, and most importantly because post-repair inspections and assessment of the structure

become difficult since the FRP effectively hides the conditions underneath the repair system.

Cement-based composites are a relatively new strengthening and rehabilitation system. They have almost all of the same benefits of typical FRP systems such as low weight, ease of installation and non-corroding properties, but overcome some of the drawbacks such of using epoxy as bonding agent in FRP systems as poor compatibility with concrete substrate, lack of vapour permeability and fire resistance. A cement-based composite system replaces the epoxy with cementitious mortar and the fiber sheets are replaced with fabrics or FRP grids. Cement-based systems are generally categorized into two types. The first type of cement-based composite system consists of an open-weave fabric and mortar. This type of cement-based system has been referred to as fabric reinforced cementitious matrix (FRCM), textile reinforced concrete (TRC), and textile reinforced mortar (TRM). The second type of cement-based composite system consists of an FRP grid and mortar. This type of cement-based system has been referred to in the literature as a mineral-based composites (MBC) system.

Only limited research has been conducted to investigate the shear strengthening of RC deep beams with cement-based composites (Al-Salloum et al., 2012; Bruckner et al., 2006 & 2008). Al-Salloum et al. (2012) investigated the effectiveness of basalt FRCM (BFRCM) to increase the shear resistance of RC beams. The FRCM used in this study consisted of basalt fabric with a cementitious bonding agent and was denoted as textile reinforced

mortar (TRM). A total of 10 RC beams were tested. The test variables included: the type of mortar (cementitious versus polymer modified cementitious), the number of TRM layers (2 or 4) and the fabric orientation in the shear spans (0˚/90˚ or 45˚/-45˚). The beams were tested in four-point bending with a shear span to depth ratio of 2.5. The test results indicated that the shear strength of the RC beams increased when strengthened with basalt-based TRM; the increase in strength ranged between 36-86% for 2-4 TRM layers. It was also observed that a polymer modified cementitious mortar performed slightly better than cementitious mortar, and that the 45˚/-45˚ orientation of the textile showed better shear resistance than 0˚/90˚ orientation when four TRM layers were applied. Bruckner et al. (2006 & 2008) investigated the performance of Glass FRCM (GFRCM) for shear strengthening of RC beams. The GFRCM used consisted of an alkali-resistant glass fabric with cementitious bonding agent and was denoted as textile reinforced concrete (TRC). A total of twelve T-shaped beams were tested: three identical control beams and nine strengthened beams. The test variables included the number of fabric layers (2, 3, 4, and 6), presence of mechanical anchorage (without anchorage and with anchorage) and different anchorage methods. The beams were tested in three-point bending with a shear span to depth ratio of about 2.1. The results showed that the load carrying capacity of the beams was increased by TRC strengthening; however, in order to fully utilize the TRC strengthening, mechanical anchorage was needed. The load carrying capacity of the strengthened beams was increased by 17% with the

application of two or four TRC layers without mechanical anchorage, whereas the increase in strength was 33% with the application of four TRC layers with mechanical anchorage.

The existing studies have been conducted on the first type of cement-based system (fabric and mortar) and no research has been conducted using the second type of cement-based system (FRP grid and mortar). In addition, the existing studies have been conducted using low stiffness fabric (glass and basalt fabric), which may be why up to six strengthening layers were used. The use of a high stiffness fabric (such as carbon fabric) may allow effective shear strengthening with fewer strengthening layers, and needs to be investigated in future studies.

A few studies have been reported in the literature to investigate the shear strengthening of RC deep beams with epoxy-based composite (externally bonded FRP sheets) systems (Zhang et al. 2004; Islam et al. 2005 and Lee et al. 2011). Zhang et al. (2004) investigated the shear behaviour of RC deep beams (with rectangular cross section) without stirrups strengthened with CFRP sheets and concluded that CFRP sheets are effective to restore or increase the shear capacity of deep beams. Islam et al. (2005) investigated the effectiveness of externally bonded FRP sheets for RC deep beams (with rectangular cross section) with stirrups and concluded that the CFRP sheets are effective in enhancing the ultimate load carrying of deep beams by restraining the growth of diagonal cracks. Lee et al. (2011) investigated the structural behaviour of RC deep

beams (with T-shaped section) without stirrups strengthened with CFRP sheets and concluded that the strengthening length (quarter length of shear span, half length of shear span and full length of shear span) direction of fibers in the CFRP sheets (0˚,45˚ and 90˚) and the anchorage of the CFRP sheets all have a significant effect on the structural performance of the strengthened beams. It was also concluded that the horizontal direction fibers (0˚ angle with beam longitudinal axis) are the most effective in enhancing the load carrying capacity of deep beams.

The literature review revealed that the cement-based composite system is a promising strengthening technique. However, a very limited research has been conducted on this topic, and to the authors' knowledge, there is no previous work that investigated the effectiveness of cement-based system in comparison to epoxy-based system in RC deep beams. Therefore, a need exists for further investigation of the effectiveness of cement-based composite system strengthening for RC deep beams. In particular, the effectiveness of cement-based system in comparison to the more common epoxy-based system needs to be explored. The current study was designed to investigate the effectiveness of both types of cement-based composite systems in comparison to a typical epoxy-based CFRP system to strengthen RC deep beams in shear. Carbon fabric and CFRP grid was used in the current study for the two types of cement-based systems. This study is part of a large research program on the strengthening of reinforced concrete structures using cement-based strengthening systems.

7.2 Experimental Program

A total of eight reinforced concrete deep beams were tested. The experimental program is summarized in Table 7.1. The variables included the strengthening system (CFRCM, CFRP grid embedded in mortar and CFRP sheet) and the amount of internal transverse reinforcement. The test beams were divided into two series: series S0 (beams without stirrups) and series S250 (beams with 6mm stirrups @ 250 mm c/c). Each series contained four beams: one control unstrengthened beam and three strengthened beams.

Table 7.1 : Experimental Program

Strengthening System	Amount of Transverse Reinforcement	
	S0 Series	S250 Series
None	S0-N	S250-N
CFRP grid in mortar	S0-CGM	S250-CGM
CFRCM	S0-CM	S250-CM
CFRP sheet	S0-CP	S250-CP

7.2.1 Test Specimens

The details of the test specimens are presented in Figure 7.1 and Table 7.2. All beams were 250 mm wide, 400 mm deep and 1700 mm long. The longitudinal tensile reinforcement in all of the beams was 6-25M bottom bars and 3-25 top bars were used as compression reinforcement. The side and vertical covers to the tension reinforcement were kept at 40 mm for all beams. The internal transverse steel reinforcement used in

the S250 series was 6 mm stirrups @ 250 mm c/c. Three additional stirrups were provided in the anchorage zone for the longitudinal reinforcement.

The beam designation used in this study is as follows: YY-ZZ with YY = steel reinforcement and ZZ= strengthening system. The steel reinforcement is specified as S0 (beams without stirrups), and S250 (beams with 6 mm stirrups @ 250 mm c/c) and the strengthening system is specified as N (none), CGM (CFRP grid embedded in mortar), CM (CFRCM) and CP (CFRP sheet).

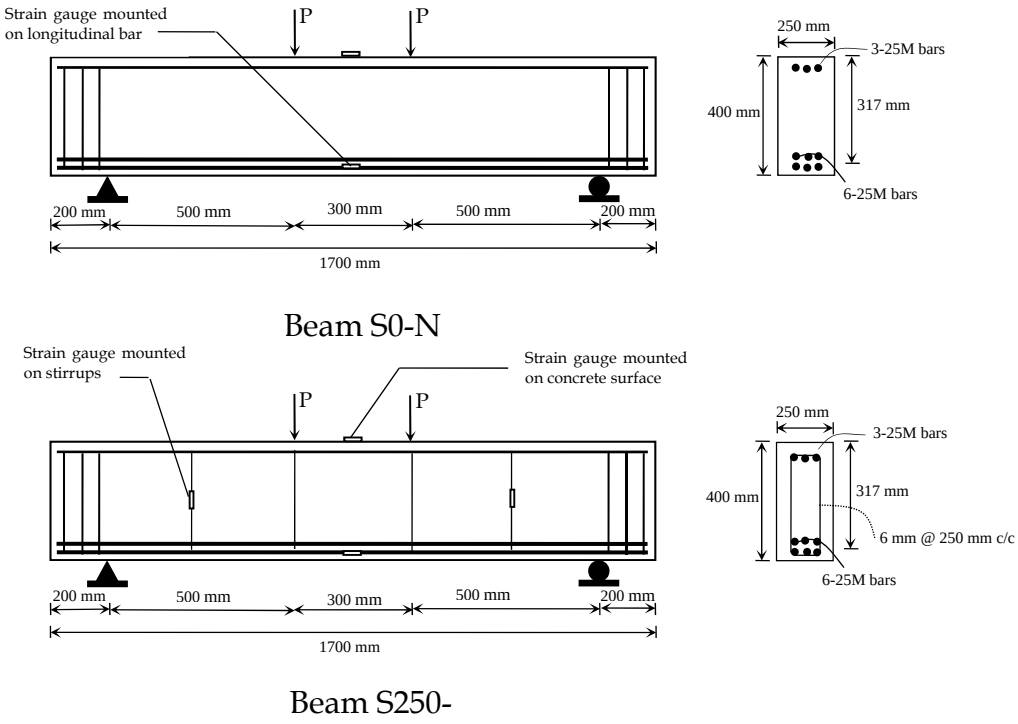

Figure 7.1 : Beam geometry, reinforcement details and layout of strain gauges

Table 7.2 : Details of test specimens

Sr. No.	Beam Designation	Longitudinal Reinforcement			Shear Reinforcement	
		Amount of Rebar	ρ	ρ / ρb	Steel Stirrups	External FRCM
1	S0-N	6-25M (T) + 3-25M (C)	3.79	0.55	None	None
2	S250-N				6mm @250 mm c/c	None
3	S0-CGM				None	CFRP grid in mortar
4	S250-CGM				6mm @250 mm c/c	CFRP grid in mortar
5	S0-CM				None	CFRCM
6	S250-CM				6mm @250 mm c/c	CFRCM
7	S0-CP				None	CFRP
8	S250-CP				6mm @250 mm c/c	CFRP

7.2.2 Material Properties

The concrete used to fabricate the test beams was supplied by a local ready-mix concrete company. The concrete was batched with Type GU portland cement with a maximum coarse aggregate size of 19 mm and a water-cementing material ratio of 0.45. The 28 day compressive strength of the concrete was 61 ± 1 MPa. The longitudinal and transverse steel had a yield strength of 494MPa and 365 MPa, respectively, as reported by the supplier.

The CFRP grid had tensile modulus of 234.5 GPa and elongation at rupture of 0.76%. The CFRP grid had an ultimate strength of 80 kN/m in both directions. The orthogonal spacing of CFRP grid was 41 x 46 mm (Figure 7.2). The carbon fibers used in the carbon fabric (used in CFRCM) had tensile modulus of 230 GPa and elongation at rupture of 1.6%. The carbon fabric had an ultimate strength of 325 kN/m and 250 kN/m in

longitudinal and transverse direction, respectively. The orthogonal spacing of fabric tows was 10 x 18 mm (Figure 7.2). Note that the properties of the CFRP grid and the carbon fabric listed above are as reported by the respective material Manufacturers. Sika Monotop 623, polymer modified, one component, and early strength-gaining cementitious mortar was used as the bonding agent in the strengthening layer. The compressive strength of the mortar was measured using 50 mm cubes. The compressive strengths of the mortar at 3, 7 and 28 days were 41±3.3, 45±2.4 and 58±2.8 MPa, respectively.

SikaWrap Hex 230C carbon fiber sheets and Sikadur 330 epoxy resin were used for the CFRP strengthening system (Figure 7.2). The dry carbon fibers used in the CFRP sheet had a tensile modulus of 230 GPa and elongation at rupture of 1.5%. The cured CFRP had tensile modulus of 65.4 GPa and an elongation at rupture of 1.33% as reported by the Manufacturer.

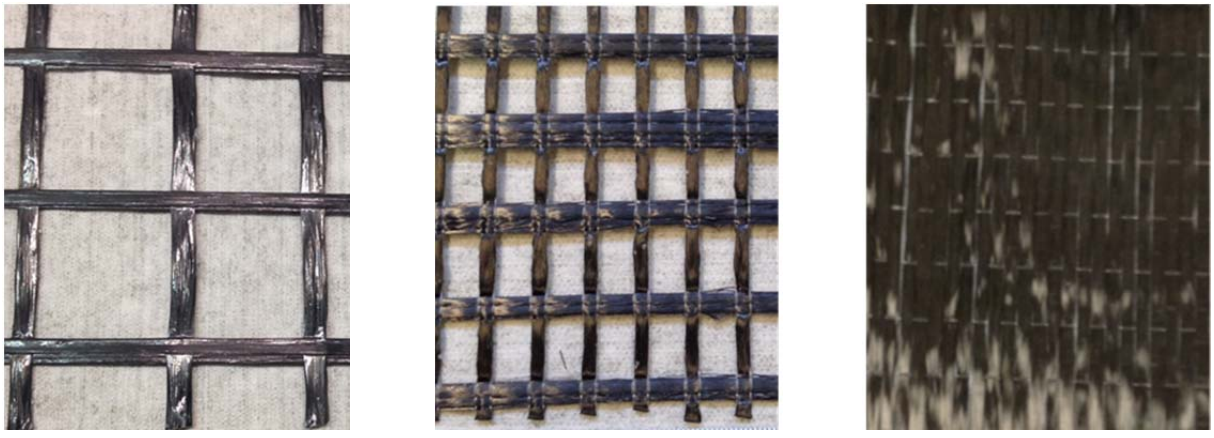

(a) **(b)** **(c)**

Figure 7.2 : Fabric/grid/sheet used in study (a) CFRP grid (b) carbon fabric (c) carbon sheet

7.2.3 Installation of Strengthening Systems

Six beams were strengthened with the three strengthening systems: two beams were strengthened with each type of strengthening system. The shear spans of beams were strengthened using a side bonded strengthening layer.

The strengthening procedure for the cement-based strengthening systems is presented in detail by Azam and Soudki (2014a). The concrete surfaces were first sand-blasted to expose the aggregates. Water was sprayed on the dry concrete surfaces of the beams until a saturated surface dry (SSD) condition was achieved. Once the SSD condition was achieved, the first layer of mortar was applied on the beams followed by pressing the fabric into the mortar. The fabrics were applied in such a way that the direction of stronger fabric tows was perpendicular to the longitudinal axis of the beam. Then a final layer of mortar was applied to completely cover the fiber textile. Finally, the beam surface was finished with a trowel. The total thickness of the strengthening system was about 6-8 mm for CFRCM and 8-12 mm for CFRP grid in mortar.

The application of the epoxy-based system (CFRP sheet) followed the Manufacturer's specifications. The concrete surfaces were first sand-blasted to expose the aggregates. Epoxy resin was then applied to the concrete surface. Then dry fiber sheets were placed by hand and a steel roller was used to apply pressure on fiber sheets to remove any air pockets.

7.2.4 Instrumentation

All beams were instrumented with one strain gauge (5 mm gauge length) mounted on one of the longitudinal bars (bottom layer) at midspan, and one strain gauge (60 mm gauge length) mounted on the concrete surface under the loading point. Two linear variable differential transformers (LVDTs) with a range of 0 to 25 mm, were placed at midspan to measure the deflection of the beam. In addition, LVDT's were mounted on the side of the beam in the shear spans to measure diagonal tensile and compressive displacements. Figure 7.1and Figure 7.3 show the layout of instrumentation.

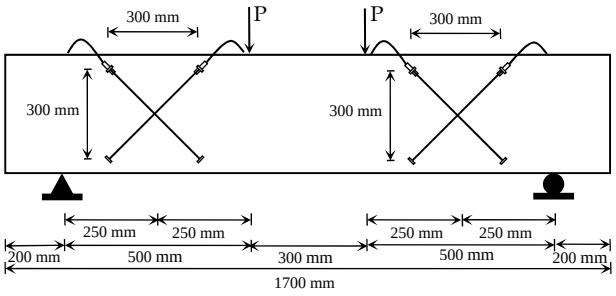

Figure 7.3 Layout of LVDT's to measure diagonal displacement in shear span

7.2.5 Test Setup and Procedure

The beams were tested in four-point bending using a test frame with closed-loop hydraulic actuator with a 2500 kN capacity. The beams were simply-supported with roller and hinge supports over a clear span of 1300 mm. The spacing between load points was 300 mm, and the shear span was 500 mm, giving a shear-span to depth ratio

of 1.62. The load was transferred from the actuator to the beam through two loading plates at mid-span. To uniformly distribute the load, the loading plates were levelled on the beam using hydro-stone. The test setup is shown in Figure 7.4.

The test procedure was as follows: the beam was placed over the supports, leveled and centered. All of the instrumentation (LVDT and strain gauges) was mounted on the beam and connected to the data acquisition system. The data acquisition system started gathering data before the application of load. The load was increased monotonically at a stroke rate of 0.18 mm/min. using a ramp function generator until failure of the beam. During the test, the initiation and progression of cracks were monitored.

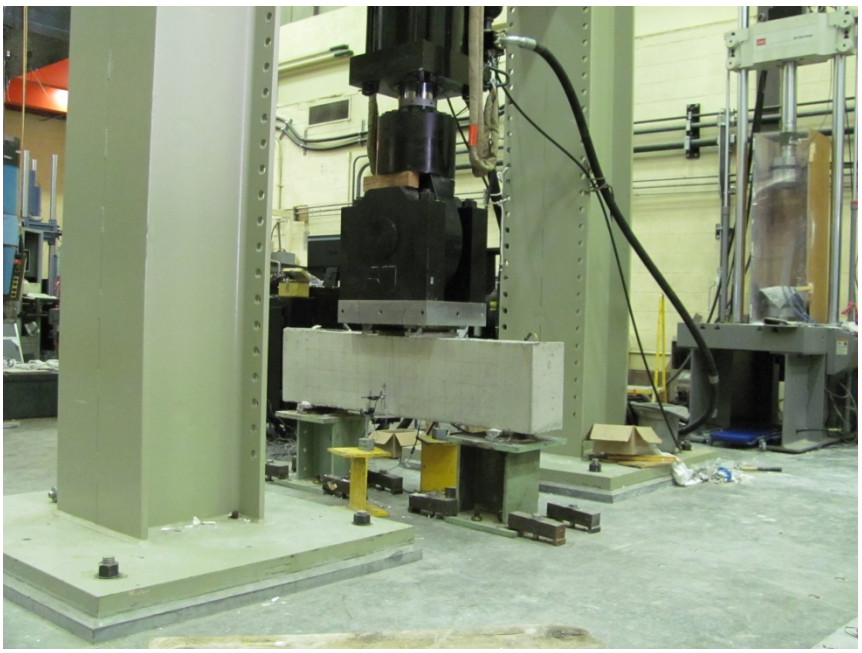

Figure 7.4 : Test setup

7.3 Test Results and Discussion

7.3.1 General Behaviour

A summary of test results is given in Table 7.3. The structural behaviour of the tested beams is discussed in terms of failure mode, load-deflection response, strain response and diagonal tensile displacement.

Table 7.3 : Summary of test results

Beam designation	Ultimate load (kN)	Increase in ultimate load (%)	Deflection at ultimate load (mm)	Strain in longitudinal reinforcement at midspan at failure (με)	Concrete strain at midspan at failure (με)	Failure mode
S0-N	1173.6	-	6.3	2253	2428	SS
S250-N	1310.1	-	6.2	2898	2067	SS
S0-CGM	1407.5	19.9	7.0	2224	3152	SS
S250-CGM	1412.7	7.8	7.7	2505	2449	SS
S0-CM	1446.6	23	6.5	2683	2893	SS
S250-CM	1522.7	16.0	8.9	-	-	SS
S0-CP	1322.3	12.6	6.4	2817	2730	SS→FR
S250-CP	1429.2	9.0	6.5	3114	2843	SS→FR

Note: Failure mode is specified as SS (splitting of strut) and SS→FR (splitting of strut → FRP rupture)

Failure Modes: The typical failure modes for the unstrengthened and strengthened beams are shown in Figure 7.5. The cracking patterns and failure modes of the unstrengthened and strengthened beams were similar. All beams failed by sudden splitting of the strut that formed. However, in the case of the strengthened beams, the

splitting of the strut was delayed due to the confinement provided by the strengthening systems. The cement-based system provided more confinement to the struts due to the bi-directional fabric tows and grid compared to the epoxy-based system which used a unidirectional sheet. At the onset of failure in the beams strengthened with the CFRP sheet, the CFRP sheet first split in the horizontal direction and then ruptured in the vertical direction which highlights the importance of bidirectional reinforcement in deep beams.

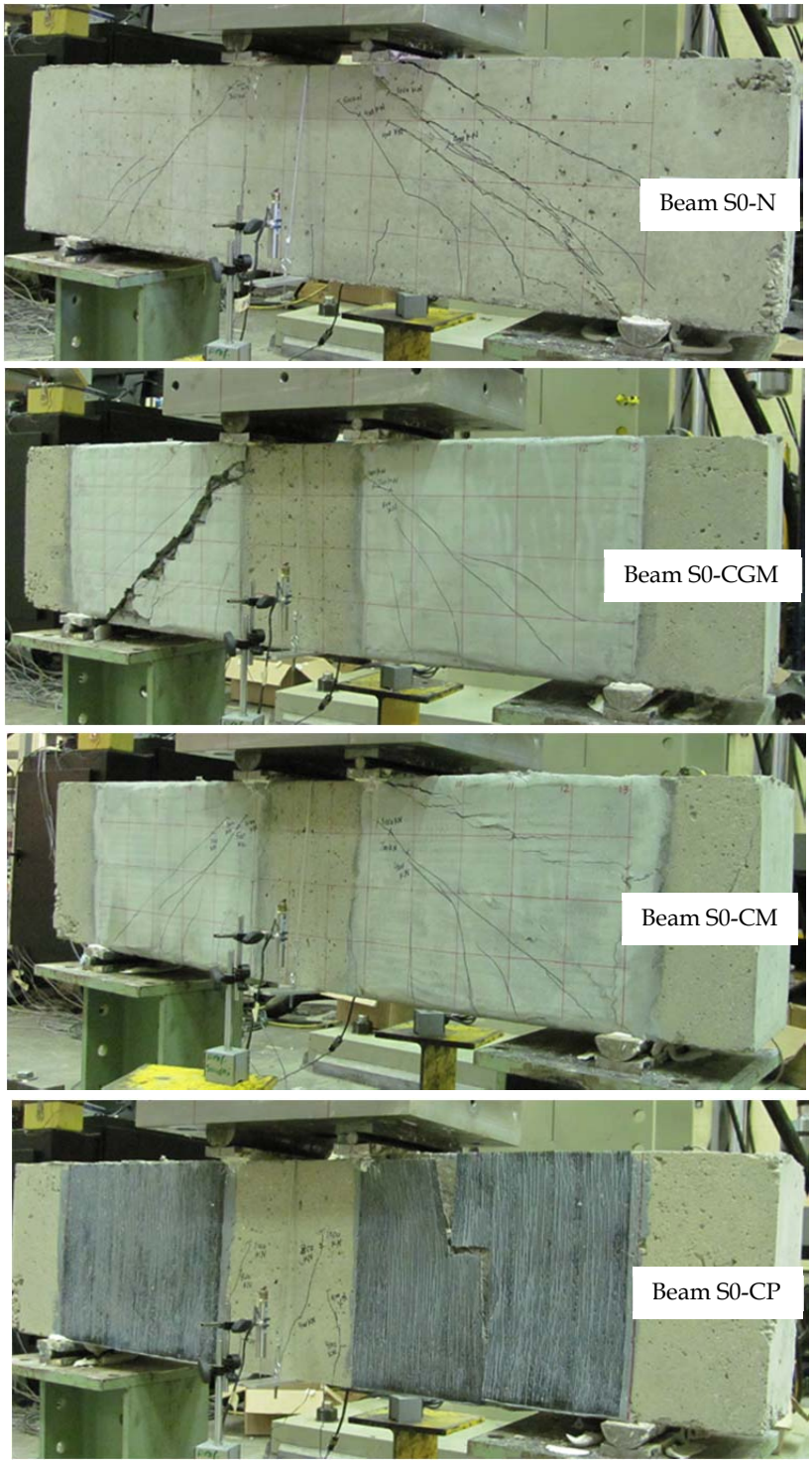

Figure 7.5 : Typical failure modes

Cracking of the beams was initiated with the appearance of flexural cracks under the concentrated load at midspan. As the load was increased, inclined cracks appeared in the shear spans. After the appearance of inclined shear cracks, the beam continued to carry load until sudden failure coincident with splitting of the struts. The appearance and propagation of shear cracks in the beams strengthened with the cement-based systems was readily visible which gave an indication of impending failure. In contrast, the beams strengthened with CFRP sheets did not have visible cracks and failed suddenly without any indication of impending failure.

*Load-Deflection Response: T*he load-deflection response of the tested beams is shown in Figure 7.6(a-b). Fig. 6a shows the load-deflection response for series S0 beams (beams without stirrups). The control unstrengthened beam without stirrups failed at a load of 1173.6 kN. The beams that were strengthened with CFRP grid in mortar, CFRCM and CFRP sheet failed at ultimate loads of 1407 kN, 1446.6 kN and 1322 kN, respectively. This represents an increase in ultimate load of 19.9%, 23.3% and 12.6% for the CFRP grid in mortar, CFRCM and CFRP sheet systems, respectively.

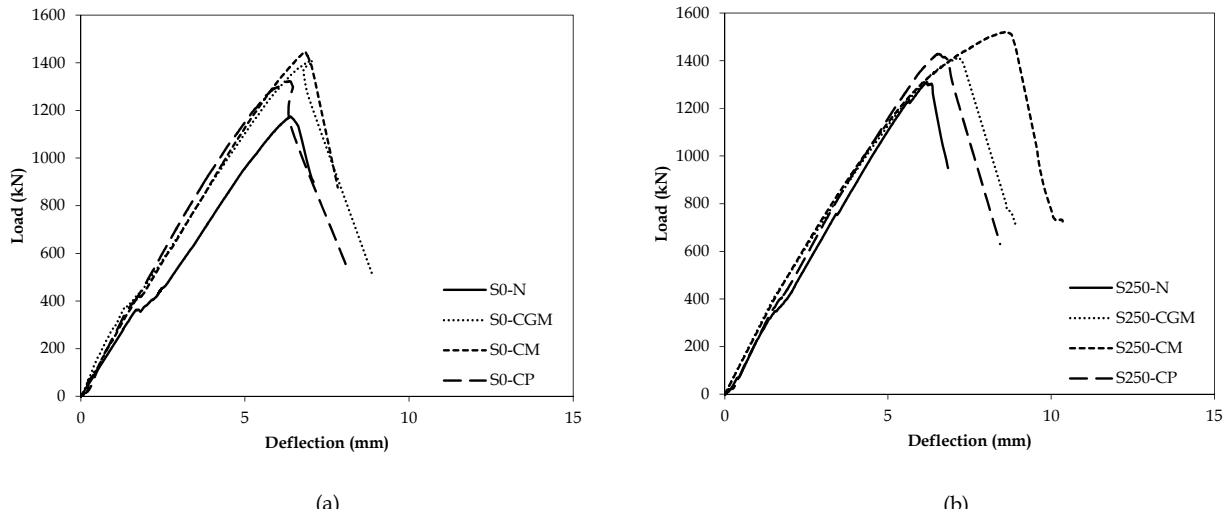

Figure 7.6 : load vs. deflection response of tested beams (a) beams without stirrups (b) beams with stirrups

mm stirrups @250 mm c/c). The control unstrengthened beam with stirrups failed at a load of 1310 kN. The beams strengthened with CFRP grid in mortar, CFRCM and CFRP sheet failed at ultimate loads of 1412 kN, 1522 kN and 1429 kN, respectively. This corresponds to 7.8%, 16.2% and 9% increase in the ultimate for the CFRP grid in mortar, CFRCM and CFRP sheet systems, respectively. The deflection at the ultimate load for the control (unstrengthened) and strengthened beams for both series ranged between 6.2 to 8.9 mm.

The beams that were strengthened with the CFRP sheet showed lower increase in ultimate load compared to the increase in ultimate load in the beams strengthened with the cement-based systems (CFRP grid in mortar, CFRCM). It is notable that the CFRP sheets have a ultimate strength (440.5 kN/m) that is five times higher than that of the

CFRP grid in mortar (80 kN/m) and 35% higher than the CFRCM (325 kN/m). This indicates that the cement-based systems (CFRP grid in mortar and CFRCM) performed more efficiently compared to the epoxy-based system (CFRP sheet).

Diagonal Tensile Displacements: Figure 7.7 (a-b) shows the load versus diagonal tensile displacement curves for series S0 and S250, respectively. In general, all strengthening systems were effective in controlling the diagonal tensile displacement for beams with or without stirrups. In order to quantify the relative effectiveness of different strengthening systems to control the diagonal cracks, the diagonal tensile displacement corresponding to the maximum load in the control beam was compared with the diagonal tensile displacement at same load level in the beams with the different strengthening systems. This quantitative analysis was only performed on beams without stirrups as the beam with stirrups did not exhibited significant effect of strengthening possibly due to low potential for strengthening.

Figure 7.7a shows the load versus diagonal tensile displacement curves for the series S0 beams. The diagonal tensile displacement at maximum load in the control beam (S0-N) was 2.57 mm compared a diagonal tensile displacement of 1.50 mm, 1.71 mm and 1.66 mm in beams strengthened with CFRP grid in mortar, CFRCM and CFRP sheet, respectively. This corresponds to a 44%, 33% and 35% decrease in the diagonal tensile displacement for the beams strengthened with CFRP grid in mortar, CFRCM and CFRP sheet, respectively.

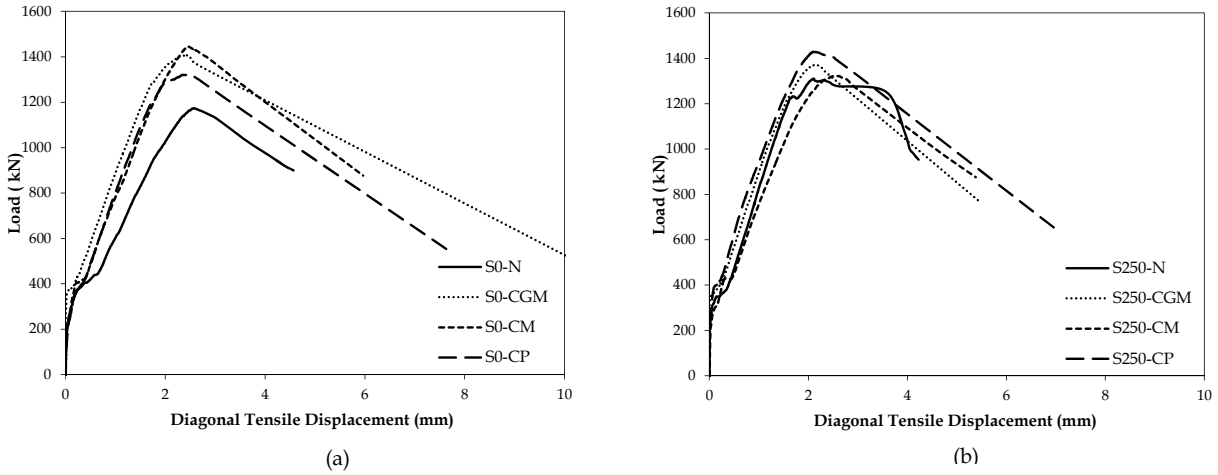

Figure 7.7 : load vs. diagonal tensile displacement (a) beams without stirrups (b) beams with stirrups

When diagonal cracking occurs in a strengthened beam, the strengthening system intersects the crack and restrains the crack opening. The effectiveness of strengthening system to control shear cracks depends on the tensile stiffness of the strengthening system and the bond between the strengthening system and the original beam concrete surface. The tensile stiffness of the fabric primarily depends on the area of the fiber tows and the modulus of elasticity of the fabric material. This means that the carbon fabric with high modulus of elasticity will provide better crack control in FRCM compared to glass fabric with a lower modulus of elasticity (assuming that the area of fibre tows is similar and that bond is adequate). Similarly, a heavier fabric with more tow area will provide better crack control compared to lighter fabric with a smaller tow area, assuming that the bond properties between the fabric and the beam surface are constant.

In the current study, the modulus of elasticity of the CFRP grid, carbon fabric and carbon fiber sheet was essentially equivalent at 230 GPa. However, the area of dry fiber or grid used was different in the three strengthening systems. The area of dry fiber or grid (in the vertical direction) per meter within the shear span was 43.6 mm^2, 88.3 mm^2 and 127.8 mm^2, respectively, for the CFRP grid in mortar, CFRCM and CFRP sheet systems. This indicates that the CFRP sheets have a tensile stiffness that is almost 200% higher than that of the CFRP grid in mortar and 45% higher than the CFRCM. In contrast, the CFRP sheet was less effective in controlling the diagonal crack width compared to the CFRP grid in mortar (the beams strengthened with CFRP sheets exhibited 35% reduction in diagonal crack width compared with a 44% reduction in beams strengthened with CFRP grid embedded in mortar). The CFRP sheets exhibited similar performance compared to the CFRCM, in spite of the 45% higher tensile stiffness of the CRFP sheet compared to the CFRCM. Considering the relative tensile stiffness of the CFRP sheet and the cement-based systems (CFRCM and CFRP grid in mortar), it can be concluded that the cement-based systems were more efficient in terms of controlling the diagonal tensile displacements. This appears to be primarily due to bi-directional fabric used in cement-based strengthening system compared to unidirectional sheets used in the epoxy-based strengthening system. The other possible reason is the better bond performance of cement-based systems compared to the epoxy-

based systems. This is explained further following the discussion of the efficiency of strengthening systems.

Strain Response; The compressive and tensile strains measured at failure in the concrete and in the longitudinal reinforcement are presented in Table 7.3. The measured compressive strains at failure in all beams were below the maximum compressive strain of 3500 με normally associated with concrete crushing in flexure for design purposes. The measured tensile reinforcement strains at failure in four beams (S250-N, S0-CM, S0-CP and S250-CP) exceeded the yield strain of 2500 με. It is important to note that all beams were reinforced with 6-25M tensile rebar placed in two layers, and the strain gauges were mounted on the bottom layer of steel. The beam responses did not suggest complete yielding of all reinforcement. In addition, no signs of flexural failure were observed in load-deflection curves.

Figure 7.8 shows the load versus strain measurements in the stirrups for all tested beams. As expected, the strengthened beams exhibited smaller strains in the stirrups compared to the control unstrengthened beams. This reduction in strain in the stirrups for strengthened beams is due to load sharing between the stirrups and the strengthening layer. The yielding of stirrups was delayed in the strengthened beams compared to unstrengthened beams. However, the stirrups yielded before shear failure in all of the beams in this study.

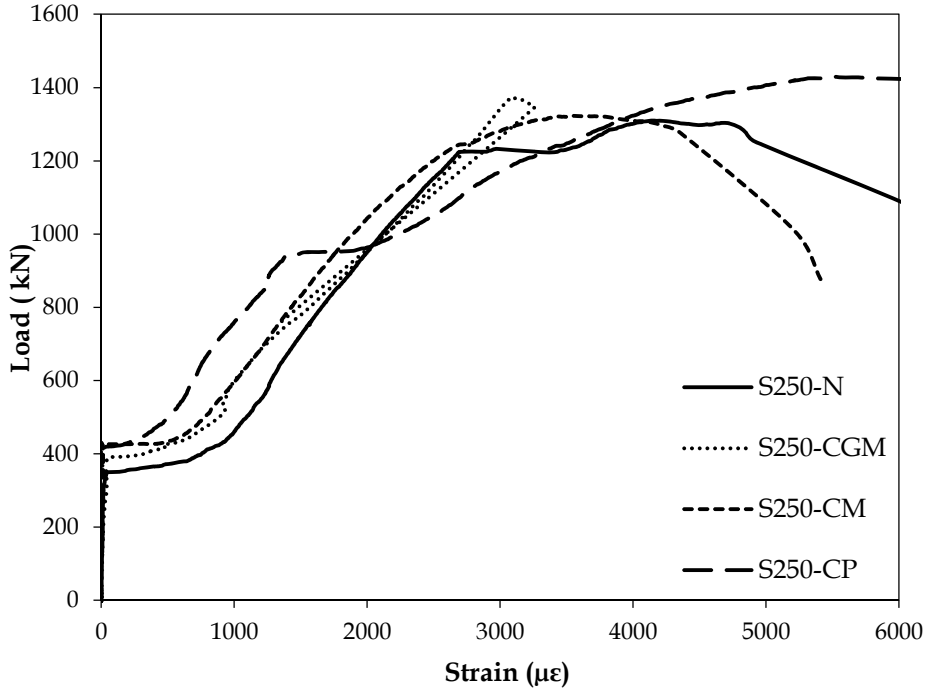

Figure 7.8 : load vs. strain in stirrups

7.3.2 Efficiency of Strengthening System

The performance of the two types of cement-based systems (CFRP grid in mortar and CFRCM) in comparison to the epoxy-based system (CFRP sheet) is illustrated by considering the efficiency of the strengthening systems. The efficiency is defined as the shear strength contribution from the strengthening system for each specimen divided by the ultimate tensile capacity per unit length of the strengthening system. The shear strength contribution from the different strengthening system is assumed to be equal to difference between the ultimate load of the companion strengthened and control beams. The tensile properties of the strengthening system are taken as the strength of the sheet,

fabric or grid without the contribution of the bonding agent (without epoxy for CFRP sheet and without mortar for CFRCM and CFRP grid embedded in mortar). As mentioned previously, the ultimate tensile capacities of the fiber strengthening systems in the beams strengthened with CFRP grid in mortar, CFRCM and CFRP were equal to 80 kN/m, 325 kN/m and 440.5 kN/m, respectively. Table 7.4 and Figure 7.9 present the efficiency of the different strengthening systems used. It is evident from Figure 7.9 that the CFRP grid embedded in mortar is the most efficient strengthening system followed by the CFRCM system. The CFRP sheet is the least efficient strengthening system among the three strengthening systems investigated in current study.

Table 7.4 : Efficiency of different strengthening methods

Strengthening Method	Beam Designation	Ultimate Tensile Capacity per unit length/shear span (kN)	Increase in Shear Strength due to strengthening (kN)	Efficiency of Strengthening system (%)
CFRP grid in mortar	S0-CGM	80	233.4	292
	S250-CGM	80	102.0	127
CFRCM	S0-CM	325	273.0	84
	S250-CM	325	213.0	65
CFRP	S0-CP	440	148.4	34
	S250-CP	440	119.0	27

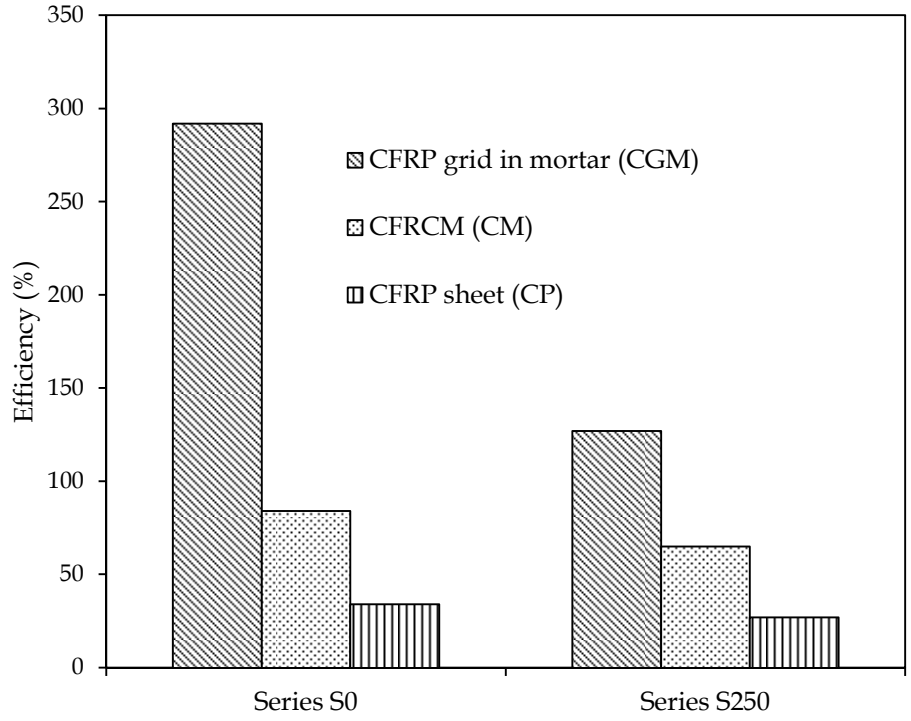

Figure 7.9 : Efficiency of cement-based shear strengthening systems in comparison to CFRP sheets

The apparent higher efficiency of the cement-based systems is attributed to the bi-directional fabric used in cement-based strengthening system compared to unidirectional sheets used in the epoxy-based strengthening system. For deep beams, horizontal (longitudinal) web reinforcement is also effective in controlling diagonal shear cracking. Therefore, beams with horizontal web reinforcement (bi-directional fabric) showed higher ultimate loads compared to beams without horizontal web reinforcement (unidirectional sheets). The other possible reason for this increased strength is the better bond performance of the cement-based systems compared to the epoxy-based systems. In the case of the cement-based systems, the bond between the

vertical (transverse) fibers of the strengthening system and the concrete appears to be significantly enhanced by the anchorage provided by the orthogonal (horizontal or longitudinal) tows of the fabric or grid. This distributes the bond stresses over a much larger area than in the CFRP sheet systems where bond of the vertical fibers to the concrete is provided by the epoxy over a more localized region.

The enhanced bond provided by the orthogonal tows in the cement-based systems is even more pronounced in the CFRP grid in mortar in comparison to the CFRCM since the orthogonal tows in the CFRP grid are strongly connected (woven and epoxy-bonded) compared to the orthogonal tows of carbon fabric used in CFRCM which are weakly connected (woven or tied with string). The more strongly connected tows of the CFRP grid in more appear to further enhance the anchorage of the vertical tows, thus improving shear resistance and system efficiency.

7.4 Analytical Predictions

The strut and tie model (STM) is generally used to predict the ultimate load carrying capacity of RC deep beams. The STM-based design provisions given in CSA A23.3-04 and ACI 318-08 do not include the effect of strengthening. Therefore, a simplified STM is proposed to predict the ultimate load carrying capacity of strengthened deep beams.

In a strut and tie model, the struts are subjected to compressive stresses and the tie is subjected to tensile force. The compression in the diagonal struts spreads out causing

transverse tension near mid-height of the strut. The struts will fail by splitting before yielding of the tie occurs in tension if the struts are not reinforced to prevent splitting. In ACI 318-08, a compressive stress limit of 0.51 f'_c has been proposed for such cases. Some researchers have recommended a different compressive stress limit of 0.6f'_c for such cases (Adebar and Zhou, 1993, Azam and Soudki 2012). In these studies, this limit was determined based on a uniform strut width. Therefore, if the geometry of diagonal strut is different at the two nodes, the average value of the strut width should be used in calculations.

Shear strengthening provides confinement to the diagonal struts and enhances the load carrying capacity of deep beams. This suggests that a higher compressive stress limit could be used for strengthened beams, although this is not addressed by any design codes or guidelines. Furthermore, none of the published literature reports a proposed compressive stress limit for a strut in deep beam strengthened with externally bonded system. Based on the experimental results from the current study, a compressive stress limit of 0.7f'_c for the concrete struts in RC deep beams strengthened with externally bonded systems gives a reasonable prediction of the ultimate load for the strengthened beams in the current study. However, this limit needs to be verified by more studies.

The first step in a strut and tie model analysis is to establish the geometry of the model. The geometry of strut and tie model for a tested beam is shown in Figure 7.10. The geometry of the strut and tie model is based on the recommendations of Martin and

Sanders (2007). The width of the strut is based on the width of the bearing plate (loading plate and reaction plate) and the height of the centroid of the tension and compression reinforcement. The upper edge of the strut starts from one end of the loading plate and ends at double the height of the centroid of the tension reinforcement above the reaction plate. The lower edge of the strut starts from double the height of the centroid of the compression reinforcement under the loading plate and ends at the other end of the reaction plate. Once geometry of the strut and tie model has been established, the next step is to determine the capacity of strut and followed by estimating the failure load based on capacity of the strut.

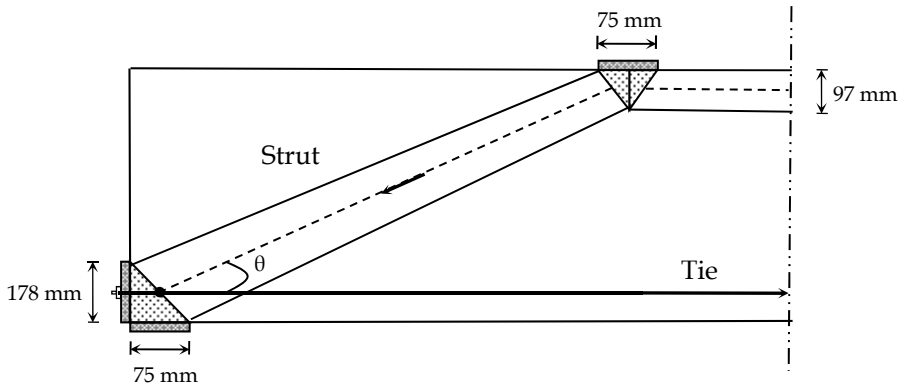

Figure 7.10 : Geometry of strut and tie model

Table 7.5 presents the experimental and predicted ultimate load of strengthened deep beams. It is evident from Table 7.5 that the predicted failure loads correlate well with experimental failure loads; the average ratio of experimental to predicted ultimate load was 1.07 with a coefficient of variation of 0.05.

Table 7.5 : Experimental and predicted ultimate loads for the strengthened beams

Strengthening Method	Beam Designation	Experimental Failure Load (kN)	Predicted Failure Load (kN)	Experimental/Predicted
CFRP grid in mortar	S0-CGM	1407.5	1328	1.06
	S250-CGM	1412.7	1328	1.06
CFRCM	S0-CM	1446.6	1328	1.09
	S250-CM	1522.7	1328	1.15
CFRP	S0-CP	1322.3	1328	1.00
	S250-CP	1429.2	1328	1.07

7.5 Conclusions

An experimental study was conducted to investigate the effectiveness of cement-based composite systems in comparison to existing epoxy-based system (carbon fiber reinforced polymer, CFRP) to strengthen shear-critical RC deep beams. Based on results of this study, the following conclusions can be drawn:

- Cement-based composite systems were effective in enhancing the load carrying capacity of RC deep beams. The beam without stirrups strengthened with CFRCM exhibited 23% increase in ultimate load, whereas a 20% increase in ultimate load was observed for RC beams without stirrups strengthened with CFRP grid embedded in mortar.
- Cement-based composite systems performed better compared to the existing epoxy-based FRP strengthening systems to strengthen shear-critical RC beams: the increase in ultimate load carrying capacity of beams without stirrups strengthened with

CFRCM was 23% compared to an increase of 13% in beams without stirrups strengthened with CFRP sheet. This is attributed to the bi-directional fabric used in cement-based strengthening system compared to unidirectional sheets used in the epoxy-based strengthening system; the horizontal tows of the bi-directional fabric appear to provide enhanced control of diagonal shear cracking in comparison to the unidirectional vertical sheets of the FRP system. The effect of horizontal web (shear) reinforcement is known to be more pronounced in deep beams than in slender beams. The other possible reason is the better bond performance of the cement-based systems compared to the epoxy-based systems.

- CFRP grid embedded in mortar is the most efficient shear strengthening system in terms of shear strength increase relative to system strength. This efficiency appears to be due to improved bond between the strengthening system and concrete substrate provided by anchorage of the vertical tows of the grid by the longitudinal tows.
- The failure loads of tested beams were predicted using simple strut and tie model by incorporating the effect of the strengthening system by increasing the diagonal strut capacity. The predicted strength of the strengthened beams using the existing code-specified strut and tie model parameters does not show any effect of the strengthening system, in contrast to the experimental results. The predicted failure loads with increased strut capacity correlated well with experimental failure loads.

Chapter 8: Discussion, Conclusions and Recommendations

8.1 Overall Discussions

A comprehensive study was conducted to investigate the behaviour of shear-critical RC beams strengthened with cement-based composite systems. Two types of cement-based systems were investigated in this study: fabric reinforced cementitious mortar (FRCM) and carbon fiber reinforced polymer (CFRP) grid embedded in mortar (CGM). The major objectives of the thesis included: 1) to evaluate the effectiveness of cement-based composite strengthening for shear-critical RC beams, 2) to compare the effectiveness of cement-based composite strengthening to that of FRP strengthening for shear-critical RC beams., 3) to investigate the contribution of the individual shear resisting components and their interaction and 4) to evaluate the applicability of existing FRP shear strengthening code provisions for use with cement-based systems, and propose modifications to existing models as required.

A research program was established to fulfill research objectives stated above. The research program consisted of experimental and analytical programs. The experimental program consisted of a total of 27 medium to large scale beams tested in two phases. Phase I focused on flexural testing of seven medium-scale shear-critical reinforced concrete (RC) beams. The beams measured 150 mm wide, 350 mm deep ad 2400 mm long. The objective of this phase was to evaluate the potential of FRCM shear

strengthening. The results of phase I study are presented in chapter 3. Phase II was designed based on results of Phase I study, and consisted of flexural testing of twenty (20) large-scale shear-critical RC beams strengthened with cement-based systems. Phase II was divided in to two groups: group A (12 slender beams) and group B (8 deep beams). All beams in phase II had the same cross section (250 mm wide x 400 mm deep) but had two different lengths of 2700 mm and 1700 mm for slender and deep beam, respectively. The objective of this phase was to evaluate the effectiveness of the two types of cement-based strengthening systems in comparison to the existing epoxy-based FRP system. The results of phase II study are presented in chapters 4 to 7.

Three types of analyses were performed in the analytical program 1) interaction between shear resisting components 2) efficiency of strengthening systems and 3) ultimate strength prediction. For slender beams, all three types of analysis were performed whereas for deep beams only last two types of analysis were performed. The details about these analyses are presented in chapter 3-7 and a summary of these analyses is presented in the following sections.

Chapters 3 through 7 of this thesis present the details of the research to address the objectives. This chapter provides a summary and discussion of the overall research findings in the context of each of the four overall research objectives. Recommendations for future research are also presented.

8.1.1 Effectiveness of Cement-Based Strengthening System to Strengthen Shear-Critical RC Beams

Chapter 3 presents results of an experimental study to investigate the effectiveness of different FRCM composite systems to strengthen shear-critical RC beams. The test variables included the type of FRCM (Glass FRCM (GFRCM) and carbon FRCM (CFRCM1 and CFRCM2) and the strengthening scheme (side bonded and U-wrapped). Test results indicated that the FRCM system significantly enhanced the ultimate load carrying capacity of shear-critical RC beams. The maximum increase in ultimate load was 105% for beams strengthened with u-wrapped CFRCM-2, and the lowest increase in ultimate load was 19% for beams strengthened with side bonded GFRCM. This difference was mainly due to the higher tensile stiffness of CFRCM-2 compared to GFRCM.

The side bonded and u-wrapped FRCM systems exhibited similar performance in terms of strength and failure modes. Furthermore, the side-bonded system did not exhibit a debonding failure. This suggested that the bond of the FRCM with the concrete substrate is sufficient such that u-wrapping may not be required. This is in contrast to most FRP fabric strengthening systems were u-wrapping is required for adequate bond.

8.1.2 Comparison of Cement-Based Composite Systems and Epoxy-Based Strengthening System for Strengthening of Shear -Critical RC Beams

The effectiveness of cement-based composite systems (CFRCM and CGM) in comparison to the epoxy-based system (CFRP sheets) to strengthen shear-critical RC beams was evaluated for slender and deep beams as presented in Chapters 6 and 7, respectively. The relative effectiveness of the cement-based shear strengthening systems in comparison to the existing epoxy-based system was evaluated based on several performance criteria including the load-deflection response, the ability to control diagonal or shear crack width, the internal stirrup strain response and the overall efficiency of strengthening systems (the efficiency is defined as the shear strength contribution from the strengthening system for each specimen divided by the ultimate tensile capacity per unit length of the strengthening system).

The experimental results for shear critical slender beams (Chapter 6) indicated that the cement-based composite systems performed better than the epoxy-based strengthening system, offering a similar increase in beam shear capacity in spite of the lower ultimate strength of the strengthening system. The beams that were strengthened with CFRCM and the CFRP sheet showed almost the same increase in ultimate load (Table 6.3) whereas the carbon fabric used in the CFRCM has ultimate strength of 325 kN/m compared to 440.5 kN/m ultimate strength of the carbon sheet used in the CFRP system. In addition, the cement-based systems exhibited a better ability to control

diagonal (shear) crack widths compared to the epoxy-based systems, providing a greater reduction in diagonal crack width despite the relative lower ultimate strength and stiffness of the cement-based systems. Moreover, the test results indicated that the CFRP grid embedded in mortar was the most efficient shear strengthening system in terms of shear strength increase relative to system strength. This efficiency appears to be due to improved bond between the strengthening system and concrete substrate provided by anchorage of the vertical tows of the rigid CFRP grid by the longitudinal tows.

The test results for shear critical RC deep beams (Chapter 7) indicated that the cement-based composite systems performed better than the existing epoxy-based FRP strengthening systems for deep beams. The increase in the ultimate load carrying capacity of beams without stirrups strengthened with CFRCM was 23% compared to an increase of 13% for beams strengthened with CFRP sheet. This improvement was attributed to the bi-directional fabric used in the cement-based strengthening system compared to unidirectional sheets used in the epoxy-based strengthening system. The horizontal tows of the bi-directional fabric appeared to provide enhanced control of diagonal shear cracking in comparison to the unidirectional vertical sheets of the FRP system. The effect of horizontal web (shear) reinforcement is known to be more pronounced in deep beams than in slender beams. As in case of deep beams horizontal web (shear) reinforcement is also effective in controlling the diagonal shear cracking.

The other possible reason is the apparent better bond performance of the cement-based systems compared to the epoxy-based systems. The research results indicate that the CFRP grid embedded in mortar is the most efficient shear strengthening system in terms of shear strength increase relative to system strength. This efficiency appears to be due to improved bond between the strengthening system and concrete substrate provided by anchorage of the vertical tows of the grid by the longitudinal tows, as well as the shear contribution of the horizontal tows of the CFRP grid.

8.1.3 Interaction Between Shear Resisting Components

A shear component analysis was performed to investigate the interaction between the different shear resisting components. In this analysis, the shear resistance provided by the cement-based composite strengthening layer and the internal transverse reinforcement (steel stirrups) were estimated using experimentally measured strains. The shear resistance provided by the concrete cannot be determined directly from the experimental results, and thus was estimated by subtracting the estimated shear resistance contributions provided by the stirrups and strengthening layer from the experimentally observed total shear strength. The shear component analysis for beams strengthened with the carbon fabric reinforced cementitious mortar (CFRCM) and carbon fiber reinforced polymer (CFRP) grid embedded in mortar (CGM) is presented in Chapter 4 and Chapter 5, respectively. The primary findings of the shear component analysis are presented in Figure 4.13 and Figure 5.13.

The shear component analysis indicated that for the control unstrengthened beams, the shear resistance provided by the concrete increased with the addition of stirrups since the beams did not fail suddenly after yielding of the stirrups. The shear resistance provided by concrete increased further with the addition of the strengthening layer. Overall, the shear resistance provided by the concrete increased with an increase in total shear reinforcement ratio. The increase in shear resistance provided by the concrete is possibly due to two reasons: 1) the confinement provided by internal and external shear reinforcement, or 2) the shear transfer mechanism changes to arch action, or both.

The addition of the shear strengthening system reduced the shear strength contribution from the stirrups. The strengthened beams with stirrups exhibited steeper shear cracks compared to the control unstrengthened beams with stirrups. The steeper shear cracks intersected fewer stirrups, resulting in a reduced shear strength contribution from the stirrups in strengthened beams. Similarly, the presence of stirrups reduces the shear strength contribution from the external strengthening system. Again, the addition of stirrups results in steeper shear cracks which intersect fewer fibers tows in the strengthening system, which results in a reduced shear strength contribution from strengthening layer.

8.1.4 Applicability of Existing FRP Design Guidelines for Use with Cement-Based Strengthening Systems

In slender beams, the shear strength contribution from externally bonded materials (FRP sheets or FRCM) is normally determined using a truss analogy approach similar to that used for steel stirrups. The primary difference is the stress level used in the different materials: yield stress is used for the steel stirrups, while the effective stress is used for the FRP and FRCM. The effective stress for FRP is the lesser of (1) the effective stress based on debonding of FRP sheet, or (2) the effective stress based on the aggregate interlock limit (strain limit at which shear resistance provided by aggregate interlock is lost). A maximum strain of 0.4 % is generally recommended to preclude failure by aggregate interlock. The experimental results from the current study indicate that a debonding failure of the FRCM or CGM system does not occur, and thus the effective stress can be assumed to be dependent on the aggregate interlock limit only.

In chapter 3, the shear strength contribution from FRCM strengthening was calculated using the ACI 440.2R (2008) and CAN/CSA-S6 (2006) provisions for externally bonded FRP sheets using the proposed modification (debonding failure can be neglected when determining the effective stress). The predicted ultimate loads correlated well with the experimental ultimate loads, indicating that the existing FRP shear design guidelines can be used FRCM shear strengthening with the effective stress modification described above.

In chapter 4, the shear strength contribution from CFRCM strengthening was calculated using ACI 549.4R-13, a new design guide for the design and construction of externally bonded FRCM systems. The ACI 549.4R-13 provisions to calculate the shear strength contribution from externally bonded FRCM are similar to the ACI 440.2R (2008) provisions except ACI 549.4R-13 do not consider effective strain based on debonding similar to modification proposed by author in chapter 3 and discussed above. The CFRCM shear strength predictions using ACI 549.4R-13 were in good correlation with experimental CFRCM shear contributions estimated using experimental strain measurements. However, the CFRCM shear strength predictions using ACI 549.4R-13 were underestimated when compared with the experimental CFRCM shear contributions estimated from capacity subtraction ($V_{FRCM} = V_{STRENGTHENED} - V_{CONTROL}$). Unlike the experimental strain measurements method, the capacity subtraction method does not take into account the interaction between different shear resisting components. Hence it can be concluded that ACI 549.4R-13 reasonably predicts CFFRCM shear strength contribution. However, the existing methods to calculate the shear contribution from concrete do not account for the effect of strengthening and need to be studied further.

In chapter 5, the shear strength contribution from CGM strengthening was calculated using the ACI 440.2R (2008) and CAN/CSA-S6 (2006) provisions for externally bonded FRP sheets using the proposed modification (debonding failure can be neglected when

determining the effective stress). The CGM shear strength predictions were in reasonable correlation with experimental CGM shear contributions estimated using experimental strain measurements. However, the CGM shear strength predictions using the ACI 440.2R (2008) and CAN/CSA-S6 (2006) were underestimated when compared with the experimental CGM shear contributions estimated from capacity subtraction ($V_{FRCM} = V_{STRENGTHENED} - V_{CONTROL}$). This further reinforces the observation made in chapter 4 that the existing methods to calculate the shear contribution from concrete do not account for the effect of strengthening and need to be studied further.

In conclusion, existing FRP shear design guidelines with proposed modifications reasonably predicts the shear strength contribution from cement-based composite systems. However, shear resistance provided by concrete is significantly under predicted by existing methods. Therefore, the effect of strengthening on the shear strength contribution from concrete need to be studied further.

The strut and tie model (STM) is generally used to predict the ultimate load carrying capacity of RC deep beams. Existing STM-based design provisions do not include the effect of strengthening. However, shear strengthening provides confinement to the diagonal compression struts and enhances the load carrying capacity of deep beams. This suggests that a higher compressive stress limit could be used for strengthened beams, although this is not addressed by any design codes or guidelines. Furthermore, none of the published literature reports a proposed compressive stress limit for a strut

in deep beam strengthened with externally bonded system. Based on the experimental results from the current study, a compressive stress limit of $0.7f'_c$ for the concrete struts in RC deep beams strengthened with externally bonded systems gives a reasonable prediction of the ultimate load for the strengthened beams in the current study. However, this limit needs to be verified by more studies.

8.2 Conclusions

8.2.1 Main Conclusions

The overall conclusions from this research are as follows:

- Cement-based composite systems performed better than the epoxy-based strengthening system to strengthen shear-critical RC beams in terms of shear strength increase relative to system strength. The CFRP grid embedded in mortar (CGM) was the most efficient shear strengthening system by this measure.
- The bond of cement–based system with the concrete substrate is sufficient that u-wrapping may not be required; the side-bonded systems studied did not exhibit signs of premature debonding. This is in contrast to most FRP fabric strengthening systems where u-wrapping is required for adequate bond.
- Cement-based systems exhibited a better ability to control diagonal (shear) crack widths compared to the epoxy-based system tested, providing a greater

reduction in diagonal crack width despite the relative lower ultimate strength and stiffness of the cement-based systems.

- An increase in the amount of transverse reinforcement (internal and/or external) resulted in steeper diagonal crack angles. As the total transverse reinforcement ratio was increased, the crack angle was greater than 45˚. Therefore, the shear strength predictions of strengthened beams with an assumed crack angle smaller than 45˚ may lead to an overestimation of the shear strength contribution from the strengthening system.
- Shear strengthening resulted in reduced shear strength contribution from stirrups. The strengthened beams with stirrups exhibited steeper shear cracks compared to control unstrengthened beams with stirrups. The steeper shear cracks intersect fewer stirrups, resulting in reduced shear strength contribution from stirrups in strengthened beams. Similarly, the presence of stirrups reduces the shear strength contribution from strengthening. Again, the addition of stirrups results in steeper shear cracks which intersect fewer fibers tows in the strengthening system which results in a reduced shear strength contribution from strengthening layer.

8.2.2 Detailed Conclusions

The results of this study were presented five journal papers. The main findings from each paper are summarized as follows:

1. **FRCM Strengthening of Shear-Critical RC Beams:** In this study, the effectiveness of different types of fabric reinforced cementitious matrix (FRCM) composite systems to strengthen shear-critical RC beams was investigated. Seven shear-critical RC beams were tested. The test variables included the strengthening material (glass FRCM or carbon FRCM) and the strengthening scheme (side bonded or u-wrapped). The experimental results were also compared with theoretical predictions according to FRP design guidelines in North America with some modifications (ACI 440.2R 2008 and CAN/CSA-S6 2006). The conclusions from this study are presented below:
    a. The FRCM system significantly enhanced the ultimate load carrying capacity of shear-critical RC beams. The maximum increase in ultimate load was 105% for beams strengthened with u-wrapped CFRCM-2, and the lowest increase in ultimate load was 19% for beams strengthened with side bonded GFRCM.
    b. The FRCM system slightly increased the stiffness of the strengthened beams compared to the control (unstrengthened) beams. The maximum increase in stiffness was for beams strengthened with CFRCM-2 (11% increase) followed by beams strengthened with CFRCM-1 (9% increase).
    c. Side bonded vs. u-wrapped FRCM exhibited similar performance in terms of strength and failure modes. This suggests that the bond of the FRCM with the concrete substrate is sufficient that u-wrapping may not be required. This is

in contrast to most FRP fabric strengthening systems were u-wrapping is required for adequate bond.

2. **Strengthening of Shear-Critical RC Beams with CFRCM:** In this study, the behaviour of shear-critical RC beams strengthened with carbon fabric reinforced cementitious matrix (CFRCM) composite systems was investigated. Six large scale shear-critical RC beams were tested. The test variables included the amount of internal transverse reinforcement and CFRCM strengthening. The experimental shear strength contributions were also compared with theoretical predictions using a new design guide for FRCM (ACI 549.3R-13). Lastly, the shear transfer mechanism in the CFRCM strengthening layer was also discussed. The conclusions from this study are presented below:

    a. CFRCM strengthening is effective in enhancing the load-carrying capacity of shear-critical RC beams. The maximum increase in the ultimate load (87.4%) was observed for beams without stirrups.

    b. An increase in the amount of transverse reinforcement (internal and/or external) results in steeper diagonal crack angles. As the total transverse reinforcement ratio is increased, the crack angle could be greater than 45˚. Therefore, the shear strength predictions of strengthened beams with an assumed crack angle smaller than 45˚ may lead to an overestimation of the shear strength contribution from the strengthening system.

c. CFRCM strengthening reduces the shear strength contribution from stirrups. The CFRCM strengthened beams with stirrups exhibited steeper shear cracks compared to control unstrengthened beams with stirrups. The steeper shear cracks intersect fewer stirrups, resulting in reduced shear strength contribution from stirrups in strengthened beams. Similarly, the presence of stirrups reduces the shear strength contribution from CFRCM strengthening. Again, the addition of stirrups results in steeper shear cracks which intersect fewer fibers tows in the CFRCM system which results in a reduced shear strength contribution from CFRCM strengthening layer.

d. CFRCM strengthening resulted in lower strains in the internal shear reinforcement (stirrups) at a given load level. However, the stirrups in all beams tested yielded before beam failure. Therefore, it is safe to assume that the stirrups are yielded while calculating the shear strength of strengthened beams.

e. The average CFRCM strain across shear crack at failure for all specimens was 5083 με; with a coefficient of variation of 6%. Thus, it appears that the CFRCM strain limit of 4000με specified in ACI 549.4R-13 is adequate for design.

f. Based on the observed shear transfer mechanism of the CFRCM strengthening layer, it can be concluded that shear in the transverse (vertical) tows of the fabric is mainly transferred to the concrete surface through the

longitudinal tows which act as anchorage for the transverse tows. Therefore, to achieve better performance of the CFRCM strengthening layer, a fabric in which the tows are strongly connected in orthogonal directions should be used.

g. The CFRCM shear strength predictions using ACI 549.4R-13 were in good correlation with experimental CFRCM shear contributions estimated using experimental strain measurements.

3. **CFRP Grid Embedded in Mortar for Strengthening of Shear-Critical RC Beams:** In this study, the effectiveness of the CGM composite system to strengthen shear-critical reinforced concrete (RC) beams was investigated. The experimental shear strength contributions were also compared with theoretical predictions using FRP design guidelines in North America with some modifications. The conclusions from this study are presented as follow:

   a. CFRP grid embedded in mortar (CGM) is effective in enhancing the load carrying capacity of shear-critical RC beams. Based on measured strains, the strength contribution from the CGM was similar for all beams tested (independent of internal reinforcement amount). However, based on capacity subtraction, the increase in ultimate load of the strengthened beams without stirrups was 47.5%, while the strength enhancement was lower for strengthened beams with stirrups where the average strength increase was 10.2 %.

b. CGM strengthening reduces the shear strength contribution from stirrups. The CGM strengthened beams with stirrups exhibited steeper shear cracks compared to control unstrengthened beams with stirrups. The steeper shear cracks intersected fewer stirrups, resulting in reduction in the shear strength contribution from the stirrups in the strengthened beams.

c. The average CGM strain across shear crack at failure for all specimens was 4672 με; with a coefficient of variation of 6%. Thus, it appears that the strain limit of 4000με specified in FRP design guidelines in North America (ACI 440.2R (2008) and CAN/CSA S6 (2006)) is appropriate for use with the CGM strengthening used in this study.

d. Based on the observed shear transfer mechanism of the CGM strengthening layer, it can be concluded that the failure of the strengthening layer is caused by the CFRP grid rupture provided that the CFRP grid is covered with enough mortar cover. To ensure the CFRP grid rupture failure, a thicker layer of mortar should be used in CGM strengthening layer in future studies.

e. The CGM shear strength predictions using CAN/CSA S6 (2006) were in good correlation with experimental CGM shear contributions estimated using experimental strain measurements.

4. **Strengthening of Shear-Critical RC Beams: Alternatives to Existing Externally Bonded CFRP Sheets:** In this study, the effectiveness of cement-based composite

systems in comparison to an existing epoxy-based system (carbon fiber reinforced polymer, CFRP) to strengthen shear-critical RC beams was investigated. Two types of cement-based systems were investigated in this study: carbon fiber reinforced polymer (CFRP) grid embedded in mortar and carbon fabric reinforced cementitious mortar (CFRCM). The conclusions from this study are presented as follows:

a. Cement-based composite systems performed better than the epoxy-based strengthening system to strengthen shear-critical RC beams, offering a similar increase in shear capacity in spite of the lower ultimate strength of the material: the increase in ultimate load carrying capacity of beams without stirrups strengthened with CFRCM was 87.4% compared to an increase of 84.8% in beams without stirrups strengthened with CFRP sheet.

b. Cement-based systems exhibited a better ability to control diagonal (shear) crack widths compared to the epoxy-based systems, providing a greater reduction in diagonal crack width despite the relative lower ultimate strength and stiffness of the cement-based systems.

c. CFRP grid embedded in mortar is the most efficient shear strengthening system in terms of shear strength increase relative to system strength. This efficiency appears to be due to improved bond between the strengthening system and concrete substrate provided by anchorage of the vertical tows of the grid by the longitudinal tows.

5. **Shear Strengthening of RC Deep Beams with Cement-Based Composites:** In this study, the effectiveness of cement-based composite systems in comparison to an existing epoxy-based carbon fiber reinforced polymer (CFRP) system to strengthen RC deep beams was investigated. The results are presented as follows:
    - Cement-based composite systems were effective in enhancing the load carrying capacity of RC deep beams. The beam without stirrups strengthened with CFRCM exhibited 23% increase in ultimate load, whereas a 20% increase in ultimate load was observed for RC beams without stirrups strengthened with CFRP grid embedded in mortar.
    - Cement-based composite systems performed better compared to the existing epoxy-based FRP strengthening systems to strengthen shear-critical RC beams: the increase in ultimate load carrying capacity of beams without stirrups strengthened with CFRCM was 23% compared to an increase of 13% in beams without stirrups strengthened with CFRP sheet. This is attributed to the bi-directional fabric used in cement-based strengthening system compared to unidirectional sheets used in the epoxy-based strengthening system; the horizontal tows of the bi-directional fabric appear to provide enhanced control of diagonal shear cracking in comparison to the unidirectional vertical sheets of the FRP system. The effect of horizontal web (shear) reinforcement is known to be more pronounced in deep beams than in slender beams. The other possible

reason is the better bond performance of the cement-based systems compared to the epoxy-based systems.

- CFRP grid embedded in mortar is the most efficient shear strengthening system in terms of shear strength increase relative to system strength. This efficiency appears to be due to improved bond between the strengthening system and concrete substrate provided by anchorage of the vertical tows of the grid by the longitudinal tows.
- The failure loads of tested beams were predicted using simple strut and tie model by incorporating the effect of the strengthening system by increasing the diagonal strut capacity. The predicted strength of the strengthened beams using the existing code-specified strut and tie model parameters does not show any effect of the strengthening system, in contrast to the experimental results. The predicted failure loads with increased strut capacity correlated well with experimental failure loads.

8.3 Recommendations for Future Work

A number of parameters affect the behaviour of shear-critical RC beams strengthened with cement-based strengthening systems. A few parameters have been investigated in the current study and the remaining parameters should be investigated in future studies. It is recommended that the following be considered for future work:

- In the current study, the interaction between different shear components was investigated. The analysis revealed that a significant interaction exists between different shear components. In future studies, this interaction should be further studied and new design approaches should be developed to quantify the effects of interaction between shear components.
- In general, the interaction between internal stirrups and external strengthening was investigated. However, the analysis of current study results showed that this interaction was negligible compared to the interaction between concrete and transverse reinforcement (internal and external). In future studies, this aspect of interaction between shear components should be further investigated.
- The current study was conducted under monotonic loading. It is recommended for future studies to investigate the effect of cyclic loading on the behaviour of cement-based strengthening systems.
- In the current study, the thickness of the mortar (strengthening layer) was 8-12 mm. The analysis of results showed that the thickness of mortar was an important parameter which affected the failure of strengthening layer especially in case of CGM strengthening layer. In future studies, a thicker layer of mortar should be investigated.

- In the current study, a very light (0.04 mm thick) CFRP grid was used in CGM strengthening. In future studies, heavier CFRP grids embedded in mortar should be investigated.

References

ACI Committee 318, (2014). “Building Code Requirements for Structural Concrete” ACI 318M-14, American Concrete Institute, Farmington Hills, Michigan, U.S.A.

ACI-440.2R (2008). “Guide for the Design and Construction of Externally Bonded FRP Systems for Strengthening Concrete Structures,” American Concrete Institute, Farmington Hills, Michigan, USA.

ACI-549.4R (2013). “Guide to Design and Construction of Externally Bonded Fabric-Reinforced Cementitious matrix Systems for Repair and Strengthening Concrete and Masonry Structures,” American Concrete Institute, Farmington Hills, Michigan, U.S.A.

Adebar, Perry and Zongyu Zhou. 1993. "Bearing Strength of Compressive Struts Confined by Plain Concrete." *ACI Structural Journal* 90 (5): 534-541.

Al-Salloum, Y. A., H. M. Elsanadedy, S. H. Alsayed, and R. A. Iqbal. 2012. "Experimental and Numerical Study for the Shear Strengthening of Reinforced Concrete Beams using Textile-Reinforced Mortar." *Journal of Composites for Construction* 16 (1): 74-90.

Al-Sulaimani, G. J., Shariff, A., Basanbul, I. A., Baluch, M. H, and Ghaleb, B. N. 1994. "Shear Repair of Reinforced Concrete by Fiber Glass Plate Bonding." *ACI Structural Journal* 91 (4): 295-303.

Arboleda, D., G. Loreto, A. De Luca, and A. and Nanni. 2012. "Material Characterization of Fiber Reinforced Cementitious Matrix (FRCM) Composite Laminates." Havana, Cuba, X International Symposium on Ferrocement and Thin Reinforced Cement Composites (FERRO 10), October 12-17.

Azam, R. and K. Soudki. 2012. "Structural Performance of Shear-Critical RC Deep Beams with Corroded Longitudinal Steel Reinforcement." *Cement and Concrete Composites* 34 (8): 946-57.

Azam, R. and K. Soudki. 2014b. "Strengthening of Shear-Critical RC Beams with Cement-based Composites: A Pilot Study.".

Azam, R. and K. Soudki. 2013. "Structural Behavior of Shear-Critical RC Slender Beams with Corroded Properly Anchored Longitudinal Steel Reinforcement." *Journal of Structural Engineering* 139 (12): 04013011 (11 pp.).

Azam, R. and K. Soudki. 2014a. "FRCM Strengthening of Shear-Critical RC Beams." *Journal of Composites for Construction* 18 (5): 04014012 (9 pp.).

Azam, R., Soudki, K., and West, J.S. (2016). "Strengthening of RC Beams with GFRCM." ACI Special Publication (in press)

Belarbi, A., S-W Bae, A. Ayoub, D. Kuchma, A. Mirmiran, and A. and Okeil. 2011. *Design of FRP Systems for Strengthening Concrete Girders in Shear*: NCHRP Report.

Blanksvard, T (2007). “Strengthening of Concrete Structures by the use of Mineral-Based Composites,” *Doctoral Thesis, Lulea University of Technology, Lulea, Sweden.*

Blanksvärd, T., B. Täljsten, and A. Carolin. 2009. "Shear Strengthening of Concrete Structures with the use of Mineral-Based Composites." *Journal of Composites for Construction* 13 (1): 25-34.

Bousselham, Abdelhak and Omar Chaallal. 2004. "Shear Strengthening Reinforced Concrete Beams with Fiber-Reinforced Polymer: Assessment of Influencing Parameters and Required Research." *ACI Structural Journal* 101 (2): 219-227.

Bruckner, A., R. Ortlepp, and M. Curbach. 2006. "Textile Reinforced Concrete for Strengthening in Bending and Shear." *Materials and Structures/Materiaux Et Constructions* 39 (292): 741-748.

Bruckner, A., R. Ortlepp, and M. Curbach. 2008. "Anchoring of Shear Strengthening for T-Beams made of Textile Reinforced Concrete (TRC)." *Materials and Structures/Materiaux Et Constructions* 41 (2): 407-418.

CAN/CSA-A23.3-04, (2004).”Design of Concrete Structures” Canadian Standard Association, Rexdale, Ontario, Canada, 240p.

CAN/CSA-S6-06. (2006). “Canadian Highway Bridge Design Code” Canadian Standards Association, Toronto.

Carolin, Anders and Bjorn Taljsten. 2005. "Theoretical Study of Strengthening for Increased Shear Bearing Capacity." *Journal of Composites for Construction* 9 (6): 497-506.

Chaallal, O., M. Shahawy, and M. Hassan. 2002. "Performance of Reinforced Concrete T-Girders Strengthened in Shear with Carbon Fiber-Reinforced Polymer Fabric." *ACI Structural Journal* 99 (3): 335-343.

Chajes, M. J., Jansuska, T. F., Mertz, D. R., Thomson, T. A., and Finch, W. W. 1995. "Shear Strength of RC Beams using Externally Applied Composite Fabrics." *ACI Structural Journal* 92 (3): 295-303.

Chen, G. M., J. G. Teng, J. F. Chen, and O. A. Rosenboom. 2010. "Interaction between Steel Stirrups and Shear-Strengthening FRP Strips in RC Beams." *Journal of Composites for Construction* 14 (5): 498-509.

Chen, J. F. and J. G. Teng. 2003. "Shear Capacity of Fiber-Reinforced Polymer-Strengthened Reinforced Concrete Beams: Fiber Reinforced Polymer Rupture." *Journal of Structural Engineering* 129 (5): 615-625.

Chen, J. F. and J. G. Teng. 2003b. "Shear Capacity of FRP-Strengthened RC Beams: FRP Debonding."Elsevier Ltd, 2002.

Colalillo, M. A. and S. A. Sheikh. 2014. "Behavior of Shear-Critical Reinforced Concrete Beams Strengthened with Fiber-Reinforced Polymer-Experimentation." *ACI Structural Journal* 111 (6): 1373-1384.

Collins, M. P., E. C. Bentz, and E. G. Sherwood. 2009. "Where is Shear Reinforcement Required? Review of Research Results and Design Procedures." *ACI Structural Journal* 106 (4): 556.

De Caso, y. Basalo, F. Matta, and A. Nanni. 2012. "Fiber Reinforced Cement-Based Composite System for Concrete Confinement." *Construction and Building Materials* 32: 55-65.

Escrig, C., L. Gil, E. Bernat-Maso, and F. Puigvert. 2015. "Experimental and Analytical Study of Reinforced Concrete Beams Shear Strengthened with Different Types of Textile-Reinforced Mortar." *Construction and Building Materials* 83: 248-260.

Hashemi, S. and R. Al-Mahaidi. 2012. "Experimental and Finite Element Analysis of Flexural Behavior of FRP-Strengthened RC Beams using Cement-Based Adhesives." *Construction and Building Materials* 26 (1): 268-73.

Hegger, J. and Voss, S. 2004. "Textile Reinforced Concrete Under Biaxial Loading." Varenna, Italy, Proceedings of 6th Rilem Symposium on Fiber Reinforced Concrete (FRC), BEFIB 2004, .

Hegger, J., N. Will, O. Bruckermann, and S. Voss. 2006. "Load-Bearing Behaviour and Simulation of Textile Reinforced Concrete." *Materials and Structures/Materiaux Et Constructions* 39 (292): 765-776.

Higgins, C. and W. C. Farrow III. 2006. "Tests of Reinforced Concrete Beams with Corrosion-Damaged Stirrups." *ACI Structural Journal* 103 (1): 133-141.

ISIS Design Manual 4 Version 2 (2008). "FRP rehabiliatation of reinforced concrete structures," *ISIS Canada Research Network, Winnipeg, Canada.*

Islam, M. R., M. A. Mansur, and M. Maalej. 2005. "Shear Strengthening of RC Deep Beams using Externally Bonded FRP Systems." *Cement and Concrete Composites* 27 (3): 413-420.

Johnson, P.M., Couture, A., and Nicolet, R. 2007. *Commission of Inquiry into the Collapse of a Portion of the De La Concorde Overpass*: Government of Quebec.

Jumaat, M. Z., M. A. Rahman, M. A. Alam, and M. M. Rahman. 2011. "Premature Failures in Plate Bonded Strengthened RC Beams with an Emphasis on Premature Shear: A Review." *International Journal of Physical Sciences* 6 (2): 156-168.

Khalifa, Ahmed and Antonio Nanni. 2000. "Improving Shear Capacity of Existing RC T-Section Beams using CFRP Composites." *Cement and Concrete Composites* 22 (3): 165-174.

Khalifa, Ahmed, William J. Gold, Antonio Nanni, and Abdel M. I. Aziz. 1998. "Contribution of Externally Bonded FRP to Shear Capacity of RC Flexural Members." *Journal of Composites for Construction* 2 (4): 195-202.

Lee, H. K., S. H. Cheong, S. K. Ha, and C. G. Lee. 2011. "Behavior and Performance of RC T-Section Deep Beams Externally Strengthened in Shear with CFRP Sheets." *Composite Structures* 93 (2): 911-922.

MacGregor, J.G., (1997) "Reinforced Concrete-Mechanics and Design" *Prentice Hall International Series.*

Malek, A. M. and H. Saadatmanesh. 1998. "Ultimate Shear Capacity of Reinforced Concrete Beams Strengthened with Web-Bonded Fiber-Reinforced Plastic Plates." *ACI Structural Journal* 95 (4): 391-399.

Martin, B. T. and D. H. and Sanders . 2007. *Verification and Implementation of Strut –and Tie Model in LRFD Bridge Design Specifications*: NCHRP project 20-07, Task 217.

Mofidi, A. and O. Chaallal. 2014. "Effect of Steel Stirrups on Shear Resistance Gain due to Externally Bonded Fiber-Reinforced Polymer Strips and Sheets." *ACI Structural Journal* 111 (2): 353-361.

Monti, G. and Liotta, M. A. 2005. "FRP-Strengthening in Shear: Tests and Design Equations." Kansas City, Missouri, Proceedings, 7th International RILEM Symposium on Non-Metallic (FRP) Reinforcement for Concrete Structures (FRPRCS-7).

Mörsch, E. (1908). Der eisenbetonbau – seine theorie und anwendung. 3. Auflage, Verlag Konrad Wittwer, Stuttgart, pp. 376.

Mörsch, E. (1922). Der eisenbetonbau - seine theorie und anwendung. 5. Auflage, Verlag Konrad Wittwer, Stuttgart, pp. 460.

Mufti, A. A. 2003. "FRPs and FOSs Lead to Innovation in Canadian Civil Engineering Structures." *Construction and Building Materials* 17 (6-7): 379-387.

Ombres, L. 2011. "Structural Performances of PBO FRCM-Strengthened RC Beams." *Proceedings of the Institution of Civil Engineers: Structures and Buildings* 164 (4): 265-272.

Ortlepp, R., U. Hampel, and M. Curbach. 2006. "A New Approach for Evaluating Bond Capacity of TRC Strengthening." *Cement and Concrete Composites* 28 (7): 589-97.

Pellegrino, Carlo and Claudio Modena. 2002. "Fiber Reinforced Polymer Shear Strengthening of Reinforced Concrete Beams with Transverse Steel Reinforcement." *Journal of Composites for Construction* 6 (2): 104-111.

Potisuk, T., Miller, T. H., C. C. Higgins, and S. C. Yim. 2011. "Finite Element Analysis of Reinforced Concrete Beams with Corrosion Subjected to Shear." *Advances in Civil Engineering* 2011.

Ritter, W. (1899). "Die bauweise Hennebique. Schweizerische Bauzeitung," 17, 41-43, 49-52 and 59-61.

Sherwood, Edward G., Adam S. Lubell, Evan C. Bentz, and Michael P. Collins. 2006. "One-Way Shear Strength of Thick Slabs and Wide Beams." *ACI Structural Journal* 103 (6): 794-802.

Sneed, L. H., and Ramirez, J. A. 2008. "Effect of Depth on the Shear Strength of Concrete Beams without Shear Reinforcement – Experimental Study," *SN2921, Portland Cement Association, Skokie, Illinois, USA*, 182 pages, 2008

Suffern, C., El-Sayed, A., and Soudki, K.A. 2011. "Shear Strength of Distributed Regions with Corroded Stirrups in Reinforced Concrete Beams," *Canadian Journal of Civil Engineering*, 37(8), 1045-1056.

Triantafillou, T. C. 1998. "Shear Strengthening of Reinforced Concrete Beams using Epoxy-Bonded FRP Composites." *ACI Structural Journal* 95 (2): 107-115.

Triantafillou, Thanasis C. and Catherine G. Papanicolaou. 2006. "Shear Strengthening of Reinforced Concrete Members with Textile Reinforced Mortar (TRM) Jackets." *Materials and Structures/Materiaux Et Constructions* 39 (285): 93-103.

Triantafillou, Thanasis C. and Costas P. Antonopoulos. 2000. "Design of Concrete Flexural Members Strengthened in Shear with FRP." *Journal of Composites for Construction* 4 (4): 198-205.

Tzoura, E., and Triantafillou, T.C. 2016. "Shear Strengthening of Reinforced Concrete T-Beams under cyclic loading with TRM FRP jackets" *Materials and Structures* 49(1): 17-28.

Zhang, Zhichao, Cheng-Tzu Thomas Hsu, and Jon Moren. 2004. "Shear Strengthening of Reinforced Concrete Deep Beams using Carbon Fiber Reinforced Polymer Laminates." *Journal of Composites for Construction* 8 (5): 403-414.